Universidade de Aveiro Departamento de Ciências Médicas
2017

Tânia Cristina Soares Martins

Exossomas como ferramentas para a descoberta de biomarcadores

Exosomes as tools for biomarker discovery

Universidade de Aveiro Departamento de Ciências Médicas
2017

Tânia Cristina Soares Martins

Exossomas como ferramentas para a descoberta de biomarcadores

Exosomes as tools for biomarker discovery

Dissertação apresentada à Universidade de Aveiro para cumprimento dos requisitos necessários à obtenção do grau de Mestre em Biomedicina Molecular, realizada sob a orientação científica da Professora Doutora Ana Gabriela Henriques, Professora Auxiliar Convidada do Departamento de Ciências Médicas da Universidade de Aveiro

Esta tese contou com o apoio financeiro da FCT (PTDC/DTPPIC/5587/2014) e do Instituto de Biomedicina (iBiMED) - UID/BIM/04501/2013.

Dedico esta tese aos meus pais, António e Laurinda por todo o amor, força e dedicação que sempre me deram. Dedico também esta tese em memória do meu avô Arlindo, por quem nutro um carinho muito especial, e que sempre foi para mim um exemplo de trabalho e superação.

o júri

presidente

Professora Doutora Sandra Maria Tavares da Costa Rebelo
Professora Auxiliar Convidada, Universidade de Aveiro

Professora Doutora Maria de Lourdes Gomes Pereira
Professora Associada C/ Agregação, Universidade de Aveiro

Professora Doutora Ana Gabriela da Silva Cavaleiro Henriques
Professora Auxiliar Convidada, Universidade de Aveiro

agradecimentos

O meu muito obrigada à Prof. Dra. Ana Gabriela Henriques por toda a ajuda e dedicação. Obrigada por todo o encorajamento e por ter acreditado em mim. Obrigada por ter contribuído tanto para o meu enriquecimento científico e também pessoal.

Muito obrigada,
Prof. Dra. Odete da Cruz e Silva por todas as sugestões, incentivo e confiança.
Prof. Ilka Martins Rosa pela sua ajuda e disponibilidade.
Dr. Ricardo Pinto pela sua ajuda e por tão bem me ter recebido.

Agradeço de forma muito especial a todos os voluntários participantes no estudo, famílias e profissionais de saúde, sem os quais este projeto não seria possível.

Um especial agradecimento à Joana Oliveira, que tanto me ajudou nos primeiros tempos, ao Roberto Dias, à Marlene Marafona e à Filipa Martins. Agradeço também a todos os meus restantes colegas e amigos do laboratório de Neurociências e Sinalização Celular que tão bem me receberam, sem esquecer todos os outros amigos que sempre me apoiaram.

Obrigado,
Ao iBiMED pelo financiamento deste projeto (UID/BIM/04501/2013) e por todos os equipamentos essenciais à realização desta dissertação.
À FCT pelo financiamento do projeto PTDC/DTPPIC/5587/2014.

Agradeço muito aos meus pais por todo o amor, coragem e valores transmitidos. Obrigada por nunca me terem deixado desistir e sempre terem acreditado nas minhas capacidades. Obrigada aos meus avós pelo carinho e encorajamento.

Obrigado Micael Monteiro, por todo o carinho, o amor e por teres estado sempre ao meu lado a dar-me força.

palavras-chave

Exossoma, métodos de isolação de exosomas, Doença de Alzheimer, sAPPα, sAPPβ, biomarcador

resumo

Os exossomas são pequenas vesículas extracelulares envolvidas em vários processos fisiológicos e patológicos. O potencial dos exosomas como fontes de biomarcadores para o diagnóstico, prognóstico e mesmo para a terapêutica tem intensificado a investigação nesta área, apoiando o potencial dos exosomas na descoberta de biomarcadores. A centrifugação diferencial é o método mais usado, mas é demorado, requer grandes volumes de amostra e as altas velocidades de centrifugação podem comprometer a integridade dos exossomas. Apesar das várias opções disponíveis, nenhum consenso foi atingido quanto à melhor metodologia para isolar exossomas.

Neste estudo, dois métodos baseados em precipitação e um método baseado em colunas foram comparados para a isolação de exosomas a partir de soro, plasma e líquido cefalorraquidiano humano (LCR). Foi realizada uma completa caracterização dos exosomas isolados, incluindo a análise do tamanho e estabilidade das partículas, análise da morfologia por microscopia eletrónica de transmissão, incluindo métodos de quantificação de partículas e proteína. Todos os métodos isolaram exosomas a partir dos três biofluidos, contudo apresentaram performances diferentes em termos de rendimento exossomal. Estes dados apoiam a hipótese de que para além da ultracentrifugação outros métodos podem ser aplicados para isolar exosomas no contexto da investigação clínica e translacional. Neste estudo foi também explorado o potencial dos exosomas derivados do soro humano como transportadores de biomarcadores candidatos para a Doença de Alzheimer (DA). Estes podem representar métodos menos invasivos do que o atual diagnóstico neuroquímico para a DA, baseado no LCR. Neste caso, foi monitorizado o potencial de sAPPα e sAPPβ nos exosomas extraídos de soro de indivíduos com demência moderada, severa e casos de DA diagnosticados. Foi observada uma diminuição nas médias de sAPPα e sAPPβ dos exosomas neuronais derivados do soro, suportando o potencial dos exosomas na descoberta de biomarcadores para a DA.

keywords Exosome, exosome isolation methods, Alzheimer's disease, sAPPα, sAPPβ, biomarker.

abstract Exosomes are small extracellular vesicles involved in various physiological and pathological processes. The potential of exosomes as biomarker resources for diagnostics, prognostics and even for therapeutics has intensified research in the field supporting the potential of exosomes in AD biomarker discovery. Differential centrifugation is the most used method but is time-consuming, requires larger volumes of sample, and the high centrifuge speed compromise exosome integrity. Despite the various approaches available, no consensus on which is the best methodology to isolate exosomes have been reached thus far. Thus, in this study, two precipitation-based methods and one column-based method were compared for exosome isolation from human serum, plasma and cerebrospinal fluid. A complete exosome characterization was carried out, including size and particle stability analysis, morphological assessment by transmission electron microscopy and yield quantification methods. All methods isolated exosomes from the three biofluids although in terms of exosome yield they performed differently. These data support the notion that other methods than ultracentrifugation can be successfully applied to isolate exosomes, that can be further used in the context of translational and clinical research.
It was also explored the value of serum-derived exosomes as carriers of candidate Alzheimer's disease (AD) biomarkers. These may represent less invasive approaches than CSF-based neurodegenerative diagnostic currently used for AD. In this case, the potential of serum-derived exosome sAPPα and sAPPβ was monitored, in cognitive demented individuals including AD diagnosed cases. A decrease in sAPPα and sAPPβ levels of serum-derived neuronal exosomes was obtained in individuals with moderate, severe dementia and AD confirmed from respective controls, supporting the potential of exosome in AD biomarker discovery.

Index

Abbreviations

Aβ	Amyloid-beta peptide
AD	Alzheimer's disease
ADAM	A desintegrin and metalloproteinase
AICD	APP intracellular domain
ALIX	Programmed cell death 6-interacting protein
APH-1	Anterior pharynx-defective 1
APLP1	APP like protein 1
APLP2	APP like protein 2
APOE	Apolipoprotein E
APP	Amyloid precursor protein
APP-CTFα/β	APP Carboxy-terminal Fragment of a/b-secretase processing
APS	Ammonium persulfate
ATP	Adenosine triphosphate
BACE	β-site APP cleaving enzyme
BCA	Bicinchoninic acid
CCD	Charge-coupled device
CDR	Clinical dementia rate
CHMP4	Charge multivesicular body protein 4
CSF	Cerebrospinal fluid
CTF	Carboxy-terminal fragment
DGKα	Diacyl glycerol kinase α
DNA	Deoxyribonucleic acid

DLS	Dynamic light scattering
ECL	Enhanced chemiluminescence
ELISA	Enzyme-linked immunosorbent assay
EOAD	Early-onset Alzheimer's disease
ESCRT	Endosomal Sorting Complex Required for Transport
ExoQ	Exoquick
ExoS	Exospin
FAD	Familiar Alzheimer's disease
flAPP	Full-length amyloid precursor protein
GSAP	γ-secretase activating protein
GTP	Guanosine triphosphate
HRP	Horseradish peroxidase
HRS	Tyrosine kinase substrate
Hsp	Heat shock protein
IDE	Insulin degrading enzyme
ILV	Intraluminal vesicle
IRS	Insulin receptor substrate
KPI	Kunitz protease inhibitor
LGB	Lower gel buffer
LOAD	Late-onset Alzheimer's disease
LTP	Long term potentiation
MCI	Mild cognitive impairment
MHC	Major histocompatibility complex
mRNA	Messenger RNA

miRNA	MicroRNA
MTBP	Microtubule binding protein
MVB	Multivesicular bodies
NCAM	Neural cell adhesion molecule
NAD	Non-Alzheimer's disease types of dementia
NDD	Neurochemical dementia diagnostic
NFT	Neurofibrillary tangle
nSMase	Neutral sphingomyelinases
PAD	Putative and Alzheimer's disease
PAGE	PolyAcrylamide gel electrophoresis
PBS	Phosphate buffered saline
PCB	Primary care setting
PDI	Polydispersity index
PEN2	Presenilin enhancer protein 2
PI3P	Phosphatidylinositol 3-phosphate
PLP	Proteolipid protein
PM	Plasma membrane
PrP^{C}	Cellular Prion Protein
PS	Presenilin
p-Tau	Tau phosphorylated form
RAB	Ras-related protein
RIPA	Radioimmunoprecipitation assay
RNA	ribonucleic acid
ROC	Receiver operating characteristic curves

RT	Room temperature
SAD	Sporadic Alzheimer's disease
sAPPα/β	Secreted APP forms after α-cleavage/β-cleavage
SD	Standard deviation
SDS	Sodium docecilsulfate
SEC	Size Exclusion Chromatography
shRNA	Short hairpin RNA
siRNA	short interfering RNA
SNARE	Soluble NSF-attachment protein receptors
SP	Senile plaque
STAM	Signal transducing adaptor molecule
TBS	Tris-buffered saline
TBS-T	Tris-buffered saline + Tween
TEI	Total Exosome Isolation
TEM	Transmission electron microscopy
TGN	Trans-Golgi network
TMB	3,3'5,5-tetramethylbenzidine
Tris-HCl	Tris (hydroxymethyl)-aminoethane chloride
TSG101	Tumor susceptibility gene 101
UGB	Upper gel buffer
VPS4	Vacuolar protein sorting 4

Chapter 1. Introduction

1. Exosomes overview

Cellular communication is essential to life and can be mediated by direct cell contact or through molecule secretion. In the 1980s, another mechanism for cell communication that involves the release of membrane vesicles (nanovesicles) into the extracellular space and consequent influence on target cells has emerged. These nanovesicles are formed by vesiculation inside an intracellular endosome, forming a multivesicular body (MVB). MVBs have the capacity to fuse with plasma membrane (PM) and release vesicles into the extracellular space [1, 2]. In 1987, the term “exosome” was adopted for these small vesicles (30-150 nm) of endosomal origin [3].

1.1. Exosome biogenesis

As mentioned, exosomes are originated from intraluminal vesicles (ILVs) of MVBs. These vesicles or early endosomes are formed by inward budding of PM with internalization of selected cargo. Early endosomes mature into late endosomes or MVBs that accumulate various endosomes inside their lumen [4]. Different subpopulations of MVBs can fuse with plasma membrane, resulting in exosome secretion, or fuse with lysosomes to destroy their content (Figure 1).

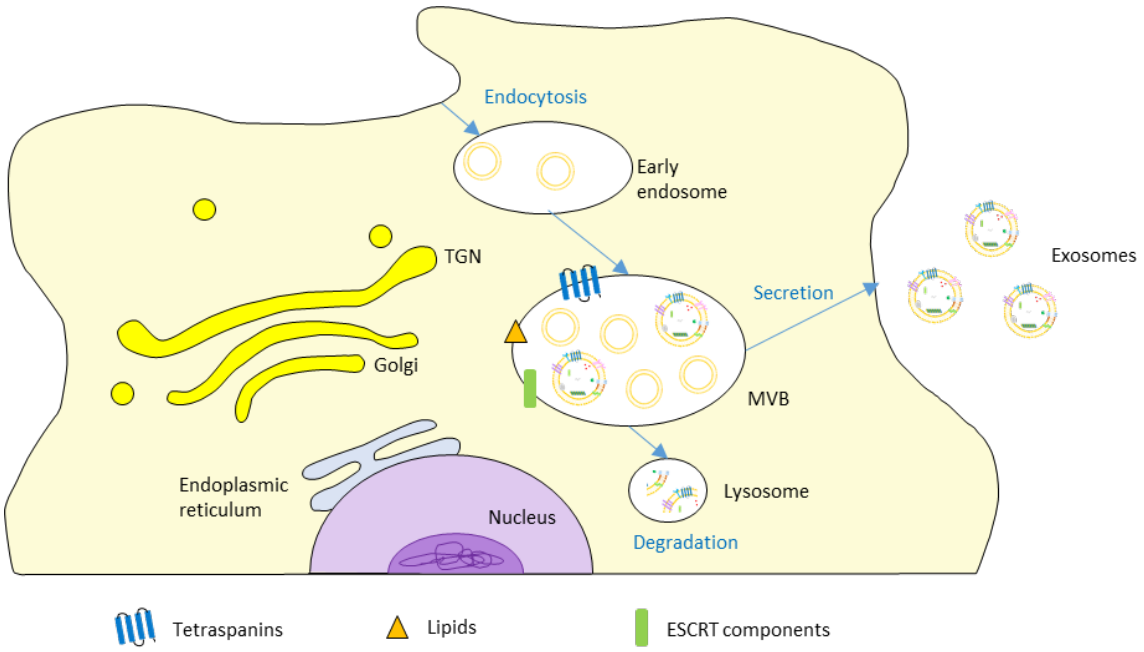

Figure 1. Mechanisms of exosome biogenesis. Plasma membrane budding inward result in early endosomes that mature in late endosomes or MVBs. MBVs can then fuse with plasma membrane resulting in exosome secretion or fuse with lysosome for degradation. MVBs: Multivesicular bodies. TGN: Trans-Golgi network.

Neither MVBs content sorting or MVBs destiny is aleatory, being those processes controlled in part by lipid metabolism and lipid composition at PM. For example, phosphatidylinositol 3-phosphate (PI3P) is present in early endosomes [5] and plays an important role in protein targeting. FYVE protein domains of Endosomal Sorting Complex Required for Transport (ESCRT)-0, involved in exosome biogenesis, directly bind to PI3P (reviewed in [6]). In addition, PI3P contributes for regulation of membrane dynamics and endosome mobility by recruiting kinesins [7]. Protein-to-protein interactions can also regulate the selection of protein cargo of ILVs, as chaperone heat shock protein 70 (Hsp70) that binds not only to endosomal acidic phospholipids but also to cytosolic proteins, conferring selectively in inclusion of proteins into ILVs [8].

Different cell types secrete different subpopulations of exosomes with distinct cargo and consequently different mechanisms for exosome biogenesis may be involved. Endosomal Sorting Complex Required for Transport is the most common studied mechanism involved in MVBs formation. It is composed by four complexes and approximately thirty proteins [9]. ESCRT-0 complex binds to transmembrane proteins that are ubiquitinated and thus destined for degradation. This interaction occurs via hepatocyte growth factor – regulated tyrosine kinase substrate (HRS) which recognizes ubiquitin. Signal transducing adaptor molecule (STAM) is another ESCRT-0 component that interacts directly with HRS. In turn, HRS can recruit the Tumour susceptibility gene 101 protein (TSG101) that is a member of ESCRT-I. Consequently, ESCRT-I recruits ESCRT-II and finally ESCRT-III via ESCRT-II. Various studies support the role of HRS in ESCRT-I recruitment as HRS inhibition resulted in decreased exosome secretion, in different cell lines [10–13]. Moreover, silencing of ESCRT-0 component STAM gene, ESCRT-I TSG101 gene or depletion of Programmed cell death 6-interacting protein (ALIX), the later involved in ESCRT-III recruitment, result in decreased exosome secretion [12].

ESCRT-I and ESCRT-II are both tetramers involved in budding formation, sequester of ubiquitinated proteins and seem to be essential for exosome secretion. Their structure helps to stabilize the bud upon interaction. Inhibition of charge multivesicular body protein 4 (CHMP4) isoforms (ESCRT-III component) in MCF-7 cell line resulted in decreased exosome secretion containing syndecan, CD63 and syntenin [14]. Lastly, ESCRT-III complex is involved in scission of ILV, dissociation and recycling of ESCRT is dependent of the AAA-ATPase Vacuolar protein sorting 4 (VPS4) activity, suggesting that ESCRT-III polymers disassembly requires ATP hydrolysis [15]. However, VPS can interact with ESCRT-III also independently of ATP hydrolysis as shown in

deficient VPS24 -VPS2 protein chimeras [16]. The role of VPS4 in ILV formation is still unclear: inhibition of VPS4B in HeLa-CIITA cells increased exosome secretion [12] but concomitant depletion of VPS4A and VPS4B in MCF-7 cells decreased exosome secretion [14]. Thus, exosome secretion can be also dependent of ESCRT-III complex [14].

Exosome biogenesis can occur also in a ESCRT independent manner, as initially shown in oligodendroglial cell line when ALIX and TSG101 were depleted [17] and in human HEp-2 cells facing depletion of ESCRT complexes [18]. Lipids, tetraspanins and heat shock proteins seems to be the essential elements involved in ESCRT independent mechanisms that probably occur concomitantly with ESCRT mechanisms.

Some lipids are also essential to exosome biogenesis as ceramide and sphingomyelin. Inhibition of neutral sphingomyelinases (nSMase), enzymes responsible for hydrolysis of sphingomyelin to ceramide, results in decreased exosome secretion, carrying the proteolipid protein (PLP), in an oligodendroglial cell line. Further, ESCRT machinery depletion still results in exosomes secretion with PLP suggesting that exosome biogenesis can be independent of ESCRT mechanisms and ceramide is crucial element [17]. In addition, induction of cholesterol accumulation results in increased levels of exosomes carrying mainly flotillin which suggests that exosomes and flotillin can be involved in cholesterol homeostasis regulation [19].

Tetraspanins can also be involved in exosome biogenesis by ESCRT independent mechanisms. CD63 was the first tetraspanin found to be involved in exosome biogenesis and secretion [20]. CD81 is another tetraspanin involved in selection of exosome cargo proteins, through interaction with specific ligands [21]. CD9 and CD82 when overexpressed in HEK293 cells increased exosome secretion of β-Catenin, although in a ceramide dependent process, suggesting that β-Catenin secretion into exosomes is associated to Wnt signalling pathway downregulation (for example, involved in cell proliferation) [22]. In addition, the expression of tetraspanin Tspan8 modified exosome protein content, mRNA and miRNA cargo with effects into tumour angiogenesis in rat pancreatic adenocarcinoma cells [23].

Considering all current knowledge about exosome biogenesis it seems likely different subpopulations of MVBs as well as different mechanisms involved in exosome biogenesis in a cell could exist.

1.2. Exosomes secretion machinery

MVBs fuse with plasma membrane leading to the secretion of exosomes. In this process, several small GTPases from RAB family are involved, depending on cell type (Figure 2). The first Ras-related protein (RAB) involved in exosome secretion identified was RAB11 [24]. Inhibition of RAB11 lead to reduction of exosome secretion bearing the transferrin receptor [24] and is crucial to MVBs docking with PM in an intracellular calcium rising-dependent mechanism [25]. RAB35 is also crucial for exosome secretion since its inhibition decreased exosome secretion in murine oligodendroglial cell line [26] and in primary oligodendrocytes [27]. Silencing of RAB2B, RAB5SA, RAB9A, RAB27A and RAB27B through small hairpin RNA also results in decreased exosome secretion in HeLa-CIITA cells [28]. These effects were more significant for RAB27A and RAB27B depletion, suggesting that these RABs could be involved in MVBs fusion with PM [28]. In contrast, RAB7 was essential for exosome secretion in MCF-7 cells [14] and RAB11 in Drosophila S2 cells [29]. RAB 11 and RAB35 depletion in RPE1 cells led to decreased exosomes secretion. Dual effects have been described for RAB27A/B (associated with late endosome and secretory compartments), silencing of RAB27A/B did not influence secretion rates [30] but depletion of RAB27A is correlated with less exosome secretion in various cells lines [13, 31–33]. Concomitant depletion of RAB27A and RAB27B in myofibroblasts cells rendered in decreased exosome secretion [33] as shRNA RAB27A/B inhibition in human breast cancer MDA-MB-231 [34].

The fusion of MVBs with PM and consequently exosome secretion is not completely understood. Soluble NSF-attachment protein receptors (SNARE) are known to be involved in fusion of lipid membranes however SNAREs effects on exosome secretion are controversial. Inhibition of SNARE protein VAMP7 in canine MDCK cells did not impair the secretion of exosomes [35]. However, exosome secretion in HEK293 cells containing Wnt was found to be dependent of the R-SNARE protein Ykt6 [11] which is present in the MVBs [36]. Hence, controversial results may be explained by involvement of different SNARE complexes in the secretion of different exosome subpopulations.

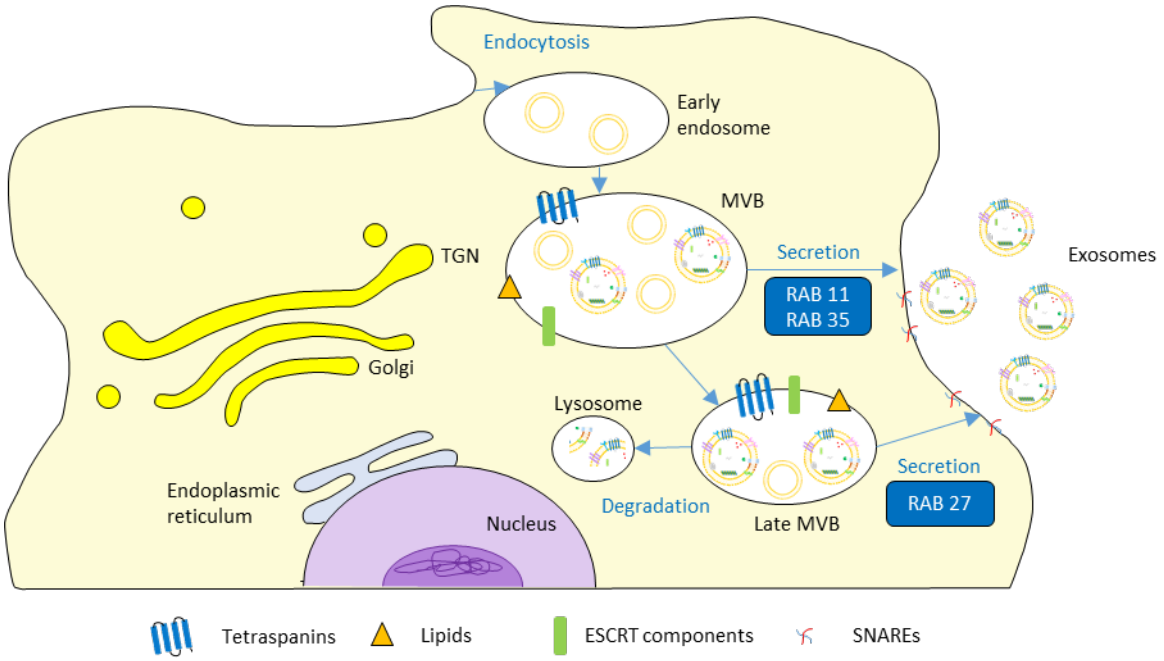

Figure 2. Machinery of exosome secretion. Outward budding for exosome secretion is regulated by endosomal sorting complex required for transport complex (ESCRT) components and many Ras-related proteins in the brain (RABs). SNARE: soluble NSF attachment receptor. MVBs: Multivesicular bodies. TGN: Trans-Golgi network. SNARE: Soluble NSF-attachment protein receptors.

There are also several molecules involved in exosome secretion beyond SNARE proteins, although it is not well clear whether their role is related to ILVs biogenesis in MVBs or with exosome secretion. Diacyl glycerol kinase α (DGKα) is one of those molecules. T cells inhibitions by DGKα decreased exosome secretion bearing Fas ligand [37] and regulated the polarised secretion of exosomes [38]. Using the nematode *Caenorhabditis elegans,* the V0 complex of the H^+- vacuolar ATPase was found to promote exosome secretion and recently it was found that the GTPase RAL-1 regulates MVB formation and exosome secretion [39].

1.3. Exosome composition

Exosomes composition is very similar to endosomes and, in a less closer manner, similar to the composition of plasma membrane and cytosol (Figure 3) [40]. The study of protein content of exosomes, isolated from cell cultures and body fluids has been based in antibody detection techniques as western blotting, protein staining or proteomic analysis as mass spectrometry. However, there is still a large number of proteins and nucleic acids secreted into exosomes to be identified. Exosomes are specially enriched in proteins derived of the plasma membrane, endosomal compartment or cytosol and in some lipids as phosphatidylethanolamide [41], ceramide [17], cholesterol [42, 43] and saturated fatty acids [44] but it can also include nucleic acids. Indeed, since it was discovered that exosomes carry various species of mRNA [45], miRNA [45] and small non-coding RNAs [46], exosome genetic cargo under physiological and pathological conditions have been the focus of intensive research. Moreover, the sorting of miRNA into exosomes is not aleatory and seems to be regulated by a motif of 4 nucleotides (GGAG). This motif is recognized by sumoylated nuclear ribonucleoprotein A2B that loads miRNA into exosomes of human embryonic kidney cells 293 [47]. Moreover, in macrophages miRNA cargo into exosomes was shown to be also regulated by the levels of target mRNA [48].

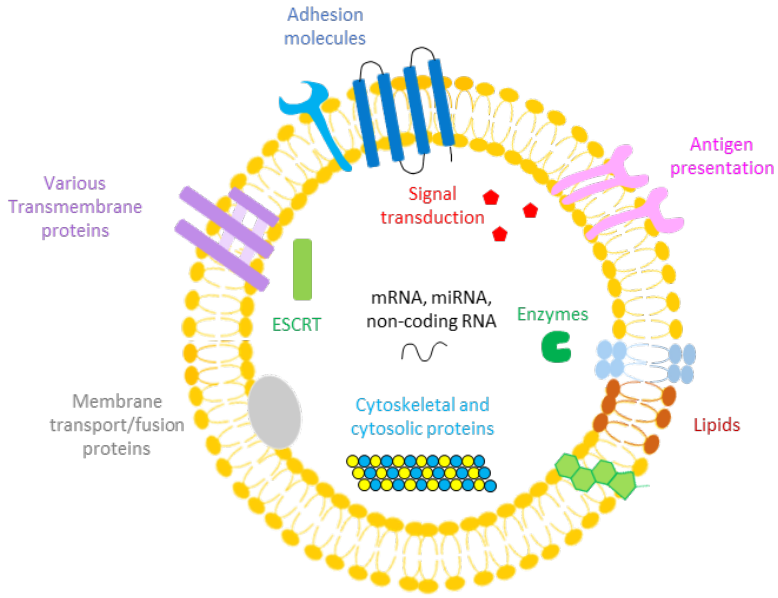

Figure 3. Exosomes general composition. Exosomes are composed by various protein, lipids and nucleic acids. Among those are adhesion molecules as tetraspanins and integrins; antigen presentation as MHC class I and MHC class II proteins; signal transduction proteins as G proteins; membrane and fusion proteins as annexins and RABs; cytoskeletal and cytosolic proteins as actin, tubulin and ribosomal proteins; enzymes as glyceraldehyde 3-phosphate dehydrogenase and lipids as ceramide, cholesterol and sphingomyelin. ESCRT: Endosomal sorting complex required for transport; mRNA: Messenger RNA; miRNA: microRNA.

1.4. Exosome isolation methods

Exosome isolation from cell culture supernatants or biofluids is a big challenge, especially in the last case. Generally, exosome purification techniques are based in exosome characteristics as size, density, shape or surface proteins.

The most common technique for exosome isolation is differential ultracentrifugation which includes low speed centrifugation to remove cells and debris (important contaminants of exosome suspensions), high speed cycles to remove larger vesicles and then a high ultracentrifugation step to pellet exosomes. It consists in a time-consuming method which requires expensive material (ultracentrifuge), precipitates protein aggregates and other contaminants, resulting in low exosome yields. Further, biofluids viscosity is related to lower particle sedimentation so it requires longer ultracentrifugation steps, usually with higher centrifugation periods that can comprise the exosome integrity. As an advantage, ultracentrifugation does not require sample pre-treatments or any other reagents [49–51].

Density gradient ultracentrifugation is a variation of ultracentrifugation and is based on exosome size, mass and density, efficiently separating exosomes from other vesicles with distinct densities. According to this method the sample is placed in the top of a density gradient medium (higher densities in the top). Then, it is applied an ultracentrifugation step and various vesicles including exosomes move through density gradient medium. Exosomes float until get equilibrium density, ranging from 1.08 to 1.22 g/ml on a sucrose gradient, and form a fraction zone that can be easily recovered [49–51].

The discovery of exosome surface proteins and receptors allowed the development of additional methods as immunoaffinity exosome isolation that is based on interactions between the antigens, for example highly abundant exosome proteins, and specific antibodies which may be coupled to magnetic beads. These magnetic beads can then be analysed by several techniques as flow cytometry, electron microscopy, providing higher exosome yields than ultracentrifugation. However, exosome immunocapture methods only isolates subpopulations of exosomes, depending on exosome marker that was targeted and it is difficult to elute exosomes from beads resulting in low exosome yields, requires cell-free suspensions and expensive reagents [49–51].

The main size-based exosome isolation methods are ultrafiltration and size exclusion chromatography (SEC). Ultrafiltration requires a previous centrifugation step to remove cells and then fluid suspensions are filtered through membranes in which pores are defined according to

exosome size or molecular weight. This is a rapid method however it may co-isolate other vesicles, various proteins and lead to vesicles damage due to pressure forces. SEC isolates exosomes based on their size, since macromolecules pass thought a porous polymeric phase with beads and multiple tunnels and pores. Vesicles with small hydrodynamic diameters ranging from 30 to 200 nm are trapped into pores and lately eluted. Particles with sizes higher than 1 μm do not enter the porous phase and other particles than exosomes enter in the porous zone but are not retained. SEC provides purest exosome isolations, preserving exosome integrity but is time-consuming method [49–51], although less than ultracentrifugation methods.

Water-excluding polymers isolate exosomes by altering its solubility. This method requires a low speed centrifugation step to remove cells and debris, mixing and incubating with polymers such as polyethylene glycol that link to water molecules and enhances the precipitation of less soluble components as exosomes. Further, the mixture is centrifugated at low speed, pelleting exosomes. Polymer-based exosome isolation gives good exosome yields, preserves exosome integrity, however it also precipitates protein aggregates and other materials as lipoproteins. The solely polymer reagent can interfere with downstream analysis as mass spectrometry [49–51].

Recently, microfluidic techniques have been used to isolate exosomes. This method is based on specific binding of exosomes to antibody coated surfaces starting from very small sample volumes. The fluid is pumped through a chip, resulting in exosome isolation. Microfluidic devices isolate exosomes in cost-effective manner and rapidly, with high sensitivity. As microfluids are recent, it still lacks validation and large scale tests. The smaller starting volume is another important issue when using this method, especially in the clinical scale exosome isolation [49–51].

2. Alzheimer's disease overview

Alzheimer's disease (AD), first described by Alois Alzheimer in 1907 is a multifactorial disorder like most of the neurodegenerative diseases [52]. Nowadays, it is the most prevalent neurodegenerative disease worldwide estimated to affect 46 million people in 2015 and it is expected to reach the double by 2030 and triple by 2050 [53–55]. AD mainly affects individuals between ages of 60 and 85 years, representing a major public health challenge with huge impacts on patient's quality of life, but it also represents a major economic problem [53–55]. In Portugal, AD cases are increasing, in 2013 it represented from 50% to 70% of dementia cases and affected around 160 287 individuals [56].

AD is characterized by progressive cognitive decline, starting with memory loss and progressive hindering of daily activities performance, until language, perception and orientation impairment. In late stages of disease, individuals lose autonomy and become completely dependent on others. Neurodegeneration starts about 20 to 30 years before clinical symptoms but typically AD is diagnosed in later stages of disease and, in some cases, it can even be misdiagnosed due to overlap of symptoms of other diseases [57, 58]. There is a huge need for reliably biomarkers to assist in AD diagnosis in asymptomatic stages which will permit an earlier intervention with consequent improving of patient's health and quality of life.

2.1. Alzheimer's disease neuropathological hallmarks

Alzheimer's disease major hallmarks are neurofibrillary tangles (NFTs) and senile plaques (SP).

NFTs were described as fibrous inclusions inside perikaryal cytoplasm of pyramidal neurons (Figure 4) [58]. NFTs are composed by paired abnormal fibrils (helical filaments), formed mainly by hyperphosphorylated and misfolded Tau proteins [59] and for other proteins as ubiquitin [60, 61], cholinesterase [62] and amyloid beta peptide (Aβ) [63]. Tau belongs to the family of microtubule proteins and the interaction between Tau and microtubules is highly regulated by phosphorylation. Excessive phosphorylation affects Tau interactions [64].

NFTs are initially distributed along entorhinal cortex and hippocampus (medial temporal lobe) [65] and then extend to primary motor, sensory and visual areas [66]. NFTs extend and distribution are correlated with AD degree of dementia and disease duration. Neurofibrillary degeneration on medial temporal lobe can lead to the initial episodic memory impairment and progressive neurodegeneration in other areas, such as prefrontal cortex or anterior temporal cortex, associated respectively to executive dysfunctions and semantic memory impairment [66–69].

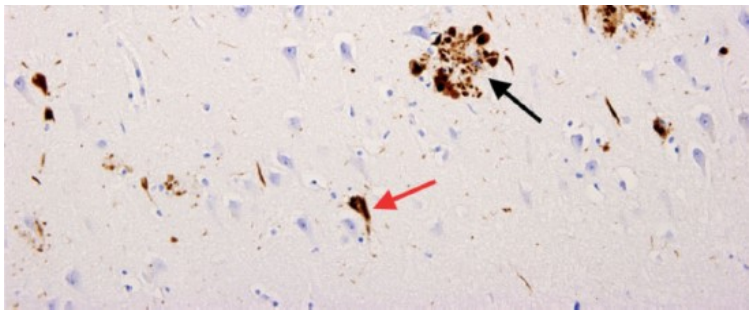

Figure 4. Immunohistochemical preparation of temporal cortex of a patient with Alzheimer's disease. Red arrow points for neurofibrillary tangles and black arrow points for senile neuritic plaques. Adapted from: [58].

SPs are another AD hallmark (Figure 4). These are mainly composed by atypical extracellular deposition and accumulation of Aβ 1-40 or 1-42 which are products of normal Alzheimer's amyloid precursor protein (APP) processing. The Aβ1-42 is highly hydrophobic and fibrillogenic so it is the main component of SPs [70]. Central core of plaques is composed by a mass of extracellular amyloid, surrounded by dystrophic neurites (neuronal, astrocytic, microglial processes and paired helical filaments) supporting the Aβ potential for neurotoxicity [71, 72].

Amyloid plaques accumulate mainly in isocortex, at basal portions of temporal, frontal and occipital lobes extending then to association areas and primary isocortical areas sometimes without exclude cerebellum and basal ganglia [66].

Besides the two main hallmarks, other morphological alterations which have an impact on cognitive performance are neuropil threads, resulting from breakdown of dendrites and axons, and dystrophic neurites [58, 73]. Additionally, AD brains face cerebral cortical atrophy with impairment of primary motor, sensory and visual areas, hippocampus atrophy and loss of brain tissue accompanied by lateral ventricles dilation [58].

2.2. FAD and sporadic AD

The majority of AD cases have an onset after 65 years and are considered late onset AD (LOAD) cases. Few cases appear between ages of 30 and 65 and are known by early onset AD (EOAD) cases. Etiologically, AD can be considered familiar (FAD), when various individuals of the same family are affected by Mendelian inheritance, or sporadic AD (SAD) cases, without familiar cases. Most of FAD cases are EOAD and most of LOAD cases are sporadic. FAD is characterized by mutations in APP, presenilin 1 (PS1) and presenilin 2 (PS2) [74].

In humans, the *APP* gene is located on chromosome 21 (21q21.3) and contains at least 18 exons [75–77]. APP is a type-I transmembrane protein that belongs to a three-member family of homologs identified in mammals: APP [78, 79], APP like protein 1 (APLP1) [80] and 2 (APLP2) [81, 82]. These members share a conserved structure as E1 and E2 domains, a short C-terminal intracellular tail and a large extracellular domain however Aβ domain is specific of APP and do not exist in the other homologs (reviewed in [83]). *APP* autosomal mutations are rare and mainly located in exons 16 and 17, located near the α-secretase cleavage site (within Aβ sequence) or near γ-secretase site which alter APP processing and increase Aβ1-42 production [84].

The majority of FAD cases is caused by *PS1* and *PS2* autosomal mutations which are related with increase production of Aβ1-42, the main component of SPs [74]. *PS1* and *PS2* genes have a similar structure although *PS1*, located on chromosome 14, encodes the catalytic core of γ-secretase, and *PS2*, located in the chromosome 1, codifies for active sites of the γ-secretase complex [85, 86]. Recently, a *PS1* loss of function mutation was identified as correlated with overproduction of Aβ1-43 which is highly amyloidogenic [87].

SAD results from a combination of genetic and environmental factors. Apolipoprotein E (*APOE*) alleles presence is the highest risk factor for SAD, especially *APOE4* alleles increase which encodes apolipoproteins in brain [88], but *APOE2* has a protective role [89]. *APOE* genes encode for lipoprotein binding amyloid peptides. Besides *APOE4* allele, environmental risk factors as low educational levels, hypertension, high cholesterol levels, smoking, pesticides, traumatic brain injury and depression also contribute to SAD. Protective AD factors may be physical exercise, hormonal replacement therapy and moderate alcohol consume [90].

2.3. Alzheimer's amyloid precursor protein

2.3.1. APP processing

APP can be proteolytic cleaved by two pathways: the non-amyloidogenic pathway, mediated by α- and γ-secretases (Figure 5A), or the amyloidogenic pathway where Aβ generation occurs by sequential cleavage of β- and γ-secretases (Figure 5B).

In the non-amyloidogenic pathway, APP is cleaved by α-secretase within the Aβ domain (between Lys^{16}-Leu^{17} bond) [91, 92], releasing the large soluble ectodomain sAPPα and generating the membrane bound carboxy-terminal fragment APP-CTFα or C83 [93], which lacks the amino terminal portion of Aβ. C83 can be further cleaved by γ-secretase liberating small hydrophobic peptides, called P3 fragments [94] and the APP intracellular domain (AICD) [95]. APP processing by α-secretases is expected to be neuroprotective as precludes Aβ formation and originates P3 fragment that although found in diffuse amyloid plaques has been considered to be non-pathogenic [96–98].

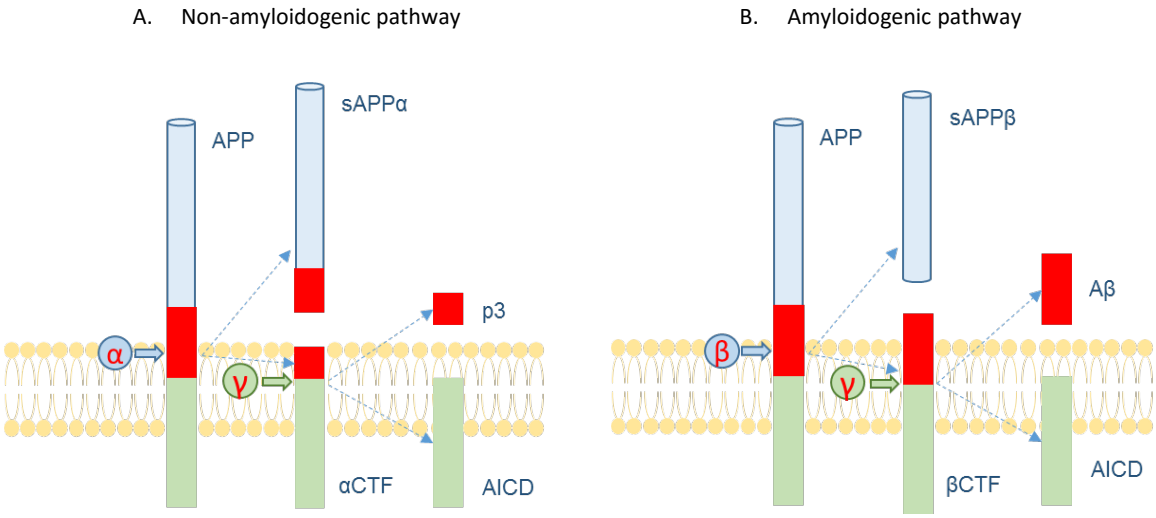

Figure 5. APP processing. A. Non-amyloidogenic processing of APP. APP is cleaved by α-secretase in amyloid peptide sequence originating sAPPα and αCTF. Then, αCTF is cleaved by γ-secretase producing p3 and AICD**. B. Amyloidogenic processing of APP.** APP is cleaved by β-secretase generating sAPPβ and βCTF. γ-secretase cleaves βCTF in AICD and in neurotoxic Aβ specie. APP: amyloid precursor protein; Aβ: amyloid beta peptide; sAPP α/β: soluble amyloid precursor protein α/β; α/βCTF: carboxy-terminal fragment α/β; AICD: APP intracellular domain. Arrows highlight cleavage sites of secretases.

α-secretases are plasma membrane proteases [99], more precisely zinc metalloproteinases [100]. Several members of ADAM family ("a desintegrin and metalloproteinase") can act as α-secretases: ADAM9 [101, 102], ADAM10 [102, 103], ADAM17 [102, 104], ADAM19 [105]. ADAM17 has found to play a crucial role in APP regulated cleavage [104], especially in neurons [106] as well as ADAM9 that when inhibited stops the regulated production of sAPPα [107]. ADAM10 seems to be responsible for the characteristic constitutive α-secretase cleavage of APP, in various cell lines [107], including in neurons. ADAM9 [108] and ADAM19 [109] are also expressed in human brain.

The amyloidogenic pathway is mediated by β-secretase cleavage of APP at amino terminal with the release of sAPPβ ectodomain and the formation of membrane-bound APP-CTFβ or C99 that is further processed by γ-secretase leading to Aβ generation and a long AICD (Figure 5B).

The β-site APP cleaving enzyme 1 (BACE1) was the first transmembrane aspartyl protease found, highly expressed in brain [110–115]. It cleaves APP preferentially at Asp^{1} and Glu^{11}, its optimal activity is at low pH and the enzyme is preferentially located in acidic compartments as early Golgi, late Golgi and endosomes, besides of plasma membrane [111, 116–118]. Beyond BACE1, cathepsin B was also proposed to be a β-secretase as its inhibition decreased Aβ generation in neuronal chromaffin cells and in mice [119, 120].

γ-secretase is a high molecular weight aspartyl protease complex composed by four transmembrane components: PS1 and PS2 with two aspartyl residues that are part of the catalytic domain [121, 122], and three adaptor proteins: nicastrin [123], anterior pharynx-defective 1 (APH-1) and presenilin enhancer protein 2 (PEN2) [124, 125]. All components of γ-secretase seems to be essential for its function, APH-1, nicastrin and PEN2 are necessary for complex maturation, stability and function as it was demonstrated in a *Saccharomyces cerevisiae* model [126–128]. Nicastrin interacts with APH-1 in early assembly of γ-secretase complex [129] and PEN2 regulates the proteolytic processing activity of presenilins [130]. Despite of the four already described γ-secretase components, some factors have been identified as potential new components as CD147 [131], TMP23/p21 [132] and an γ-secretase activating protein (GSAP) [133].

γ-secretase cleaves the products of α- and β-secretases at various sites, preferentially within transmembrane domains near cytoplasmic border of PM. The clear majority of species produced by γ-secretase processing are Aβ1-40 and Aβ1-42 and respective AICD's.

2.3.2. APP intracellular trafficking

Full length APP is synthetized in the endoplasmic reticulum, transported through Golgi to trans-Golgi network (TGN) (Figure 6) where most part of post translational modifications occur such as phosphorylation, N- and O-glycosylation and sulfation [134]. A small portion of APP is transported into TGN vesicles to plasma membrane where APP can suffer α-secretase cleavage, producing sAPPα, or be reinternalized and cleaved in endosomes generating Aβ peptide and other products that can be after transferred to MVBs [135]. Aβ peptides can also be generated in various cell compartments as endoplasmic reticulum, Golgi apparatus, TGN, endosomes and lysosomes, in the presence of β and γ-secretases which contributes to intracellular accumulation of Aβ. Evidences suggest that APP amyloidogenic processing occurs mainly in lipid rafts of intracellular organelles [135–138]. Some MVBs can fuse with lysosomes to degradation and others fuse with PM, releasing ILVs as exosomes. Aβ can accumulate in some ILVs so can be released into exosomes. Various studies corroborate the presence of Aβ and other cleavage products inside exosomes [139] as described in topic 3.

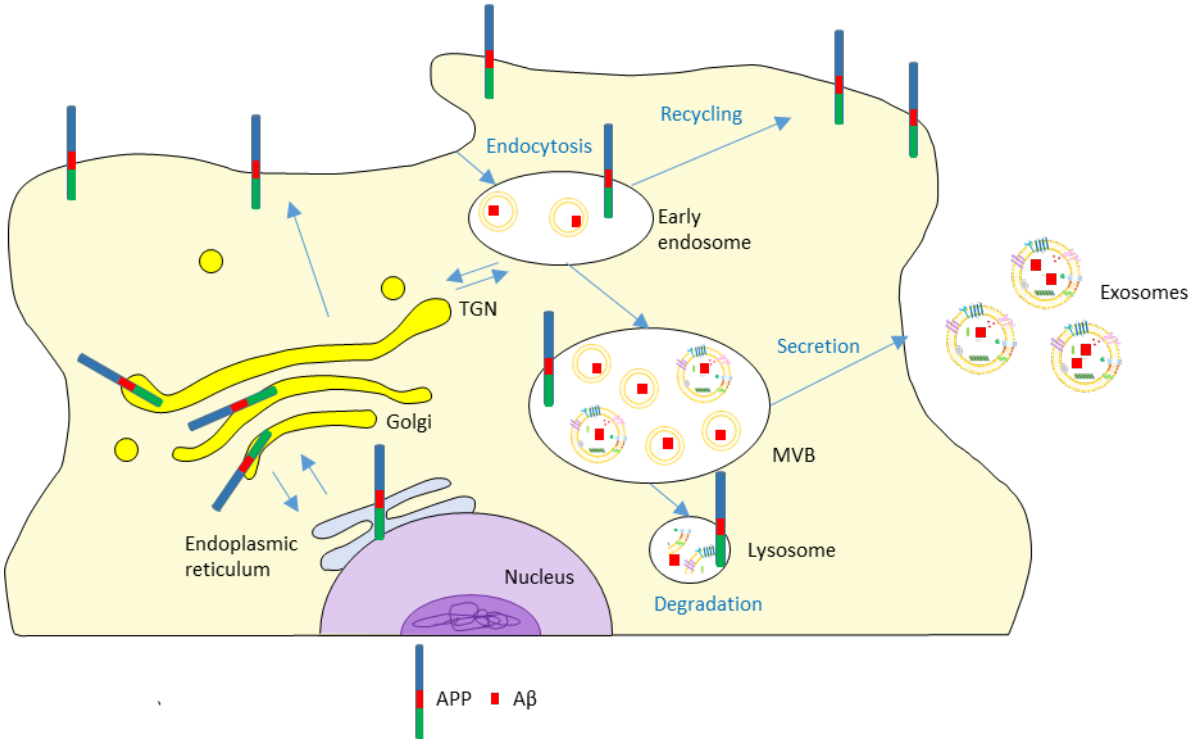

Figure 6. APP intracellular trafficking. New synthetized APP mature and is transported through secretory pathway, from endoplasmic reticulum to Golgi and TGN to PM where APP can be non-amyloidogenic processed. APP full length at PM can be internalized and further recycled or traffic to late endosomes and lysosomes to be degraded or amyloidogenic processed. APP: Amyloid precursor protein; Aβ: Amyloid beta peptide

2.4. Amyloid cascade hypothesis

Amyloid cascade hypothesis considers that amyloid peptide accumulation in brain parenchyma is the trigger event for a neurodegenerative cascade that culminates into dementia (Figure 7). This is supported not only by autosomal dominant mutations in PS1 and PS2 which impair APP metabolism and cause EOAD, but also by mutations at *APOE* gene. *APOE* alleles appear to have distinct impact on AD pathology. APOE2 proteins mediate clearance of Aβ but the presence of allele APOE4 is correlated to increased risk for develop sporadic AD, as already mentioned. Many other mutations can contribute to AD as mutations in the gene that encode Tau protein. These mutations were initially found in patients of frontotemporal dementia which is a neurodegenerative disorder characterized by Tau deposition with formation of NFTs and neuronal loss, but without amyloid plaques accumulation [140–142]. Therefore, it is thought that NFTs appear after SPs. This is supported by the fact that transgenic mice overexpressing human APP and Tau have increased formation of Tau tangles but do not exhibit alterations in SPs [143]. Despite of all efforts made, it is still uncertain the exact mechanism linking Aβ deposition and NFTs.

Neurotoxicity of Aβ peptides is sustained by small diffusible Aβ oligomers which assemble when fibril formation is not possible and impair synaptic plasticity and memory during early stage of AD [144]. Soluble oligomers formed after Aβ plaques formation also contribute for Aβ toxicity, impairing long term potentiation (LTP) *in vivo,* required for memory formation, and decreasing the number and function of synapses [145]. Different forms of Aβ oligomers were identified in human brain and transgenic organisms [145–147]. Recently, soluble oligomers were quantified in post-mortem brain tissues from healthy subjects and patients with dementia, and although similar plaque densities were identified in both cases healthy subjects had a weaker correlation between oligomers and plaque deposition when compared with AD patients [148]. Amyloid cascade hypothesis highlights the role of Aβ and its contribution to AD disease type dementia.

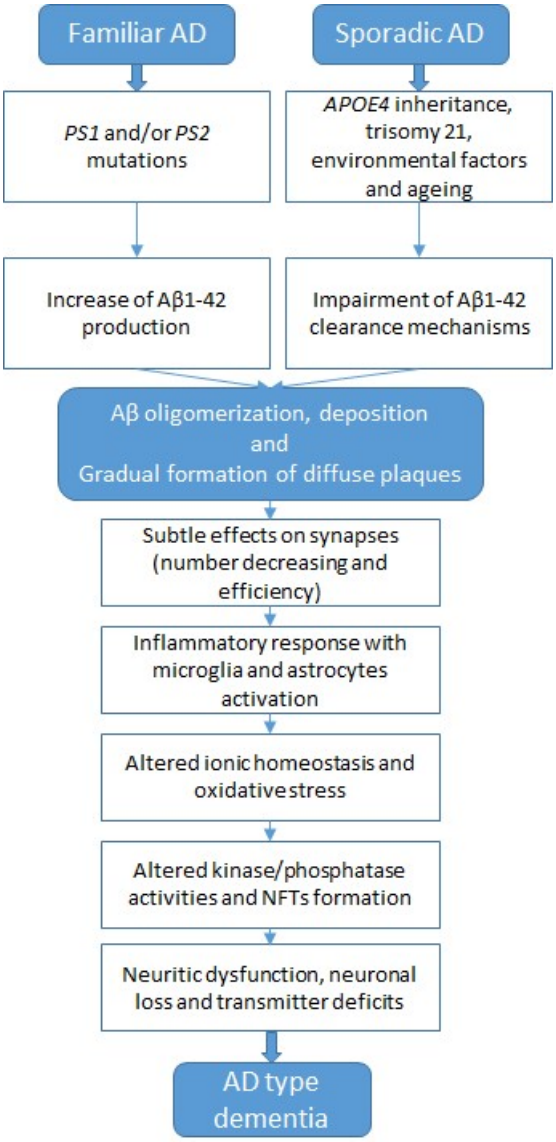

Figure 7. Schematic representation of the amyloid cascade hypothesis and the major pathogenic events leading to Alzheimer's disease. Adapted from [149]. Aβ: Amyloid beta peptide; AD: Alzheimer's disease; *APOE4*: Apolipoprotein allele 4; NFT: Neurofibrillary tangle; *PS1/2*: *Presenilin 1 or 2* genes.

2.5. Neurochemical dementia diagnostics in Alzheimer's disease

As already mentioned, AD neuropathological alterations begin several years before onset of symptoms and AD clinical diagnostic [150, 151]. During the preclinical AD stage, pathological alterations start in the medial temporal lobe and extend to neocortex [152, 153]. Then, AD can evolve to a prodromal stage, with mild symptoms presentation, and to the symptomatic stage characterized by dementia. Dementia is sometimes preceded by the mild cognitive impairment stage (MCI) which includes memory impairment [154].

A conclusive AD diagnosis based on clinical symptoms is particular difficult in early stages. In the last few years, efforts have been made to identify new biomarkers to enhance accuracy of AD diagnosis [155, 156]. The neurochemical based dementia diagnostic (NDD) is particular useful, since it allows to distinguish AD from other forms of dementia [157].

Not surprisingly, Tau, Tau hyperphosphorylated form and Aβ1-42 were the first three biomarkers, identified in cerebrospinal fluid (CSF) [66], and nowadays, these are yet the most established in AD neurochemical diagnostic. Decreased levels of Aβ1-42 in CSF of AD patients were identified by various groups [158, 159]. A decrease in Aβ1-42 was also identified in patients with Creutzfeldt-Jakob disease [160] and in cases of bacterial meningitis [161]. Thus, the use of these biomarker in combination with other biomarkers will increase AD diagnostics sensitivity and specificity. Levels of Aβ1-42 in CSF permitted to distinguish AD patients from control non-dementia patients, with sensitivities and specificities around 80% [159, 162, 163]. In addition to Aβ1-42, several other peptides were found abundant in CSF: Aβ1-37, Aβ1-38, Aβ1-39 and Aβ1-40 oxidized form, and indeed concentrations of Aβ1-38 and Aβ1-40 oxidized peptides were increased in AD patients [164, 165]. Hence other APP fragments in CSF are being explored as potential AD biomarkers. It was already reported increased CSF levels of sAPPα and sAPPβ in AD and MCI-AD with a sensitivity of 75% when compared with controls, also showing their potential as biomarkers [166].

Various studies supported the use of Tau CSF levels as a biomarker as it could predict AD with sensitivities of 81% and specificities of 92% [167, 168]. Increased levels of CSF Tau were also found in other dementias such as vascular dementia and frontotemporal dementia [169, 170], but the concentration values of phosphorylated forms of Tau (p-Tau) in CSF are specifically related to AD. In particular, increased levels of p-Tau 181 were found in CSF of AD patients [171], similarly

p-Tau 199 and p-Tau 231 increased levels were identified as putative biomarkers for AD diagnosis [172, 173].

Diagnostic biomarkers combination will enhance AD diagnosis (Table 1). This diagnosis does not exclude the need for cognitive evaluation of the patients and of the use of imaging techniques. In addition to CSF neurochemical biomarkers, AD diagnostics should also include magnetic resonance imaging and other imaging biomarkers to enhance diagnosis accuracy [174].

Table 1. **Usefulness of combinatorial CSF neurochemical-based biomarkers**. AD: Alzheimer's disease; NAD: Non-Alzheimer's disease types of dementia; MCI: Mild cognitive impairment.

CSF Biomarkers combination	Diagnosis	Sensitivity	Specificity	Study
Aβ1-42 and total Tau	AD versus NAD	85%	58%	[162]
Tau and Aβ1-42/Aβ1-40	AD versus NAD	81%	87%	[175]
p-Tau 181 and Aβ1-42/Aβ1-38	AD versus NAD	94%	85%	[176]
Tau, p-Tau 181 and Aβ1-42	AD versus MCI	68%	97%	[177]
Aβ, Tau and p-Tau	AD versus controls	>80%	>80%	[178]

The CSF-based biomarkers are currently the gold standard to assist AD diagnosis, however, this involves a lumbar puncture, which brings some limitations, as an invasive procedure and as a screening tool. Hence, blood-based biomarkers are receiving increased attention, as they can be easily obtained, proportionate early diagnosis and better disease management. Blood has appropriate conditions to be a great source of biomarkers for AD: some brain-derived products circulate in the bloodstream due to direct contact with CSF, brain-derived products are predominantly release to blood-brain barrier rather than into the CSF and Aβ was detected in blood as result of Aβ clearance from the brain parenchyma [179, 180]. Several forms of Aβ (1-37,1-38, 1-39, 1-40, 1-42) were already identified in plasma and even a new form never found in CSF: Aβ2-40 [181]. Increased plasma levels of Aβ1-40 were found in individuals with higher risk to develop dementia and increased baseline concentrations of Aβ1-40 and Aβ1-42 for AD patients [182, 183]. [184]. In addition, an elderly cohort study showed the potential of plasma Aβ1-

42/Aβ1-40 ratios to identify elderly subjects at higher risk to develop mild cognitive impairment [185]. However, a decrease in plasma Aβ1-42 was reported for AD patients [186] and no differences were found between serum levels of AD Aβ1-42 of AD patients and healthy individuals [184]. In addition, low plasma Aβ1-42/Aβ1-40 ratios were identified in AD patients [187].

Furthermore, the interest of sAPPα and sAPPβ as blood-based biomarkers is increasing however studies are still scarce. Decreased levels of sAPPβ were already found in plasma of AD patients when compared with controls or frontotemporal dementia individuals however it were not identified significant differences for sAPPα levels [188].

Controversial data on the potential of Aβ and sAPP as blood based biomarkers reflects the need for additional studies and methodologies to validate their potential as peripheral biomarker candidates for AD.

3. Exosomes in Alzheimer's disease

Exosomes have a great potential due to their diversified content and for their presence in various body fluids. Exosomes became more recently to be explored in the context of neurodegenerative diseases, as Alzheimer's and Parkinson's diseases, as potential sources for biomarkers useful either for diagnostic or therapeutics without exclude their contribution to elucidate disease mechanisms. In AD, exosomes have been addressed to elucidate Aβ formation, the spreading of amyloidogenic proteins but also the role of tau into exosomes (Figure 8).

3.1. Exosomes carrying Aβ: Neuroprotection or neurotoxicity?

The exact role of exosomes in AD is unclear. It was shown that Aβ1-42 peptide was enriched in MVBs of neurons [189] and of different cell models [139] and that it could be secreted into the extracellular space via exosomes. Further, it was also observed an enrichment of the exosome marker Alix around small SPs and into large diffuse plaques in brains of post-mortem AD patients which suggests that Aβ release into exosomes can possibly contribute for plaque formation and the progression of the disease [139]. In addition, microglia surrounding SPs appears to play a role in neurodegeneration by secreting exosomes containing Aβ1-42 [190].

Besides full-length APP (flAPP) some APP metabolites were found to be carried by exosomes such as APP CTFs and AICD [191] however the involvement of exosomes in secretion of amyloidogenic species is not well clarified. Exosomes secreted by brain mice mimicking AD, exibited higher levels of flAPP and APP CTFs than wild type mice which suggest that AD enhances accumulation of these proteins into exosomes [192]. APP CTFs and Aβ secretion into exosomes can be a protective mechanism for cells, relieving toxicity, or alternatively, potentially harmful since the secretion of exosomes enriched with APP CTFs and Aβ can contribute to the formation of SPs and also for the spread of amylogenic material between cells [192]. In addition, it was also found Aβ species, CTFs and increased levels of sAPPα into exosomes secreted by a human cell line expressing wild type APP in γ-secretase inhibition conditions. These exosomes also contained BACE, PS1, PS2 and ADAM10 which suggests that APP can be cleaved into exosomes and not only at the PM [193].

Additional, Aβ1-40 binding, conformational changes and aggregation were determined to be favoured by high membrane curvatures, for example on exosomes, and high abundance of membrane proteins [194].

Higher levels of BACE-1, γ-secretase, sAPPβ, sAPPα, Aβ1-42, p-Tau 181 and p-Tau 396 were detected into exosomes derived of astrocytes AD patients. Levels of P-T181-Tau, P-S396-Tau and Aβ1-42 were also increased in neuronal exosomes derived from plasma of AD patients [195]. Moreover, it was demonstrated *in vitro* that Aβ induces neuronal death of astrocytes surrounding SPs [196]. These secreted exosomes can induce apoptosis in astrocytes not exposed Aβ by being taken up by these cells which might represent a new mechanism for apoptosis induction by Aβ [196].

Despite the harmful effects of exosomes in the spread of amylogenic substances some beneficial actions for exosomes can also be described. Neuronal exosomes were uptake by microglia, contributing for Aβ clearance from extracellular space [197]. Moreover, the clearance of Aβ promoted by secreted exosomes of activated microglia reduces the inflammation around senile plaques and APP transgenic mice injection of exosomes resulted in a reduction of Aβ levels and Aβ deposits which support that exosomes can capture Aβ [197]. In addition, it was observed that exosomes infusions can sequester Aβ peptides which is mediated by exosome surface proteins as cellular prion protein (PrP^C). This may neutralize synaptic plasticity dysfunctions normally induced by Aβ [198].

Some Aβ degrading enzymes were found into exosomes, highlight their beneficial role in AD. A part of insulin degrading enzyme (IDE), one of the proteases responsible for Aβ extracellular degradation, was found into secreted exosomes [199]. In addition, statins administration can enhance exosome secretion carrying IDE, contributing to Aβ clearance, however the mechanism is still unknown [200]. Neprilysin, another Aβ degrading enzyme, is also carried by exosomes and internalization of these lead to a reduction of extracellular and intracellular levels of Aβ [201].

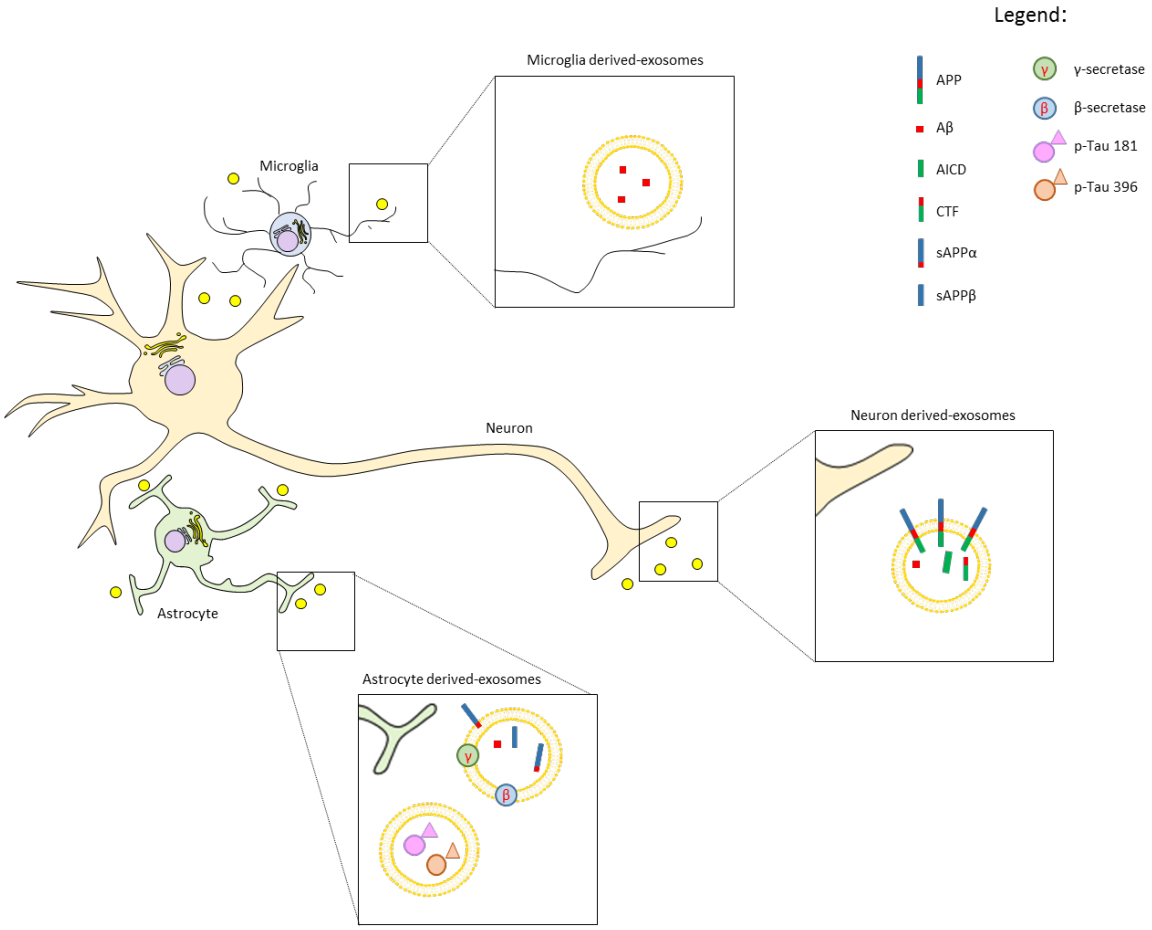

Figure 8. Content of AD nervous system cell-derived exosomes. Exosomes secreted by neurons, microglia and astrocytes contain several AD intermediators such as Aβ and sAPPα/β and enzymes involved in APP processing as γ- and β-secretases. APP: amyloid precursor protein; Aβ: amyloid beta peptide; AICD: APP intracellular domain; CTF: carboxy-terminal fragment; sAPP α/β: soluble amyloid precursor protein α/β; p-Tau: phosphorylated tau**.**

The potential of exosomes as a therapeutic approach is highly relevant and is favoured by the capacity of exosomes to cross the blood brain barrier [202–204]. Exosome mediated delivery of short interfering RNA (siRNA) to knock down beta secretase 1 (BACE1) enzyme is an example of the potential use of exosomes in this area. Exosomes can be a suitable tool for gene therapy by its capacity to deliver nucleic acids, specially targeted exosomes, which perform deliveries with good specificity [202]. As neuronal exosomes carry Aβ and contribute for amyloidogenesis it would be also of beneficity reduce exosome secretion. Inhibition of nSMase 2, the enzyme responsible for ceramide generation leads to a decrease of brain and serum exosome secretion, reduces SPs formation and neuronal apoptosis [205]. Moreover, this hypothesis is supported for further studies that observed an exosome secretion increase in serum of mice treated with ceramide [206]. It remains to be clarified if increased exosome secretion is in fact involved in SPs formation.

3.2. Tau and exosomes in AD

Tau species of 35-40 kDa were shown to be secreted into extracellular space by exosomes and Tau phosphorylated in threonine 181 was present in exosomes isolated from CSF of AD patients [207] or plasma neuron-derived exosomes [195]. It was suggested that oligomeric Tau species can be transported by exosomes and that this process could contribute to fibrillar formation in other cells [207]. Extracellular Tau truncated at C-terminal and lacking the microtubule binding region (MTBR) is the major Tau specie released by neurons to extracellular space and a minor portion of this specie can also be detected into exosomes [208].

Recently, it was observed that the depletion of microglia and inhibition of exosome secretion results in suppression of Tau propagation between neurons. Thus, microglia was hypothesized to contribute for Tau rapid spread, from entorhinal cortex to the dentate gyrus, by phagocytizing Tau and then secreting it into exosomes. This way, it emerges a new kind of transport for Tau that explains non-synaptic propagation [209].

Tau secretion into exosomes seems to correlate with a relevant pathogenic role in disease since exosomes can carry Tau forms that can act as seeds of Tau aggregation and misfolding in recipient cells, as exosome aggregated Tau and phosphorylated Tau [210].

Nonetheless, Tau secretion into exosomes is still controversial. Some research groups did not find Tau into exosomes released from SH-SY5Y [211], medium of cultured rat cortical neurons [212] and from various other cell lines and also body fluids [213].

3.3. Exosomes as biomarker resources in AD

Exosome potential as biomarker resources in AD have been addressed in various body fluids, especially in exosomes isolated from serum, plasma and CSF.

Elevated levels of blood exosomal p-Tau 396, p-Tau 181 and Aβ1-42 were observed in preclinical subjects up to 10 years before AD diagnosis and Aβ1-42 levels progressively increased from asymptomatic stage to AD diagnosis, which suggests its potential as a progression biomarker [214]. Levels of these three proteins could predict the development of AD before clinical diagnostic with a sensitivity of 96% [214]. As already mentioned, high levels of BACE1, γ-secretase, sAPPα and sAPPβ, Aβ1-42, p-Tau 396 and p-Tau 181 were found in plasma neuronal-derived exosomes from AD patients [195]. The p-Tau 181 protein was also found in exosomes derived from CSF of early AD patients [207].

Neuronal-derived plasma exosomes from AD patients exhibited distinct phosphorylation patterns of the adaptor protein receptor substrate 1 (IRS-1), in preclinical AD cases supporting its potential as an AD exosomal biomarker [215]. In fact, the brain tissues of AD individuals typically exhibit altered phosphorylation pattern of IRS-1 and IRS-2, mimicking insulin resistance [215]. Altered levels of diverse lysosomal proteins into plasma exosomes were also identified such as high levels of cathepsin D and LAMP-1 and lower levels of heat shock protein 70 (Hsp70) [216]. These different protein alterations were detected 10 years before AD being diagnosed and may be a result of lysosomal dysfunction observed in AD [216]. In addition, P-T181-Tau, P-S396-Tau, Aβ 1-42, neurogranin and RE1-Silencing Transcription factor were also identified as exosomal biomarkers with high sensitivity for distinction of controls from AD patients and evolution of MCI to AD [217].

Besides protein content, exosome genetic cargo might also represent novel biomarker candidates, special miRNA. Various neurodegenerative diseases as AD present altered miRNA expression patterns. A set of twenty miRNAs derived of from plasma exosomes were identified as potential biomarkers for AD [218]. Further, microRNA 193b was found into exosomes isolated from CSF of MCI or AD patients with stablished [219]. About 16 exosome miRNAs from serum were considered potential AD biomarkers, presenting high sensitivity (87%) and specificity (77%), and correlating age, sex and APOE4 allele status as risk factors to predict AD [220]. Recently, miRNA 34a was also identified as a potential target for AD therapeutics [221]. This miRNA is typically overexpressed in AD patients and AD transgenic mice and is known to regulate various

cellular processes as synaptic plasticity by repressing some pre-synaptic proteins and post-synaptic ion channel proteins and energy metabolism. The latter event may related with repression of some oxidative phosphorylation proteins expression, overall mitochondria activity and resting state network activity [221]. Neurons secrete exosomes with miRNA 34a which can contribute to AD progression, through impairment of resting state network activity and by worsening memory capacities due to dysregulation of many genes in brain neighbour cells [221]. Interestingly, ADAM 10 gene was also identified as a target for miRNA 34a, supporting that ADAM 10 gene decreased expression by miRNA 34a can increase Aβ secretion and contribute for AD progression [221]. Taken together data suggest that exosomes containing miRNA can be useful for AD diagnosis and therapeutic strategies.

Aims of the thesis

Exosomes are released by various cell types, are present in several biofluids [222–229] and participate either in physiological and pathological processes [197, 206, 230–232], thus represent a potential source for identification of novel AD biomarker candidates.

Nonetheless, exosome isolation from biofluids is still a challenge topic. The most used technique is differential centrifugation however has low recovery-rates, is time-consuming, is not fully reproducible between labs [233] and can compromise exosome integrity [49–51]. To overcome this issues the use of precipitation polymer-based reagents is increasing. The main advantages of these reagents are easy handling, good exosome yields and no need of special equipment. Column-based protocols are also very useful as provide exosome isolation with greater purity than precipitation-based methods [51, 234]. Therefore, the first aims of this thesis were to:

- Optimize and compare the performance of 3 commercial kits for exosome isolation from different body fluids (two exosome precipitation-based kits and one column-based method);
- Characterize exosome samples in terms of size, stability, morphology and particle yield.

After exosome isolation protocols optimization, the potential of exosomes as biomarker resources for AD was addressed by evaluating soluble APP forms in cognitive demented cases. The value of sAPP as biomarker as already been tested in CSF [166], plasma [188] and plasma derived-exosomes [195] but not in serum or serum-derived exosomes. Hence, the final goal of this thesis was to:

- Evaluate the potential of sAPPα and sAPPβ in serum and serum-derived exosomes in dementia cases.

Chapter 2. Exosome isolation from different biofluids

2.1. Materials and methods

Biofluids preparation

Serum, plasma were obtained from a pool of samples of normal individuals, and CSF from a pool including normal and patient cases. Blood samples were collected in EDTA tubes, centrifuged at 1800g during 15 min for plasma and centrifuged at 2000g during 15 min for serum. CSF was obtained by lumbar punction and centrifuged at 3000 rpm for 5 min. All samples were aliquoted and stored at -80ºC.

The study was approved by Ethics Committee for Health of the Central Regional Administration of Coimbra (CES da ARS Centro, protocol No. 012804-04.04.2012) and by the National Committee for Data Protection (Authorization Nº 369/2012).

Exosome isolation from serum and plasma

Exosomes were isolated using three commercial kits: Total Exosome Isolation from serum (Invitrogen) (TEI), ExoQuick Serum Exosome Precipitation Solution (System Biosciences) (ExoQ) and Exo-spin Blood Exosome Purification Kit (Cell guidance systems) (ExoS) (Figure 9).

TEI and ExoQ are exosome precipitation kits based on the use of water-excluding polymers as polyethylene glycol. These polymers bind water molecules leading to the exclusion of less soluble components. Prior to sample incubation with polymers, the biofluid is centrifuged to remove cells and some subcellular components. After incubation at 4ºC with polymer reagents, the mixture is centrifuged at low-speed [50, 51].

ExoS is a column-base method which comprises a precipitation-step followed by exosome sample purification by SEC. In this method, it is used a column coated with porous polymeric beads containing ciliated micropillars. Components with lower hydrodynamic diameters (about 40 to 100 nm) are retained and take more time to pass through wired area. Higher particles elute first as they are not retained in nanocilia pores [50, 51].

All exosome isolations were prepared according to manufacturer's instructions with minor modifications (Figure 9). For all cases, exosome isolation was carried out in triplicate. Exosome purification from TEI and ExoQ was carried out from a starting volume of 250 µl of

serum and plasma, except for plasma isolation using ExoS that was performed from a starting volume of 200 µl, as recommended by the manufacturer.

After all exosome isolation procedures, exosome suspensions were divided in half into two tubes. To one part, 100 µl RIPA buffer (Sigma-Aldrich) was added to lysis exosomes and samples prepared for Western blot. The other part remained in PBS for size, stability and particle quantification analysis. Exosome suspensions were freeze at -20ºC, except for transmission electron microscopy (TEM) procedure as new fresh exosome samples were prepared.

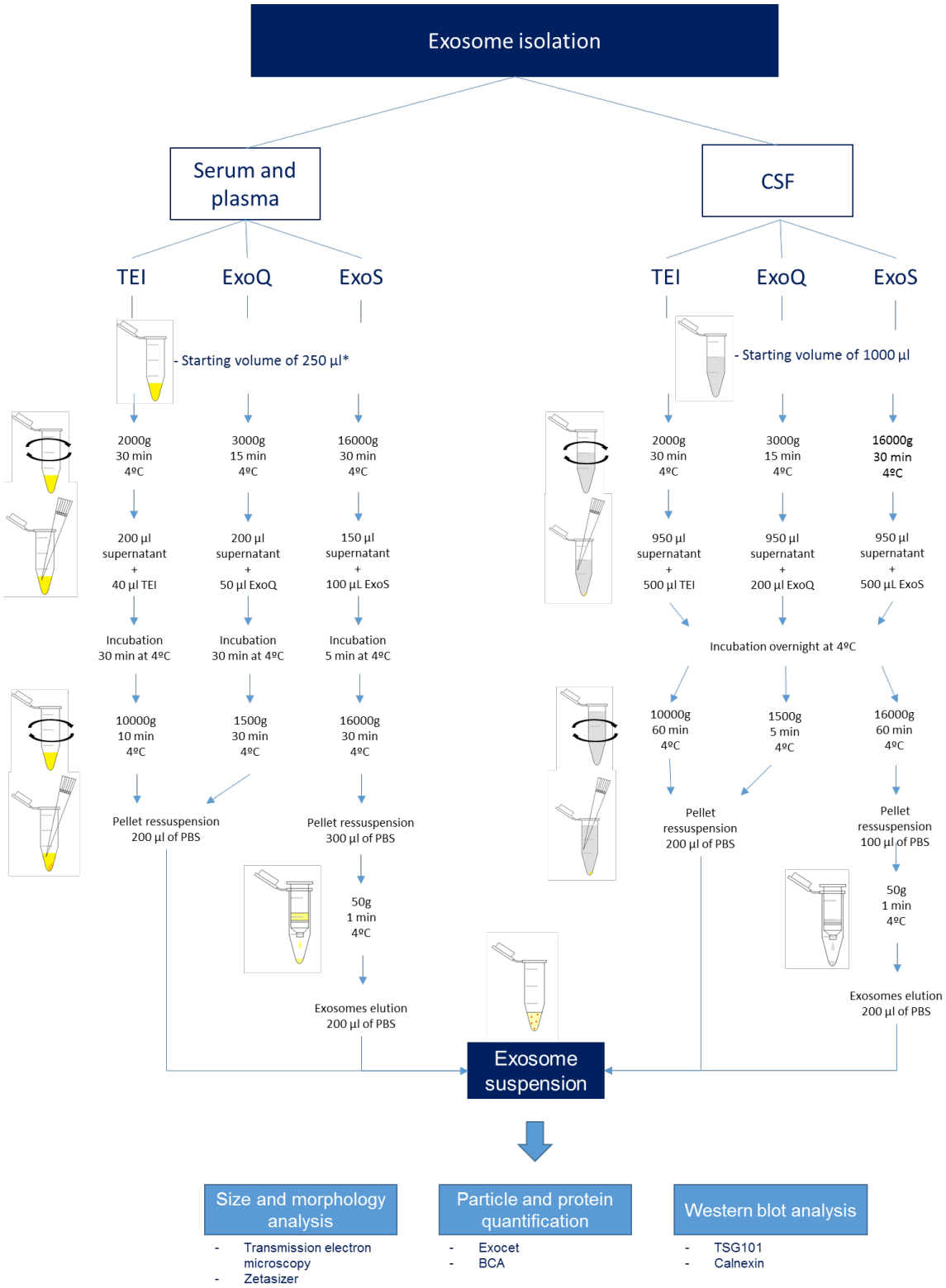

Figure 9. Exosome isolation workflow. Serum and Plasma derived exosomes were isolated using precipitation-based reagents Total Exosome Isolation from serum (Invitrogen) (TEI) and Exoquick Serum Exosome Precipitation Solution (ExoQ) and the column-based method Exo-Spin Blood Exosome Purification kit (ExoS). *The starting volume for plasma exosome isolation using ExoS was 200 µl as recommended by manufacturer. Exosome extraction from pooled CSF was also performed using equivalent methods.

Exosome isolation from CSF

Exosome isolation from CSF was performed using Total Exosome Isolation from cell culture media (Invitrogen) (TEI), ExoQuick-TC exosome precipitation solution (System Biosciences) (ExoQ) and Exo-spin Exosome Purification Kit for cell culture media/urine/saliva and other low-protein biological fluids (Cell guidance systems) (ExoS). All exosome isolations were performed in triplicate. Exosome isolations were performed according to manufacturer instructions with some minor modifications (Figure 9). For all cases, a starting volume of 1 ml of pooled CSF was used.

All exosome suspensions were divided in half into two tubes after exosome isolation procedures as already described for serum and plasma exosome suspensions. Finally, exosome samples were freeze at -20ºC, except for TEM as described above.

Exosomes size distribution and zeta potential analysis

To evaluate particle size and stability of exosomes in solution, dynamic light scattering and Zeta Potential measurements were performed using Zetasizer Nano ZS (Malvern Instruments, Paralab, Portugal) and Zetasizer software 7.12.

Dynamic light scattering (DLS) is a wide use method to measure the size of particles and molecules in suspension. When light hits in a particle, the light scatter in all directions as result of the interaction between light and the electric field of the particle. However, the scattering intensity of a particle is not constant since these moves in random way (Brownian motion) in solution. Therefore, DLS measures the speed of Brownian motion of particles. The speed of Browian motion is influenced by size of particles, viscosity and temperature. Smaller particles have a fastest Browian motion and larger ones have slower motions. These speeds are then converted in particle size by Stokes-Einstein equation. The particle size determined by DLS corresponds to the hydrodynamic diameter which depends of particle size, particle surface structure and the presence of ions in the solution [235–237].

To measure particle sizes and determine zeta potential, exosome suspensions were diluted at 1:1000 in ultrapure water and sonicated during 10 min in a water-bath at room temperature (RT). Sonication was performed to reduce exosome aggregation which influences size measurements by DLS. For each exosome sample three measurements (technical replicates)

were carried out for all experimental replicate. The following settings were used: Refractive Index = 1.330, viscosity = 0.887, temperature = 25ºC.

Transmission electron microscopy

Nano-sized particles as exosomes are outside optical microscopy resolution. Therefore, electron microscopy is the optimal choice since it can achieve resolutions in the order of few angstrom, allowing to study ultrastructure of organelles, for example. Instead of using a light source like optical microscopy, electron microscopy uses a cathode as an electron source. Tungsten filaments when heated at vacuum emit electrons at a constant accelerating voltage, so these filaments are widely used as electron sources. Then, electron beam is focused in a thin beam by condenser electromagnetic lens in the plane of specimen or very near. In transmission electron microscopy, the electron beam crosses the specimen despite some electrons are scattered, also depending of specimen density. Electron beam that crossed the specimen then crosses electromagnetic objectives lens and multiple electromagnetic lenses, to focus and magnify the virtual image. Finally, the beam hit a fluorescent screen where electrons are converted to light and the image collected by a charge-coupled device (CCD) camera [238–240]. To obtain high contrasted images negative staining is a god choice. It is based on deposition of heavy metals contained in a staining solution. Instead of binding to the specimen, heavy metals are deposited around the sample creating “shadow” zones [239].

Freshly exosome isolations were performed for TEM visualization as described above with minor modifications. For serum, plasma and CSF samples isolated using ExoQ and TEI the exosome pellet was directly fixed in 200 µl of 2% paraformaldehyde. For exosome isolations derived from serum, plasma and CSF isolated using ExoS exosomes were eluted in 100 µl of PBS and then mixed with 100 µl of 4% paraformaldehyde to a final concentration of 2% paraformaldehyde. In all cases, exosome suspensions of 20 µl were allowed to adsorb in 75 mesh Formvar/carbon coated grid (01802-F; Ted Pella), for 30 min, at RT. Grids were then washed with PBS (membrane side faced down) and dried using filter paper. For negative staining, exosome-grids were transferred to a 50 µl drop of 3% phosphotungstic acid solution (pH 7) for 10 min and then wicked off with filter paper. TEM visualizations were performed using Hitachi H-9000 transmission electron microscope at 300 kV and images were captured using a slow-scan CCD camera.

Exosome yield analysis

To estimate exosome number, the colorimetric EXOCET assay (System Biosciences) was performed. It is based in the measurement of the enriched activity of Acetyl-CoA Acetylcholinesterase activity in exosomes [241]. A volume of 10 µl of exosomes suspensions in PBS were diluted each in 90 µl of lysis buffer. To address if the buffer interferes with the assay 10 µl of PBS were diluted also in 90 µl of lysis buffer. Then, mixtures were incubated at 37ºC for 5 min, vortexed and centrifuged at 1500g at RT during 5 min to remove debris. Afterwards, 50 µl of test sample was mixed with 50 µl of reaction buffer. Following 20 min of incubation at RT the absorbance of plate was read at 405 nm, using TECAN Infinite M200. The standard curve was created by plotting absorbance by number of exosomes.

Protein quantification

Protein quantification of all exosome suspensions was performed by colorimetric bicinchoninic acid protein assay, using Pierce™ BCA Protein Assay kit (Thermo Fisher Scientific). BCA assay is based on the biuret reaction which consists in the capacity of amino acids to complex with cupric ions in an alkaline environment, producing a blue light. Then, BCA reacts with cuprous cations producing a strong violet light, whose intensity is proportional to the number of peptide bonds and can be measured at 562 nm.

Prior to protein quantification, exosome samples ressuspended in PBS were lysed by adding a half volume of RIPA buffer (Sigma Aldrich) with cOmplete, Mini, EDTA-free Protease Inhibitor Cocktail (Roche) and incubated at RT for 5 min. All samples were sonicated for 15 seconds. Samples of 2 µl of serum-derived exosomes or plasma-derives exosomes and 5 µl of CSF-derived exosomes were quantified by BCA assay. Samples and standards were homogenised with buffers (PBS and RIPA) (Table 2) and further incubated with 200 µl of working reagent prepared in the proportion of 50 parts of reagent A to 1 part of reagent B. The plate was incubated at 37ºC for 30 min and the absorbance of BCA assay was measured at 562 nm using TECAN Infinite M200.

Table 2. Standards used in BCA protein assay. BSA: Bovine serum albumin (2 mg/ml).

Standard	BSA (µl)	Buffer (µl)	Protein mass (µg)
P0	0	50	0
P1	1	49	2
P2	2	48	4
P3	5	45	10
P4	10	40	20
P5	20	30	40

SDS-PAGE

Sodium dodecyl sulphate polyacrylamide gel electrophoresis (SDS-PAGE) is the most used method to separate proteins from a mixture, based in protein molecular weight and charge. Proteins are separated through migration across gel pores when an electric field is applied. As different proteins contain different charges what would interfere in the running, SDS is applied to confer a negative charge to all proteins. One molecule of SDS can bind to two amino acid residues. Therefore, all proteins can migrate from negative to positive anode. Typically, before loading in the gel, samples are heated for few minutes with a reducing agent, as β-mercaptoethanol. These reagents cleave disulphide bonds to disrupt tertiary and quaternary protein structures, ensuring protein linearization and equal protein migration in the gel, independently of three-dimensional structure.

For serum and plasma-derived exosome samples 50 µg of protein were loaded on the gel however for CSF samples a total volume of 100 µl was loaded since BCA quantifications for these samples were near zero. Samples were boiled at 99ºC for 5 min, loaded and separated in a 5-20% SDS-PAGE gradient gel, at constant 90 mV for about 2 to 3 hours, in Hoefer SE 600 electrophoresis system. The protein marker Precision Plus Protein Dual Colour Standards (1610374; Bio-Rad) was used.

Western blotting

Western blotting is a powerful technique to detect specific proteins with specific antibodies after proteins were separated according to their size and transferred to a solid support membrane, for example made of nitrocellulose. In the electrophoretic transference proteins become immobilized at respective migration positions where the gel was stopped to run. Proteins

were electrophoretic transferred to a nitrocellulose membranes in a wet system for 18h and at 200 mA. After transference, the membrane could dry at room temperature. Transfer was further confirmed using Ponceau staining solution which is a red stain dissolved in an acidic solution. Ponceau S bounds to protein positive amino acids and to non-polar protein regions in a non-covalent form. The membrane was hydrated with Tris-buffered saline solution (TBS) during 10 min with agitation and, then, ponceau staining solution was applied during 5 min with agitation. After this incubation, the solution was removed and the membrane was washed with deionized H_2O to remove the excess of ponceau solution.

For immunodetection, after total Ponceau removal, membranes were blocked in 5% non-fat dry milk in 1x TBS-T (0.5% Tween-20), at RT during 4 hours, to reduce non-specific binding of antibodies. Following, membranes were incubated with primary antibodies mouse anti-TSG101 (1:1000) (612697; BD transduction laboratories), raised against TSG101 amino acids 229-319, and polyclonal antibody rabbit anti-Calnexin (1:200) (SPA-860; StressGene), used to detect the C-terminal conserved region of calnexin. Primary antibodies for TSG101 and calnexin were incubated for 4h and overnight, respectively. Indirect detection was performed with secondary antibodies Amersham ECL Mouse IgG, HRP-linked (1:10000; GE Healthcare Life Sciences) and Amersham ECL Rabbit IgG, HRP-linked (1:5000; GE Healthcare Life Sciences). These were incubated during 2h, with agitation and at RT. Between primary and secondary antibody incubation and after secondary antibody, membranes were four times washed with 1x TBS-T (0.5% Tween-20). Protein bands were detected using the chemiluminescence reagent Amersham ECL Select Western Blotting Detection Reagent (GE Healthcare Life Sciences) and autoradiography Amersham Hyperfilm ECL (GE Healthcare Life Sciences). Enhanced chemiluminescence (ECL) reagent is based in luminol substrate oxidation by HRP, generating chemiluminescence at 425 nm. The emitted light is directly proportional to the amount of protein.

Statistical analysis

Statistical analysis was carried out with two-tailed Student's t-test for assess differences between each exosome isolation. Only p-values less or equal to 0.05 were considered significant. In graphs, error bars represent standard deviation of three independent experiments. Analysis were performed using GraphPad Prism 7 (GraphPad Software, La Jolla, California, USA).

2.2. Results

Exosomes size analysis and zeta potential

Exosomes were isolated from different body fluids (serum, plasma and CSF) using three commercial kits, two precipitation-based reagents (TEI and ExoQ) and one colum-based kit (ExoS). After exosomal isolations samples were characterized using different methods.

Zetasizer Nano ZS based on DLS was used to assess the size of exosomes isolated from serum, plasma and CSF, using TEI, ExoQ and ExoS. All kits resulted in nanoparticle isolation within the expected size range of exosomes (30-150 nm) and samples had in general a good polydispersity index (between 0.08 and 0.70) (PDI) which indicates that nanoparticle populations are highly homogeneous (Figure 10 and Table 3).

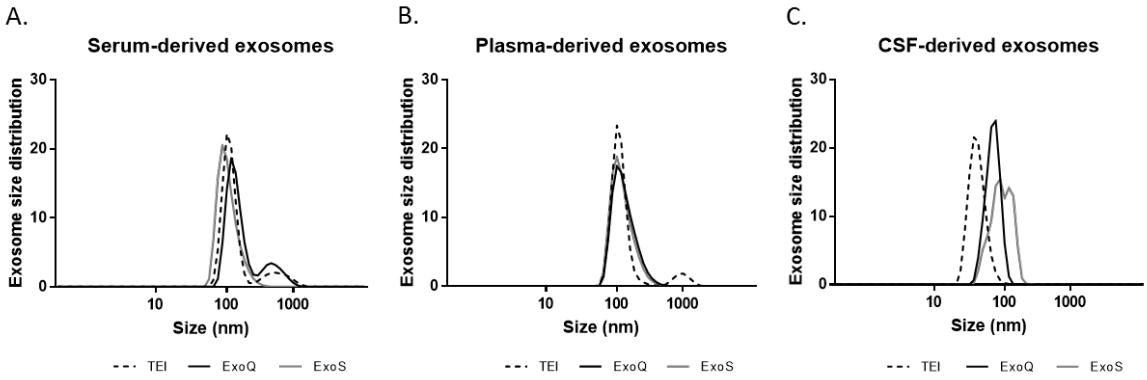

Figure 10. Size distribution of exosome samples derived from serum (A), plasma (B) and CSF (C) obtained through Zetasizer analysis. Each curve represents the average of at least 3 independent sample measurements for each corresponding exosome isolation method.

Considering serum exosome isolations, ExoS shown a homogenous population of vesicles with an average peak at 114.31±43.81 nm (only around 8% of vesicles exhibited a larger size than exosomes). Exosomes isolated with ExoQ and TEI also presented a greater intensity peek within exosome size range, 138.73±37.23 and 117.02±26.86 nm, respectively (Figure 10A and Table 3). In both cases an additional peak outside exosome size range was observed for about 18% of exosomes isolated with TEI and 31% of exosomes isolated with ExoQ. The existence of peaks that do not fit into exosome size range can be explained by nanoparticles aggregation but also due to

the fact that DLS analysis can show larger nanoparticle sizes as it measures hydrodynamic diameter of particles in movement. TEM analysis did not identified vesicles of larger proportions for any of the exosome preparations (Figure 11). In addition, all kits showed modes for diameters near 100 nm (Table 3). Plasma nanoparticles isolated with ExoQ and ExoS shown homogeneous populations with mean peaks of 138.73±37.23 and 114.31±43.81 nm, respectively, with 21% and 16% of particles, broadly distributed. Similar to serum, TEI zetasizer analysis revealed two peaks, as expected a greater one with nanoparticles within the diameter of 112.91±23.37 nm (12.8% of nanoparticles with larger diameters) (Figure 10B and Table 3). Modes of the nanoparticle size isolated from plasma with kits were around 105.7 nm for all. Nanoparticle isolated from CSF with the three kits were smaller than nanoparticles isolated from plasma and serum, although diameter peaks were unique and the exosome range as the corresponding modes; only about 1% of vesicles were outside the range for vesicles isolated with ExoS (Figure 10C and Table 3). It is important to refer that exosomes isolated from CSF with ExoS had a PDI of 0.82, which indicates a broad distribution of nanoparticles sizes (heterogenous population). No significant differences ($p \leq 0.05$) were found between particle diameter mean peaks of the various kits, for exosome preparations from serum and plasma, although differences could be detected for exosomes isolated from CSF. Moreover, TEM analysis (Figure 11) revealed spherical vesicles, with the expected exosome morphology and sizes, although for all samples microvesicles of smaller size than exosomes could also be observed.

Table 3. Complete characterization of exosome size distribution of exosomes isolated from serum, plasma and CSF. PDI: polydispersity index.

		Exosome isolation method		
		TEI	ExoQ	ExoS
Serum	Peak 1 (nm)±SD	117,02±26,86	138,73±37,23	114,31±43,81
	Peak 2 (nm)±SD	540,80±270,90	408,59±209,37	-
	Mode (nm)	105,70	122,40	91,28
	PDI (±SD)	0,41±0,05	0,27±0,07	0,22±0,09
Plasma	Peak 1 (nm)±SD	112,91±23,37	138,73±37,23	114,31±43,81
	Peak 2 (nm)±SD	925,38±266,78	-	-
	Mode (nm)	105,7	105,7	105,7
	PDI (±SD)	0,36±0,15	0,28±0,03	0,19±0,02
CSF	Peak 1 (nm)±SD	44,15±12,97	72,95±16,90	100,01±33,94
	Peak 2 (nm)±SD	-	-	-
	Mode (nm)	43,82	91,28	105,7
	PDI (±SD)	0,60±0,34	0,67±0,29	0,82±0,31

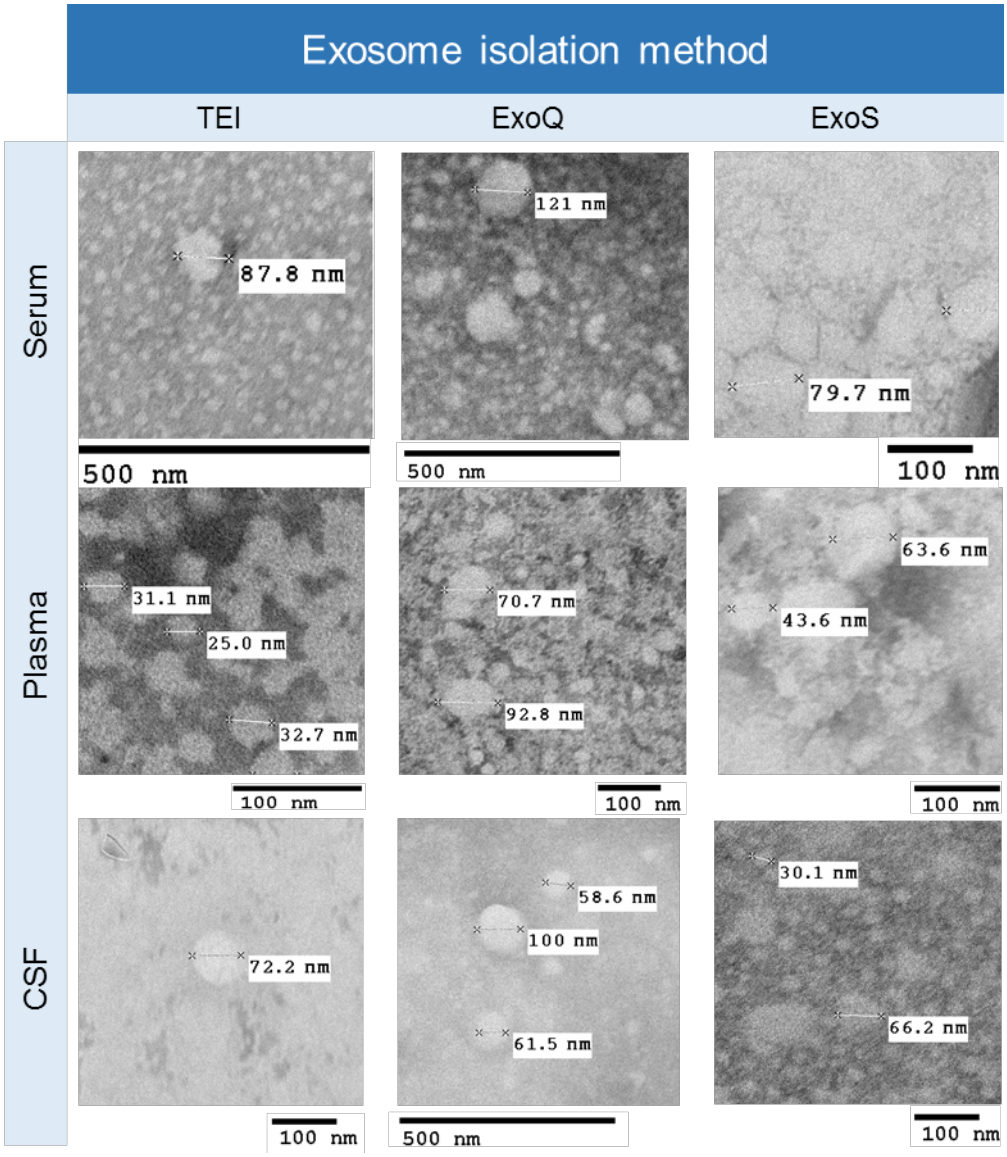

Figure 11. Morphological characterization of exosome samples by TEM negative staining. Scale bars are in scale with each corresponding image.

Zeta potentials of all exosome samples are distributed within the range of -6.11 to -20.8 mV (Figure 12) and the analysis shown that the stability of samples is distinct depending on with the exosome isolation method used, either in serum or plasma. In serum, samples isolated with ExoQ and TEI were appropriately stable (zeta potential ≤-10 mV) and significant differences were found between zeta potentials obtained among TEI and ExoS ($p \leq 0.01$) and also between ExoQ and ExoS ($p \leq 0.05$). Plasma exosomes isolated with ExoQ were properly stable in contrast with the other plasma derived-exosomes samples ($p \leq 0.01$). All CSF exosome samples had zeta potential values bellow or near -10 mV without differences between the three methods (Figure 12).

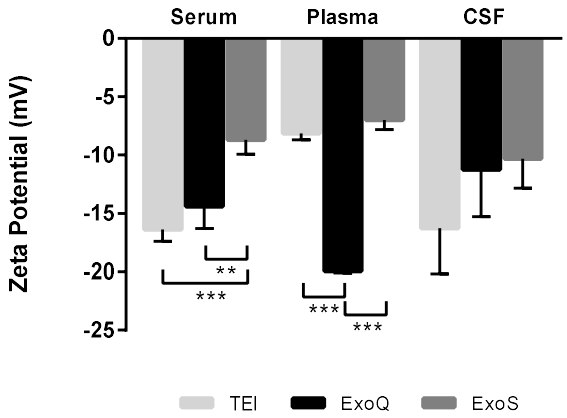

Figure 12. Zeta potential evaluation of serum, plasma and CSF-derived exosome samples. Each bar represents mean values of zeta potential (n=3) and error bars shows standard deviations. **p≤0.05; ***p≤0.01

Exosome quantification

The number of particles isolated from serum and plasma were determined by EXOCET assay. Significant differences were obtained for the three commercial kits (Figure 13). In serum, both ExoS and ExoQ isolated the highest number of particles, significantly about 2.0-fold more particles than TEI ($p \leq 0.01$ and $p \leq 0.05$, respectively). No differences were observed among ExoQ and ExoS serum exosome concentration. Following a similar pattern, for plasma, ExoQ and ExoS isolated about 2.5-fold more exosomes than TEI ($p \leq 0.01$ for both), but the performance of ExoQ and ExoS was not significantly different. In the case of CSF this method failed to quantify the number of particles, most probably due to decreased exosome concentrations obtained from 1 ml of this biofluid.

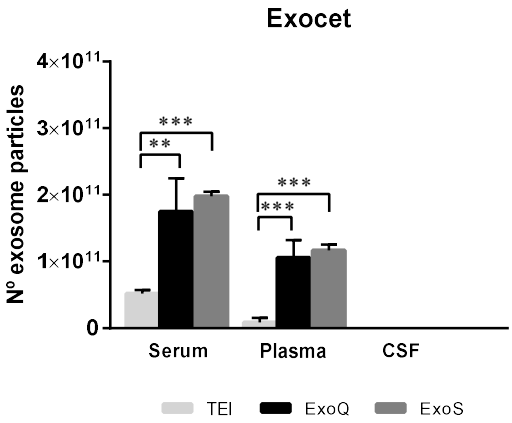

Figure 13. Quantification of exosomes isolated from serum, plasma and CSF with the various isolation methods, using EXOCET assay. Each bar represents mean number of exosomes isolated (n=3) and error bars shows standard deviations. **p≤0.05; ***p≤0.01

Protein concentration in exosome samples

The amount of protein concentration in exosome preparations was measured using BCA. For serum derived-exosomes, ExoQ was the kit that gives to the highest protein concentration although no significant differences were observed among kits (Figure 14). In plasma exosome samples, the three kits exhibited significant differences amounts of protein. ExoQ was the kit with best performance, isolating about more 1.3-fold proteins than TEI (p≤0.01) and 2.3-fold more proteins than ExoS (p≤0.01). Consistent with EXOCET results, the total protein concentration from CSF exosomal samples was unable to be detected using this method.

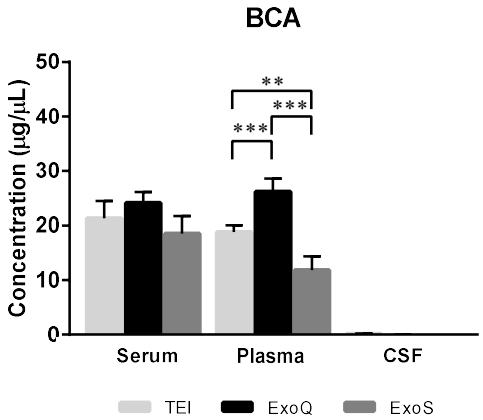

Figure 14. Protein concentration analysis of exosome samples. Protein concentration was determined using BCA. Each bar represents mean values of total protein concentration (n=3) and error bars shows standard deviations. **p≤0.05; ***p≤0.01

To address sample purity, the number of particles isolated from serum and plasma was normalized to protein concentration obtained by BCA assay (Figure 15). The total CSF was not considered due to protein concentrations near zero. Results obtained were different for serum and plasma preparations. In serum-derived exosomes, ExoS had the highest ratio between the number of exosomes isolated and total the protein concentration, 2.5-fold higher comparatively to TEI ($p \leq 0.01$) and 1.3-fold higher than ExoQ, while ExoQ ratio was 1.9-fold higher than TEI ($p \leq 0.01$). ExoS higher ratios were highlighted in plasma-derived exosome samples; about 4-fold higher than TEI ($p \leq 0.01$) and 2-fold higher than ExoQ ($p \leq 0.01$). Data suggests that ExoS is the purest method.

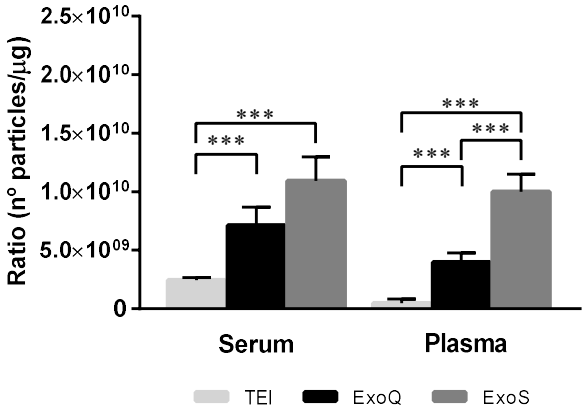

Figure 15. Normalization of particle numbers per protein concentration measured by BCA assay. Each bar represents mean values (n=3) and error bars shows standard deviations. ***p≤0.01

Western blot

Western blot analysis aimed to validate the nature of exosomal samples and to find possible differences in performances of the different methods used for exosome isolation. Analysis revealed the presence of exosome marker TSG101 and the absence of Calnexin (Figure 16), the later discards cell contamination of exosomal samples as it was expected. Similar enriched levels of TSG101 marker was observed in exosome samples isolated with precipitation-based reagents (TEI and ExoQ), comparatively to ExoS.

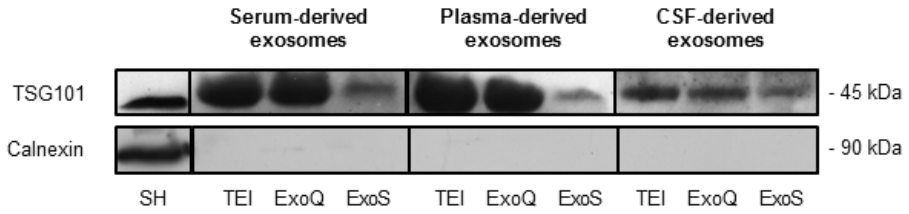

Figure 16. Western blot analysis for TSG101 and calnexin in serum, plasma and CSF exosome samples isolated with the three commercial kits. SH-SY5Y cell lysates were used as a control sample.

Chapter 3. sAPP as potential exosomal diagnostic biomarker for AD

3.1. Materials and methods

Participants and sample collection

Samples used in this study were from individuals enrolled in a primary care based cohort (pcb-cohort) from the Aveiro region, described in [242]. All volunteers provided written informed consent for the cohort study. The study was approved by Ethics Committee for Health of the Central Regional Administration of Coimbra (CES da ARS Centro, protocol No. 012804-04.04.2012) and by the National Committee for Data Protection (Authorization Nº 369/2012). Serum samples were collected in EDTA tubes, centrifuged at 2000g during 15 min, aliquoted and immediately frozen at -80ºC. The study group included thirty-two patients (n=32) with Clinical Dementia Rating (CDR) scores ≥ 1 and thirty-two sex-age matched healthy individuals (n=32) controls. CDR scale evaluates the cognitive and functional performance through six domains: memory, orientation, judgment and problem solving, community affairs, home, hobbies and personal care [243]. These domains were assessed by an interview in primary care units [242]. Scale is classified as following: normal=0, mild dementia=1, moderate dementia=2 and severe dementia=3. From the study group, 7 individuals were clinical diagnosed as AD patients. Table 4 show the characteristics (age, gender, and CDR scale) of individuals with cognitive deficits and controls enroled in the study. Individuals with cognitive deficits have mean (±SD) ages not significantly different from age-sex matched controls.

Table 4. Characteristics of individuals with cognitive deficits and healthy controls.

	Cases				Controls		
CDR scale	**Nº of individuals**	**Gender (M/F)**	**Ages (mean)±SD**	**CDR scale**	**Number of individuals**	**Gender (M/F)**	**Age (mean) ±SD**
CDR= 1 (Mild dementia)	10	4/6	70.60±11.06	**CDR=0**	10	4/6	70.50±10.89
CDR=2 (Moderate dementia)	10	4/6	80.40±6.88	**CDR=0**	10	4/6	80.40±6.31
CDR=3 (Severe dementia)	5	1/4	84.60±5.59	**CDR=0**	5	1/4	83.00±4.18
AD cases	7	1/6	77.54±4.89	**CDR=0**	7	1/6	77.14±4.67

Exosome isolations from serum

Exosomes were isolated from cases, age and sex-matched controls using the precipitation-based reagent ExoQuick Serum Exosome Precipitation Solution (System Biosciences) (ExoQ) according to manufacturer's instructions with minor modifications. Exosome purification was carried out from a starting volume of 250 µl of serum. Samples were centrifuged at 3000g for 15 min at 4ºC, 200 µl of resulting supernatant were mixed with 50 µl of ExoQ solution and incubated at 4ºC during 30 min. Supernatant was discarded, samples centrifuged again at 1500g for 5 min and exosome pellet ressuspended in 200 µl of RIPA buffer (Sigma-Aldrich) plus protein inhibitors (Roche). To ensure sample for all subsequently procedure, exosome isolations from each sample were carried out in triplicated, pooled and frozen at -20ºC.

sAPPα and sAPPβ ELISA assay using serum and serum-derived exosomes

The sAPPα levels were monitored using Human sAPPα ELISA Assay (IBL; 27734) and Human sAPPβ wild type ELISA Assay (IBL; 27732). Both kits are direct sandwich solid phase ELISA. ELISA assays are powerful quantitative immunoassays to detect and quantify a specific protein in a mixture. ELISA assays are very sensitive, in this particular case can detect low amounts of sAPPα as 0.78 to 50 ng/mL.

The first step of direct sandwich solid phase ELISA is based on the passively attachment of antibodies to a solid phase and antigen capture by coated antibodies. Washes performed after this step aim to remove unbounded antigens and then conjugated antibodies specific to antigen and labelled with enzymes are added and allowed to incubate for a period of time. Then, next washes were again performed, this time to remove the unbounded conjugated antibodies. Further, the chromogen/substrate is added and enzymatic catalysis results in colour development. This reaction is stopped within some minutes by adding a stop solution that usually changes the pH. The final colour is then quantified at appropriate wavelength, in this case at 450 nm.

Serum or serum-derived exosome samples from 32 individuals with CDR≥1 and respective controls were tested for sAPPα and sAPPβ. The assay was performed from a starting volume of 100 µl of serum or serum-derived exosome sample (isolated as described above). The standard samples were prepared out according to manufacturer instructions, performing serial dilutions. About 100 µl of diluted standard, serum or exosome sample could adsorb overnight at 4ºC, in

appropriate pre-coated wells with a specific antibody to sAPPα or sAPPβ. Following incubation, each well was washed at least 7 times with the 100 µl of recommended wash buffer before the addition of Horseradish Peroxidase conjugated Anti-human APP (R101A4) Mouse IgG MoAb Fab'. The antibody (100 µl per well) was incubated 30 minutes at 4ºC and then plate was washed at least 9 times with 100 µl of buffer. Further, 100 µl of chromogen solution containing the horseradish peroxidase (HRP) substrate TMB (3,3',5,5,-tetramethylbenzidine) was added, and plate incubated during 30 min and at RT, in the dark. In the presence of HRP enzyme, the substrate TMB is converted to a blue colour. The reaction is stopped by the addition of a solution of sulfuric acid (in this case 100 µl per well), leading to colour change to yellow and stabilization for further read of absorbance at 450 nm. Standard curve was prepared according to datasheet instructions with plotting of ELISA standard absorbance against sAPPα or sAPPβ concentrations to determine the concentration of sAPPα or sAPPβ of each serum or exosome sample. A blank sample of RIPA buffer with protease cocktail inhibitors of 100 µl was used as control to test if the buffer interfere with the procedure.

EXOCET assay

The enzymatic colorimetric EXOCET assay was performed to determine the number of exosomes in serum-derived exosome preparations from all individuals in the study group. A starting volume of 10 µl of each exosome sample in RIPA buffer was diluted with 90 µl of lysis buffer. The mixture was incubated at 37ºC for 5 min for exosome lysis, vortexed and centrifuged at 1500g during 5 min to remove general debris. Further, 50 µl of the test sample previously prepared was mixed with 50 µl of reaction buffer and added to each well. After 20 min of incubation at RT the absorbance of plate was read at 405 nm. The standard curve was created by plotting absorbance by number of exosomes, as described by manufacturer.

NCAM1 ELISA assay

The NCAM1 (CD56) ELISA assay (abcam; ab119587) was used as a neuronal exosome marker. NCAM is a neural cell adhesion molecule is expressed mainly at cell membrane of neurons and is involved in neuronal adhesion, neurite outgrowth and synaptic plasticity. This protein was also identified in neuronal exosomes. This direct sandwich ELISA assay was performed for all serum-derived exosomal samples from the study group. A starting volume of 100 µl was

used for test samples and standards (serial dilutions) and could adsorb in the precoated plate during 90 min at 37ºC, with a specific goat polyclonal antibody for NCAM. An anti-Human NCAM1 biotinylated polyclonal antibody from goat was added to each well, incubated during 60 min at 37ºC. Plate was washed 3 times with TBS too remove unbound antibodies. Next, 100 µl of avidin was added and incubated during 30 min at 37ºC. After five washes with TBS, 90 µl of TMB substrate was added and incubated during 25 min at 37ºC, producing a blue colour. An acid solution was added to stop TMB catalysis reaction and absorbance was read at 450 nm. The standard curve was created by plotting absorbance by NCAM protein concentration.

Statistical analysis

Statistical analysis was carried out using Wilcoxon signed-rank test to assess differences between individuals with cognitive deficits and age-sex matched controls in terms of sAPPα, sAPPβ and NCAM protein concentrations for serum and serum-derived exosome samples. A ratio sAPPα/ NCAM or sAPPβ/ NCAM was performed to normalize samples for exosome neuronal nature. Differences between the exosome number of individuals with cognitive deficit and controls were assessed using a two-tailed t-test. P-values less or equal to 0.10 were considered as significant. Receiver Operating Characteristic curves were carried out to determine the performance of the models for discriminating the group of moderate, severe dementia and confirmed AD cases from sex and age matched controls. All analysis were performed using GraphPad Prism 7 (GraphPad Software, La Jolla, California, USA).

3.2. Results

sAPPα and sAPPβ in serum

sAPPα and sAPPβ concentration levels in serum were assessed in two groups, the mild cognitive impairment (MCI) patients (CDR=1) and "putative and AD" (PAD) patients (CDR≥1). The last group include individuals with moderate to severe cognitive impairment and seven AD clinical confirmed cases. Respective mean protein concentrations obtained for sAPPα and sAPPβ can be found in the next table:

Table 5. Mean concentrations of sAPPα and sAPPβ in serum.

Groups	sAPPα mean (±SD)	sAPPβ mean (±SD)
MCI	41.01±9.85	5.62±5.4
Control group	34.72±11.61	6.40±4.32
PAD	34.71±10.99	5.03±5.24
Control group	33.43±8.61	5.24±3.43

The mean concentrations of sAPPα and sAPPβ in serum were not significantly different from respective controls (Table 5 and Figures 17 and 18). A small tendency for higher sAPPα means for individuals with cognitive deficits were observed for the two groups, although more accentuated in the MCI groups.

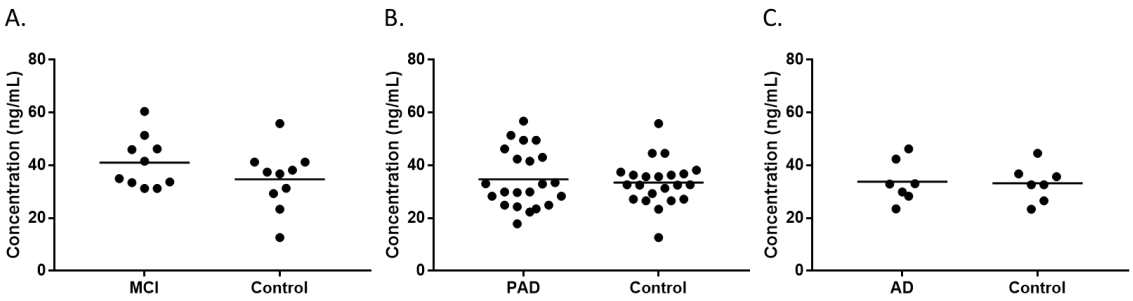

Figure 17. **sAPPα levels in dementia.** sAPPα levels in serum of MCI patients (A) and "putative and AD" cases (B). A graph was also raised for AD confirmed cases that were included in PAD group (C). The horizontal line represents the mean for each set. MCI: Mild cognitive impairment; PAD: "Putative and AD" cases.

Contrarily, sAPPβ mean levels exihibited an opposite tendency with lower values in the patients groups. However, if we only look at AD cases (Figure 18C) an accentuated decrease of sAPPβ mean in AD set when compared to controls could be observed. Noticeably, if the AD outlier (Figure 18C, red circle) and respective control were removed (Figure 18C, blue circle), this decrease tendency was significant for AD group (2.03±0.81) versus control group (5.01±3.33) ($p \leq 0.10$).

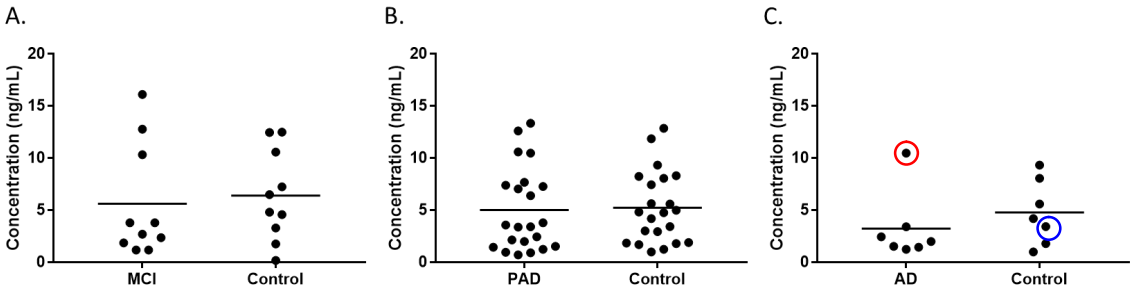

Figure 18. **sAPPβ levels in dementia**. sAPPβ levels in serum of MCI patients (A) and "putative and AD" cases (B). A graph was also raised for AD confirmed cases that were included in PAD group (C). The horizontal line represents the mean for each set. Red circle indicates exclusion of an AD patient and blue circle indicate exclusion of respective control, for the mean values calculation. MCI: Mild cognitive impairment; PAD: "Putative and AD".

sAPPα and sAPPβ levels in serum-derived exosomes

The levels of sAPPα and sAPPβ were also evaluated in exosomes. Exosomes may represent a contained source of biomarkers and thus we want to address if sAPPα and sAPPβ differences were more marked in these preparations. Mean protein concentrations for the two groups are indicated in Table 6.

Table 6. Mean concentrations of sAPPα and sAPPβ in serum-derived exosomes.

Groups	Exosome sAPPα mean (±SD)	Exosome sAPPβ mean (±SD)
MCI	31.96±12.85	5.39±3.81
Control group	30.95±8.93	4.05±2.14
PAD	25.43±9.08	3.75±2.36
Control group	26.43±5.75	4.38±2.01

As for serum, no significant differences could be observed in exosomal sAPPα and sAPPβ mean levels for MCI and PAD groups (Figures 19 and 20). Only a small decrease in sAPP concentrations for "putative and AD" cases and AD group could be detected when compared to controls, in particular for sAPPβ.

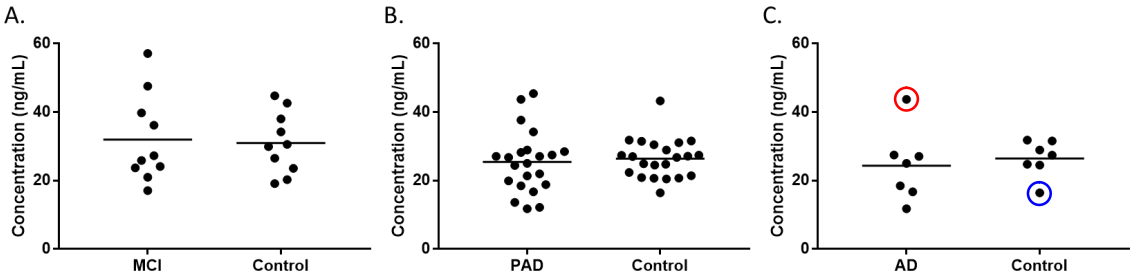

Figure 19. Exosomal sAPPα levels in dementia. sAPPα levels in serum exosomes of MCI patients (A), "putative and AD" cases (B). A graph was also raised for AD confirmed cases that were included in PAD group (C). The horizontal line represents the mean for each set. Red circle indicates exclusion of an AD patient and blue circle indicate exclusion of respective control, for the mean values calculation. MCI: Mild cognitive impairment; PAD: "Putative and AD".

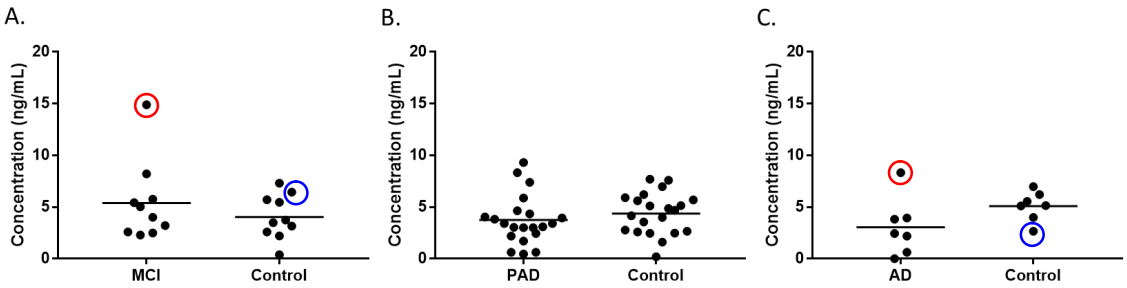

Figure 20. Exosomal sAPPβ levels in dementia. sAPPβ levels in serum exosomes of MCI patients (A), "putative and AD" cases (B). A graph was also raised for AD confirmed cases that were included in PAD group (C). The horizontal line represents the mean for each set. In A, red circle represents the removal of a mild individual outlier and the blue circle represents the removal of its respective control, for the mean values calculation. In C, red circle indicates exclusion of an AD patient and blue circle indicate exclusion of respective control, for the mean values calculation. MCI: Mild cognitive impairment; PAD: "Putative and AD".

A more detailed look at AD cases (Figures 19 and 20) did not render in significant differences. However, after removal of the AD outlier for sAPPα and sAPPβ (Figures 19C and 20C, red circle) and respective control (Figures 19C and 20C, blue circle), sAPPα and sAPPβ concentrations were significantly reduced (21.09±6.40 and 2.17±1.62, respectively) when compared with controls (28.17±3.20 and 5.49±1.03, respectively) ($p \leq 0.10$). Of note, the outlier removed was the same in all cases.

Neither mild sAPPα or sAPPβ levels were significantly different between dementia cases and controls, even with the removal of a mild outlier in sAPPβ (Figure 20A, red circle) and respective control (Figure 20A, blue circle).

Neuronal exosome sAPPα and sAPPβ levels

To evaluate if the number of exosomal particles in each preparation was different, the EXOCET assay was carried out. No significant differences could be observed for both groups: MCI versus controls ($1{,}43x10^{11}\pm5{,}57x10^{10}$ vs $1{,}29x10^{11}\pm5{,}85x10^{10}$) and "putative and AD cases" versus controls ($1{,}19x10^{11}\pm4{,}55x10^{10}$ vs $1{,}10x10^{11}\pm4{,}22x10^{10}$).

In order to determine the levels of neuronal derived exosomal sAPP, sAPPα and sAPPβ concentrations were normalized for NCAM protein concentrations. Mean concentrations of sAPPα and sAPPβ after normalization for NCAM can be found in Table 7.

Table 7. Mean concentrations of sAPPα and sAPPβ/NCAM ratio in serum-derived exosomes.

Groups	Exosome sAPPα mean (±SD)	Exosome sAPPβ mean (±SD)
MCI	17.45±7.75	2.96±2.18
Control group	14.08±3.85	1.81±0.88
PAD	12.46±5.95	1.78±1.33
Control group	13.94±4.11	2.28±1.11

The mean values for sAPPα and sAPPβ ratios were not significantly different from respective controls however a small decrease for "putative and AD" cases could be detected when compared to controls. Similar results were obtained if we look at AD confirmed cases (Figures 21 and 22, respectively).

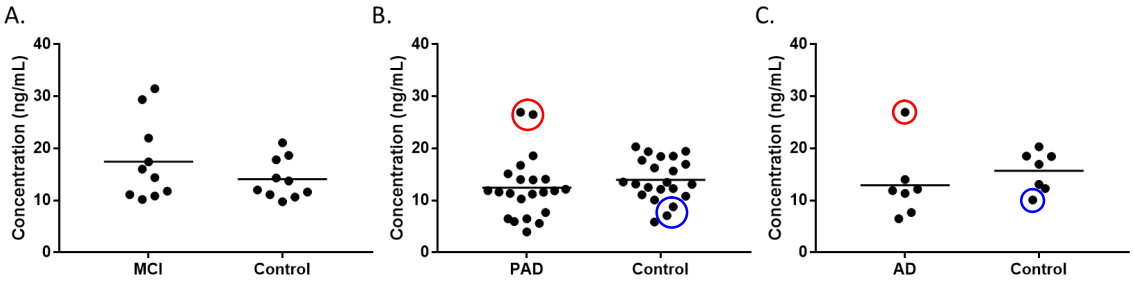

Figure 21. Neuronal exosomal sAPPα values in dementia. sAPPα levels in neuronal serum exosomes of MCI patients (A), "putative and AD" cases (B). A graph was also raised for AD confirmed cases that were included in PAD group (C). The horizontal line represents the mean for each set. In B, red circle represents the removal of two PAD patients and the blue circle represents the removal of its respective controls, for the mean values calculation. In C, red circle indicates exclusion of an AD patient and blue circle indicate exclusion of respective control, for the mean values calculation. MCI: Mild cognitive impairment; PAD: "Putative and AD".

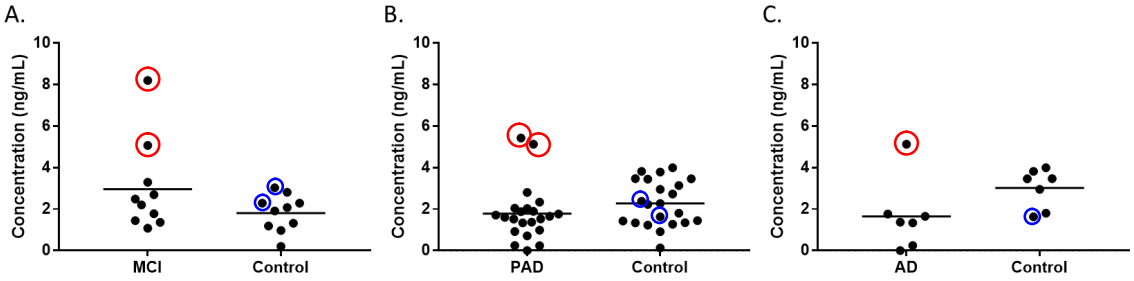

Figure 22. **Neuronal exosomal sAPPβ values in dementia.** sAPPβ levels in neuronal serum exosomes of MCI patients (A), "putative and AD" cases (B). A graph was also raised for AD confirmed cases that were included in PAD group (C). The horizontal line represents the mean for each set. Red circle represents the outlier removal of each demented individual from MCI group (A), PAD group (B) and AD cases (C) while blue circles indicates the exclusion of their respective controls. MCI: Mild cognitive impairment; PAD: "Putative and AD".

Removal of two outliers from "putative and AD" group and one from AD group and respective controls (Figures 21B/C and Figure 22B/C, red and blue circles) results in a significant decrease of mean values for both sAPPα and sAPPβ ratios between these groups and the respective controls (Figure 23). In both cases, the AD outlier removed was the same. Outlier individuals removed exhibit other comorbidities as dyslipidemia, respiratory disease and hypertension. However, outliers removal from neuronal sAPPβ MCI cases and respective controls (Figure 22A, red and blue circles, respectively) did not resulted in significant distinct means between demented individuals and controls.

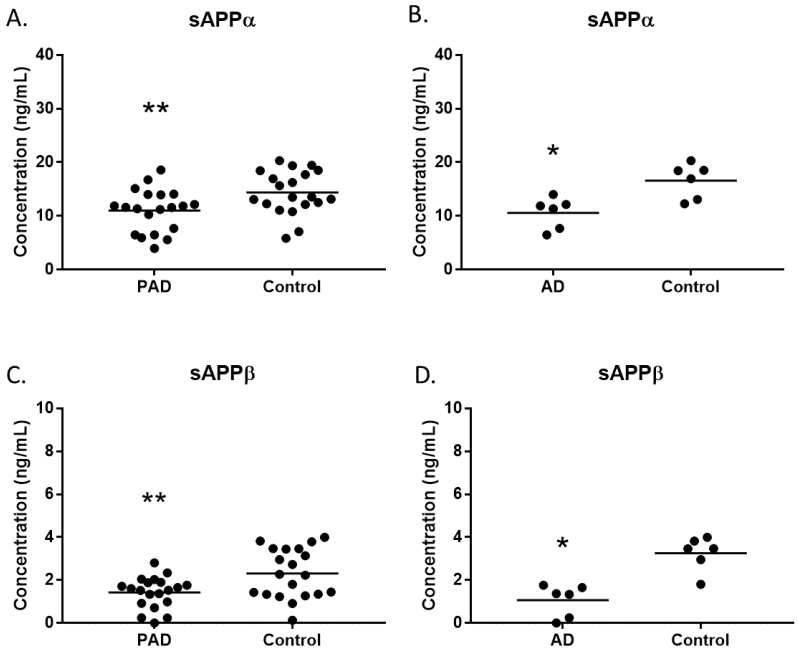

Figure 23. Neuronal exosomal sAPP ratios upon outliers removal. *p≤0.10; **p≤0.05

Considering the results of Figure 23, receiver operating characteristic curves (ROC) were performed for exosome sAPPα and sAPPβ/NCAM ratios, to determine if the profile of these neuronal exosomal sAPP was strong enough to distinguish "putative and AD" group from non-demented control cases. For exosome sAPPα/NCAM ratio the area under the curve (AUC) was 0.73 ($p \leq 0.05$) and for exosome sAPPβ/NCAM ratio it was 0.69 ($p \leq 0.05$) (Figure 24).

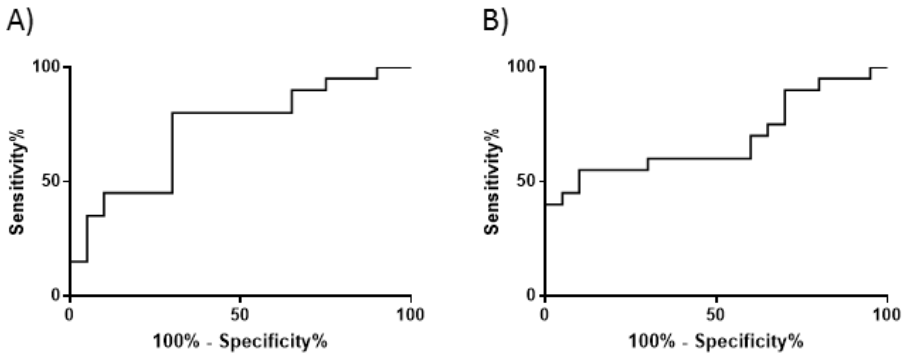

Figure 24. ROC curves for neuronal exosomal sAPP. sAPPα (A) and sAPPβ/NCAM ratios (B) for discriminating PAD patients from control individuals.

Chapter 4. Discussion

The research interest in exosomes as a resource for biomarkers linked to disease is continuously increasing however still to be stablished is the best method chose among the variety of exosome isolation methods, in particular when using biological fluids [233]. Most of literature is dedicated to compare ultracentrifugation with exosome precipitation based isolation kits, and indeed the benefits of exosome precipitation-based reagents were already shown, particularly in terms of exosome and protein yield, time consuming and cost effectiveness for biofluids and cell-derived exosomes [244, 245]. In this study, it was compared the performance of three commercial kits based on exosome precipitation reagents and one column-based method, in different body fluids namely serum, plasma and CSF. This comparative study addressed the performance of these kits in different body fluids by evaluating the number of particles isolated, the size by TEM and zeta sizer analysis, and the nature of the sample, using specific antibodies. There is a single study comparing these three kits for isolation of serum exosomes but does not provide a complete characterization [246], another study for serum exosomes comparing ExoQ and TEI [245], and a study that uses ExoQ and ExoS for plasma exosomes isolation [247]. Thus, additional studies are needed for interlaboratory validation and protocols optimization (e.g. regarding sample volumes and methods of exosome characterization).

In this study, ExoQ, TEI and ExoS were tested for exosome isolation from serum, plasma and CSF. Through DLS it was measured the hydrodynamic diameter of nanoparticles, that for all kits were within the exosome typical range (30-150 nm), representing the higher percentage of particles in the exosomal preparations (Table 3). For serum, using precipitation-based methods and for plasma using TEI, a second mean peak between 400-500 nm was identified. Other studies had already reported similar results regarding vesicles isolated being outside recommended range, with sizes from 300-1000 nm using precipitation-based reagents for serum and plasma exosomes [244, 245, 248]. TEM analysis revealed nanovesicles with exosome typical sizes and morphology for all exosome samples. All isolated vesicles observed measured less than 150 nm of diameter. However, in some preparations, aggregated like-exosome structures were detected which can explain the peaks of larger diameter obtained in DLS. In addition, it cannot be excluded the fact that DLS measures nanoparticles diameter based in the speed of particles undergoing Brownian motion, which is influenced by size, and thus, DLS is more sensitive to the presence of higher particles or aggregates. Despite that, the PDI (Table 3) measured for all particles were inside the recommended range, between 0.08 to 0.70, except for exosome-derived CSF samples isolated with ExoS, showed a polydispersity index of 0.82 which can correlate with the broad distribution of sizes obtained by DLS analysis for this sample. PDI superior to 0.7 indicates a very

broad range of sizes. Moreover, for all TEM preparations a number of small particles, bellow 30 nm were evident, these might represent some contamination with high-density, low-density and intermediate-density lipoproteins, as previously suggested [249–252]. Other possible contaminants are abundant biofluids proteins or even protein aggregates [51, 253, 254]. Additional approaches could be used to better clarify the degree of contamination as is the case of cryo-electron microscopy that focus on structural details or also immunolabelled TEM [245].

Zeta potential measures were all negative and most samples had values bellow -10mV, the minimum threshold value for what samples with higher zeta potential than this are highly subjected to aggregation. Despite the significant differences between some exosome samples, thus far there is lack of scientific knowledge to explain these differences and give them a biological mean. It was already reported that exosome storage temperature has great impacts on exosome stability, recovery and even that storage temperatures above -20ºC for long term periods can lead to exosome markers loss as well as morphological changes [255–259]. Exosome samples were all properly stored at -20ºC, for similar periods what permit to hypothesize that stability differences are not only due to storage conditions. In addition, zeta potential range are similar to others previously described for serum- derived exosomes [245, 260]. At our knowledge, this is the first study that address zeta potential of plasma and CSF-derived exosomes.

Further analysis included exosome quantification that was achieved using EXOCET assay, a method based in the characteristically enhanced activity of exosome Acetyl-CoA Acetylcholinesterase [24, 261]. Exosome quantifications were significantly different among kits. For serum and plasma-derived exosomes ExoQ and ExoS isolated about 2-fold and 2.5- fold, respectively, more particles in both biofluids than TEI. Indeed, the number of particles isolated from serum and plasma was quite similar to Nanosight-based quantifications [262, 263]. The number of exosomes isolated from serum were different between TEI and ExoQ ($p \leq 0.01$) or TEI and ExoS ($p \leq 0.01$) in contrast with previous studies that did not observed differences [245, 246]. Similar results were obtained for plasma. So, in general terms both ExoQ and ExoS render in higher exosomal yields than TEI, for serum and plasma biofluids. Unfortunately, the volume used for CSF did not render in a particle number higher enough to be detected by this method. An increase of CSF starting volume should be used to enhance exosome isolation using the same kits.

The total protein quantification was carried out using BCA assay. Regarding protein concentration, the precipitation based-reagent ExoQ performed better for serum and plasma-derived exosomes quantified by BCA assay. It was already reported that the number of exosome

particles may not necessarily correlate with protein concentration possibly because exosome samples might contain some contaminants that can affect total protein quantification. Therefore, the ratio between the number of particles and the concentrations determined by BCA was calculated for serum and plasma samples, also in order to give an idea of exosomal sample purity. Higher ratios were obtained for the column-based ExoS methods, which highlight the increase purity of exosomes isolated by this method. Western blot analysis, confirmed the nature of the samples, revealing the presence of exosomal marker TSG101, discarding cells contamination of samples with the negative results for calnexin. Taken together data suggest that either TEI or ExoQ precipitation-based reagents or ExoS column-based kit successfully isolate exosomes from small volume samples of serum and plasma, although at different yields and purity levels. However larger amounts of CSF are required to proper CSF-derived exosome isolation.

After exosome isolation optimization from biofluids, all conditions were reunited to start a pilot study directed to biomarker discovery in dementia and in AD cases. Particular emphasis was given to sAPP fragments. sAPP was shown to be a potential biomarker candidate in different studies for AD [166, 188, 195]. Currently, AD based molecular diagnostics is carried out in CSF, which involves an invasive procedure, thus many studies have focus on the search for more peripheral biomarkers. It is reasonable explore for the first time the potential of serum and serum exosome levels of sAPPα and sAPPβ. In this study, serum was the biofluid chosen and exosomes were isolated from individuals with cognitive deficit and respective controls.

No significant differences were found for the mean values of sAPPα and sAPPβ between MCI cases and controls, “putative and AD” group, AD cases and respective controls. It was observed an opposite tendency between of serum sAPPα and sAPPβ means comparatively to controls. While serum sAPPα means tend to increase in individuals with MCI, sAPPβ tend to decrease. Despite of not being significant considering all patients, with removal of an AD outlier in AD cases led to an significant sAPPβ decrease. Exosome sAPPα and sAPPβ levels follow both the same pattern with a small increase of means for mild group compared to control and reduced means for “putative and AD” group and AD cases with higher magnitude for sAPPβ. After removal of one AD outlier, AD group presented a significant decrease when compared with control individuals. The outlier removed was in both cases the same. Upon normalizations for NCAM, neuronal sAPPα and sAPPβ patterns are accentuated and a significant decrease in “putative and AD” group after removing two outliers could be observed. Significant decrease of sAPPα and sAPPβ means is specially accentuated in the case of sAPPα. ROC curves for exosome sAPPα and

sAPPβ levels normalized for neuronal nature addresses their potential for discriminate “putative and AD” group from controls. Neuronal exosome sAPPα discriminates “putative and AD” cases from controls with a modest sensibility of 73% and 69% for neuronal exosome sAPPβ levels.

A modest number of individuals were used in this study so additional studies, with increased number of samples should be carried out to address the real value of sAPP. This pilot study aims to prove the potential of these soluble APP forms as candidate biomarkers and not yet validate it use as a biomarker. Moreover, instead of normalize sAPPα and sAPPβ exosome levels for NCAM it would be interesting to isolate neuronal exosomes and evaluate the potential of sAPP, as mentioned with higher number of participants, and ideally perform a multi-centre study.

Final remarks and future perspectives

All precipitation-based and column-based methods compared in this study isolated exosomes from serum, plasma and CSF, as demonstrated by TEM visualizations and Zetasizer analysis. However, methods had different performances in terms of particle yields, protein quantifications and, more importantly, in terms of purity. Precipitation-based methods isolated more serum and plasma particles and provided an increased protein yield. For both serum and plasma, the greatest purity was achieved with the column based-method.

For CSF-derived exosomes and although some methods of characterization showed the presence of exosomal particles, there is a need to increase the CSF starting volume to enhance exosomal yield. In particular, the work carried out in this study facilitates the choice of exosome isolation methods and consequently facilitate its’ use for a wide range of downstream analysis and in biomarker research.

Considering the potential of sAPPα and sAPPβ in serum and serum-derived exosomes as candidate AD biomarkers, this work showed a decrease of serum-derived neuronal exosome means of these soluble forms, in patients scored with moderate to severe cognitive decline (CDR≥1). Neuronal exosome sAPPα levels and APPβ levels discriminates “putative and AD” cases from controls with a modest sensibility of 73% and 69%, respectively. Further studies are however required with a higher number of participants to better assess the discriminatory capacity of sAPP.

References

1. Harding C, Heuser J, Stahl P: **Receptor-mediated endocytosis of transferrin and recycling of the transferrin receptor in rat reticulocytes.** *J Cell Biol* 1983, **97**:329–39.

2. Pan BT, Teng K, Wu C, Adam M, Johnstone RM: **Electron microscopic evidence for externalization of the transferrin receptor in vesicular form in sheep reticulocytes.** *J Cell Biol* 1985, **101**:942–8.

3. Johnstone RM, Adam M, Hammond JR, Orr L, Turbide C: **Vesicle formation during reticulocyte maturation. Association of plasma membrane activities with released vesicles (exosomes).** *J Biol Chem* 1987, **262**:9412–20.

4. Stoorvogel W, Strous GJ, Geuze HJ, Oorschot V, Schwartz AL: **Late endosomes derive from early endosomes by maturation.** *Cell* 1991, **65**:417–27.

5. Gillooly DJ, Morrow IC, Lindsay M, Gould R, Bryant NJ, Gaullier JM, Parton RG, Stenmark H: **Localization of phosphatidylinositol 3-phosphate in yeast and mammalian cells**. *EMBO J* 2000, **19**:4577–4588.

6. Lemmon MA: **Membrane recognition by phospholipid-binding domains**. *Nat Rev Mol Cell Biol* 2008, **9**:99–111.

7. Hoepfner S, Severin F, Cabezas A, Habermann B, Runge A, Gillooly D, Stenmark H, Zerial M: **Modulation of receptor recycling and degradation by the endosomal kinesin KIF16B.** *Cell* 2005, **121**:437–50.

8. Sahu R, Kaushik S, Clement CC, Cannizzo ES, Scharf B, Follenzi A, Potolicchio I, Nieves E, Cuervo AM, Santambrogio L, Aniento F, Roche E, Cuervo AM, Knecht E, Arispe N, Maio A De, Bandyopadhyay U, Kaushik S, Varticovski L, Cuervo AM, Castellino F, Germain RN, Chiang HL, Terlecky SR, Plant CP, Dice JF, Cuervo AM, Cuervo AM, Dice J, Cuervo AM, et al.: **Microautophagy of cytosolic proteins by late endosomes.** *Dev Cell* 2011, **20**:131–9.

9. Katzmann DJ, Babst M, Emr SD, Amerik AY, Nowak J, Swaminathan S, Hochstrasser M, Babst M, Sato TK, Banta LM, Emr SE, Babst M, Wendland B, Estepa EJ, Emr SD, Babst M, Odorizzi G, Estepa EJ, Emr SD, Becherer KA, Reider S, Emr SD, Jones EW, Beck T, Schmidt A, Hall MN, Bishop N, Woodman P, Burd CG, Peterson M, et al.: **Ubiquitin-dependent sorting into the multivesicular body pathway requires the function of a conserved endosomal protein sorting complex, ESCRT-I.** *Cell* 2001, **106**:145–55.

10. Tamai K, Tanaka N, Nakano T, Kakazu E, Kondo Y, Inoue J, Shiina M, Fukushima K, Hoshino T, Sano K, Ueno Y, Shimosegawa T, Sugamura K: **Exosome secretion of dendritic cells is regulated by Hrs, an ESCRT-0 protein**. *Biochem Biophys Res Commun* 2010, **399**:384–390.

11. Gross JC, Chaudhary V, Bartscherer K, Boutros M: **Active Wnt proteins are secreted on exosomes**. *Nat Cell Biol* 2012, **14**:1036–1045.

12. Colombo M, Moita C, van Niel G, Kowal J, Vigneron J, Benaroch P, Manel N, Moita LF, Thery C, Raposo G: **Analysis of ESCRT functions in exosome biogenesis, composition and secretion highlights the heterogeneity of extracellular vesicles**. *J Cell Sci* 2013, **126**:5553–5565.

13. Hoshino D, Kirkbride KC, Costello K, Clark ES, Sinha S, Grega-Larson N, Tyska MJ, Weaver AM: **Exosome Secretion Is Enhanced by Invadopodia and Drives Invasive Behavior**. *Cell Rep* 2013, **5**:1159–1168.

14. Baietti MF, Zhang Z, Mortier E, Melchior A, Degeest G, Geeraerts A, Ivarsson Y, Depoortere F, Coomans C, Vermeiren E, Zimmermann P, David G: **Syndecan–syntenin–ALIX regulates the biogenesis of exosomes**. *Nat Cell Biol* 2012, **14**:677–685.

15. Babst M, Wendland B, Estepa EJ, Emr SD: **The Vps4p AAA ATPase regulates membrane association of a Vps protein complex required for normal endosome function**. *EMBO J* 1998, **17**:2982–2993.

16. Ghazi-Tabatabai S, Saksena S, Short JM, Pobbati A V., Veprintsev DB, Crowther RA, Emr SD, Egelman EH, Williams RL: **Structure and Disassembly of Filaments Formed by the ESCRT-III Subunit Vps24**. *Structure* 2008, **16**:1345–1356.

17. Trajkovic K, Hsu C, Chiantia S, Rajendran L, Wenzel D, Wieland F, Schwille P, Brugger B, Simons M: **Ceramide Triggers Budding of Exosome Vesicles into Multivesicular Endosomes**. *Science (80-)* 2008, **319**:1244–1247.

18. Stuffers S, Sem Wegner C, Stenmark H, Brech A: **Multivesicular Endosome Biogenesis in the Absence of ESCRTs**. *Traffic* 2009, **10**:925–937.

19. Strauss K, Goebel C, Runz H, Möbius W, Weiss S, Feussner I, Simons M, Schneider A: **Exosome secretion ameliorates lysosomal storage of cholesterol in Niemann-Pick type C disease.** *J Biol Chem* 2010, **285**:26279–88.

20. van Niel G, Charrin S, Simoes S, Romao M, Rochin L, Saftig P, Marks MS, Rubinstein E, Raposo G: **The tetraspanin CD63 regulates ESCRT-independent and -dependent endosomal sorting during melanogenesis.** *Dev Cell* 2011, **21**:708–21.

21. Perez-Hernandez D, Gutierrez-Vazquez C, Jorge I, Lopez-Martin S, Ursa A, Sanchez-Madrid F, Vazquez J, Yanez-Mo M: **The Intracellular Interactome of Tetraspanin-enriched Microdomains Reveals Their Function as Sorting Machineries toward Exosomes**. *J Biol Chem* 2013, **288**:11649–11661.

22. Chairoungdua A, Smith DL, Pochard P, Hull M, Caplan MJ: **Exosome release of β-catenin: a novel mechanism that antagonizes Wnt signaling**. *J Cell Biol* 2010, **190**:1079–1091.

23. Nazarenko I, Rana S, Baumann A, McAlear J, Hellwig A, Trendelenburg M, Lochnit G, Preissner KT, Zoller M: **Cell Surface Tetraspanin Tspan8 Contributes to Molecular Pathways of Exosome-Induced Endothelial Cell Activation**. *Cancer Res* 2010, **70**:1668–1678.

24. Savina A, Vidal M, Colombo MI: **The exosome pathway in K562 cells is regulated by Rab11.** *J Cell Sci* 2002, **115**(Pt 12):2505–15.

25. Savina A, Fader CM, Damiani MT, Colombo MI: **Rab11 Promotes Docking and Fusion of Multivesicular Bodies in a Calcium-Dependent Manner**. *Traffic* 2005, **6**:131–143.

26. Hsu C, Morohashi Y, Yoshimura S-I, Manrique-Hoyos N, Jung S, Lauterbach MA, Bakhti M, Grønborg M, Möbius W, Rhee J, Barr FA, Simons M: **Regulation of exosome secretion by Rab35 and its GTPase-activating proteins TBC1D10A-C.** *J Cell Biol* 2010, **189**:223–32.

27. Fruhbeis C, Frohlich D, Kuo WP, Amphornrat J, Thilemann S, Saab AS, Kirchhoff F, Mobius W, Goebbels S, Nave KA, Schneider A, Simons M, Klugmann M, Trotter J, Kramer-Albers EM: **Neurotransmitter-Triggered Transfer of Exosomes Mediates Oligodendrocyte-Neuron Communication**. *PLoS Biol* 2013, **11**.

28. Ostrowski M, Carmo NB, Krumeich S, Fanget I, Raposo G, Savina A, Moita CF, Schauer K, Hume AN, Freitas RP, Goud B, Benaroch P, Hacohen N, Fukuda M, Desnos C, Seabra MC, Darchen F, Amigorena S, Moita LF, Thery C: **Rab27a and Rab27b control different steps of the exosome**

secretion pathway. *Nat Cell Biol* 2010, **12**:19–30.

29. Beckett K, Monier S, Palmer L, Alexandre C, Green H, Bonneil E, Raposo G, Thibault P, Borgne R Le, Vincent J-P: **Drosophila S2 Cells Secrete Wingless on Exosome-Like Vesicles but the Wingless Gradient Forms Independently of Exosomes**. *Traffic* 2013, **14**:82–96.

30. Abrami L, Brandi L, Moayeri M, Brown MJ, Krantz BA, Leppla SH, van der Goot FG: **Hijacking multivesicular bodies enables long-term and exosome-mediated long-distance action of anthrax toxin.** *Cell Rep* 2013, **5**:986–96.

31. Bobrie A, Krumeich S, Reyal F, Recchi C, Moita LF, Seabra MC, Ostrowski M, Thery C: **Rab27a Supports Exosome-Dependent and -Independent Mechanisms That Modify the Tumor Microenvironment and Can Promote Tumor Progression**. *Cancer Res* 2012, **72**:4920–4930.

32. Peinado H, Alečković M, Lavotshkin S, Matei I, Costa-Silva B, Moreno-Bueno G, Hergueta-Redondo M, Williams C, García-Santos G, Ghajar CM, Nitadori-Hoshino A, Hoffman C, Badal K, Garcia BA, Callahan MK, Yuan J, Martins VR, Skog J, Kaplan RN, Brady MS, Wolchok JD, Chapman PB, Kang Y, Bromberg J, Lyden D: **Melanoma exosomes educate bone marrow progenitor cells toward a pro-metastatic phenotype through MET**. *Nat Med* 2012, **18**:883–891.

33. Webber JP, Spary LK, Sanders AJ, Chowdhury R, Jiang WG, Steadman R, Wymant J, Jones AT, Kynaston H, Mason MD, Tabi Z, Clayton A: **Differentiation of tumour-promoting stromal myofibroblasts by cancer exosomes**. *Oncogene* 2015, **34**:290–302.

34. Zheng Y, Campbell EC, Lucocq J, Riches A, Powis SJ: **Monitoring the Rab27 associated exosome pathway using nanoparticle tracking analysis**. *Exp Cell Res* 2013, **319**:1706–1713.

35. Fader CM, Sánchez DG, Mestre MB, Colombo MI: **TI-VAMP/VAMP7 and VAMP3/cellubrevin: two v-SNARE proteins involved in specific steps of the autophagy/multivesicular body pathways**. *Biochim Biophys Acta - Mol Cell Res* 2009, **1793**:1901–1916.

36. Meiringer CTA, Auffarth K, Hou H, Ungermann C: **Depalmitoylation of Ykt6 Prevents its Entry into the Multivesicular Body Pathway**. *Traffic* 2008, **9**:1510–1521.

37. Alonso R, Mazzeo C, Mérida I, Izquierdo M: **A new role of diacylglycerol kinase α on the secretion of lethal exosomes bearing Fas ligand during activation-induced cell death of T lymphocytes**. *Biochimie* 2007, **89**:213–221.

38. Alonso R, Mazzeo C, Rodriguez MC, Marsh M, Fraile-Ramos A, Calvo V, Avila-Flores A, Merida I, Izquierdo M: **Diacylglycerol kinase α regulates the formation and polarisation of mature multivesicular bodies involved in the secretion of Fas ligand-containing exosomes in T lymphocytes**. *Cell Death Differ* 2011, **18**:1161–1173.

39. Hyenne V, Apaydin A, Rodriguez D, Spiegelhalter C, Hoff-Yoessle S, Diem M, Tak S, Lefebvre O, Schwab Y, Goetz JG, Labouesse M: **RAL-1 controls multivesicular body biogenesis and exosome secretion**. *J Cell Biol* 2015, **211**:27–37.

40. Théry C, Boussac M, Véron P, Ricciardi-Castagnoli P, Raposo G, Garin J, Amigorena S: **Proteomic analysis of dendritic cell-derived exosomes: a secreted subcellular compartment distinct from apoptotic vesicles.** *J Immunol* 2001, **166**:7309–18.

41. Vidal M, Sainte-Marie J, Philippot JR, Bienvenue A: **Asymmetric distribution of phospholipids in the membrane of vesicles released during in vitro maturation of guinea pig reticulocytes: Evidence precluding a role for "aminophospholipid translocase."** *J Cell Physiol* 1989, **140**:455–462.

42. Laulagnier K, Motta C, Hamdi S, Roy S, Fauvelle F, Pageaux J-F, Kobayashi T, Salles J-P, Perret B,

Bonnerot C, Record M: **Mast cell- and dendritic cell-derived exosomes display a specific lipid composition and an unusual membrane organization.** *Biochem J* 2004, **380**(Pt 1):161–71.

43. Wubbolts R, Leckie RS, Veenhuizen PTM, Schwarzmann G, Mobius W, Hoernschemeyer J, Slot J-W, Geuze HJ, Stoorvogel W: **Proteomic and biochemical analyses of human B cell-derived exosomes. Potential implications for their function and multivesicular body formation.** *J Biol Chem* 2003, **278**:10963–10972.

44. Subra C, Grand D, Laulagnier K, Stella A, Lambeau G, Paillasse M, De Medina P, Monsarrat B, Perret B, Silvente-Poirot S, Poirot M, Record M: **Exosomes account for vesicle-mediated transcellular transport of activatable phospholipases and prostaglandins.** *J Lipid Res* 2010, **51**:2105–20.

45. Valadi H, Ekström K, Bossios A, Sjöstrand M, Lee JJ, Lötvall JO: **Exosome-mediated transfer of mRNAs and microRNAs is a novel mechanism of genetic exchange between cells**. *Nat Cell Biol* 2007, **9**:654–659.

46. Nolte-'t Hoen ENM, Buermans HPJ, Waasdorp M, Stoorvogel W, Wauben MHM, 't Hoen PAC: **Deep sequencing of RNA from immune cell-derived vesicles uncovers the selective incorporation of small non-coding RNA biotypes with potential regulatory functions**. *Nucleic Acids Res* 2012, **40**:9272–9285.

47. Villarroya-Beltri C, Gutiérrez-Vázquez C, Sánchez-Cabo F, Pérez-Hernández D, Vázquez J, Martin-Cofreces N, Martinez-Herrera DJ, Pascual-Montano A, Mittelbrunn M, Sánchez-Madrid F: **Sumoylated hnRNPA2B1 controls the sorting of miRNAs into exosomes through binding to specific motifs**. *Nat Commun* 2013, **4**:2980.

48. Squadrito ML, Baer C, Burdet F, Maderna C, Gilfillan GD, Lyle R, Ibberson M, De Palma M: **Endogenous RNAs Modulate MicroRNA Sorting to Exosomes and Transfer to Acceptor Cells**. *Cell Rep* 2014, **8**:1432–1446.

49. Momen-Heravi F, Balaj L, Alian S, Mantel P-Y, Halleck AE, Trachtenberg AJ, Soria CE, Oquin S, Bonebreak CM, Saracoglu E, Skog J, Kuo WP: **Current methods for the isolation of extracellular vesicles**. *Biol Chem* 2013, **394**.

50. Yakimchuk K: **Exosomes: isolation methods and specific markers**. *Mater Methods* 2015, **5**.

51. Li P, Kaslan M, Lee SH, Yao J, Gao Z: **Progress in Exosome Isolation Techniques.** *Theranostics* 2017, **7**:789–804.

52. **About a peculiar disease of the cerebral cortex. By Alois Alzheimer, 1907 (Translated by L. Jarvik and H. Greenson)**. *Alzheimer Dis Assoc Disord* 1987, **1**:3–8.

53. Duthey B: **Background Paper 6.11 Alzheimer Disease and other Dementias**. 2013.

54. **World Alzheimer Report 2015** [http://www.worldalzreport2015.org/]

55. **Alzheimer's Statistics** [http://www.alzheimers.net/resources/alzheimers-statistics/]

56. Santana I, Farinha F, Freitas S, Rodrigues V, Carvalho Å: **[The Epidemiology of Dementia and Alzheimer Disease in Portugal: Estimations of Prevalence and Treatment-Costs].** *Acta Med Port* 2013, **28**:182–8.

57. Hof PR, Glannakopoulos P, Bouras C: **The neuropathological changes associated with normal brain aging.** *Histol Histopathol* 1996, **11**:1075–88.

58. Perl DP: **Neuropathology of Alzheimer's Disease**. *Mt Sinai J Med A J Transl Pers Med* 2010, **77**:32–42.

59. Iqbal K, del C. Alonso A, Chen S, Chohan MO, El-Akkad E, Gong C-X, Khatoon S, Li B, Liu F, Rahman A, Tanimukai H, Grundke-Iqbal I: **Tau pathology in Alzheimer disease and other tauopathies**. *Biochim Biophys Acta - Mol Basis Dis* 2005, **1739**:198–210.

60. Perry G, Friedman R, Shaw G, Chau V: **Ubiquitin is detected in neurofibrillary tangles and senile plaque neurites of Alzheimer disease brains.** *Proc Natl Acad Sci U S A* 1987, **84**:3033–6.

61. Love S, Saitoh T, Quijada S, Cole GM, Terry RD: **Alz-50, ubiquitin and tau immunoreactivity of neurofibrillary tangles, Pick bodies and Lewy bodies.** *J Neuropathol Exp Neurol* 1988, **47**:393–405.

62. Mesulam M-M, Asuncion Morán M: **Cholinesterases within neurofibrillary tangles related to age and Alzheimer's disease**. *Ann Neurol* 1987, **22**:223–228.

63. Hyman BT, Van Hoesen GW, Beyreuther K, Masters CL: **A4 amyloid protein immunoreactivity is present in Alzheimer's disease neurofibrillary tangles.** *Neurosci Lett* 1989, **101**:352–5.

64. Billingsley ML, Kincaid RL: **Regulated phosphorylation and dephosphorylation of tau protein: effects on microtubule interaction, intracellular trafficking and neurodegeneration.** *Biochem J* 1997:577–91.

65. Morrison JH, Hof PR: **Life and death of neurons in the aging brain.** *Science* 1997, **278**:412–9.

66. Braak H, Braak E: **Neuropathological stageing of Alzheimer-related changes.** *Acta Neuropathol* 1991, **82**:239–59.

67. Arriagada P V, Growdon JH, Hedley-Whyte ET, Hyman BT: **Neurofibrillary tangles but not senile plaques parallel duration and severity of Alzheimer's disease.** *Neurology* 1992, **42**(3 Pt 1):631–9.

68. Bierer LM, Hof PR, Purohit DP, Carlin L, Schmeidler J, Davis KL, Perl DP: **Neocortical neurofibrillary tangles correlate with dementia severity in Alzheimer's disease.** *Arch Neurol* 1995, **52**:81–8.

69. Braak H, Alafuzoff I, Arzberger T, Kretzschmar H, Del Tredici K: **Staging of Alzheimer disease-associated neurofibrillary pathology using paraffin sections and immunocytochemistry.** *Acta Neuropathol* 2006, **112**:389–404.

70. Jarrett JT, Berger EP, Lansbury PT: **The carboxy terminus of the beta amyloid protein is critical for the seeding of amyloid formation: implications for the pathogenesis of Alzheimer's disease.** *Biochemistry* 1993, **32**:4693–7.

71. Serpell LC: **Alzheimer's amyloid fibrils: structure and assembly**. *Biochim Biophys Acta - Mol Basis Dis* 2000, **1502**:16–30.

72. Fiala JC, Feinberg M, Peters A, Barbas H: **Mitochondrial degeneration in dystrophic neurites of senile plaques may lead to extracellular deposition of fine filaments**. *Brain Struct Funct* 2007, **212**:195–207.

73. Armstrong RA: **The molecular biology of senile plaques and neurofibrillary tangles in Alzheimer's disease.** *Folia Neuropathol* 2009, **47**:289–99.

74. Bekris LM, Yu C-E, Bird TD, Tsuang DW: **Genetics of Alzheimer disease.** *J Geriatr Psychiatry Neurol* 2010, **23**:213–27.

75. Yoshikai S, Sasaki H, Doh-ura K, Furuya H, Sakaki Y: **Genomic organization of the human amyloid beta-protein precursor gene.** *Gene* 1990, **87**:257–63.

76. Lamb BT, Sisodia SS, Lawler AM, Slunt HH, Kitt CA, Kearns WG, Pearson PL, Price DL, Gearhart

JD: **Introduction and expression of the 400 kilobase precursor amyloid protein gene in transgenic mice**. *Nat Genet* 1993, **5**:22–30.

77. **APP amyloid beta precursor protein** [https://www.ncbi.nlm.nih.gov/gene/351]

78. Tanzi RE, Gusella JF, Watkins PC, Bruns GA, St George-Hyslop P, Van Keuren ML, Patterson D, Pagan S, Kurnit DM, Neve RL: **Amyloid beta protein gene: cDNA, mRNA distribution, and genetic linkage near the Alzheimer locus.** *Science* 1987, **235**:880–4.

79. Goldgaber D, Lerman MI, McBride OW, Saffiotti U, Gajdusek DC: **Characterization and chromosomal localization of a cDNA encoding brain amyloid of Alzheimer's disease.** *Science* 1987, **235**:877–80.

80. Wasco W, Bupp K, Magendantz M, Gusella JF, Tanzi RE, Solomon F: **Identification of a mouse brain cDNA that encodes a protein related to the Alzheimer disease-associated amyloid beta protein precursor.** *Proc Natl Acad Sci U S A* 1992, **89**:10758–62.

81. Wasco W, Gurubhagavatula S, Paradis M d., Romano DM, Sisodia SS, Hyman BT, Neve RL, Tanzi RE: **Isolation and characterization of APLP2 encoding a homologue of the Alzheimer's associated amyloid β protein precursor**. *Nat Genet* 1993, **5**:95–100.

82. Slunt HH, Thinakaran G, Von Koch C, Lo AC, Tanzi RE, Sisodia SS: **Expression of a ubiquitous, cross-reactive homologue of the mouse beta-amyloid precursor protein (APP).** *J Biol Chem* 1994, **269**:2637–44.

83. Müller UC, Zheng H: **Physiological functions of APP family proteins.** *Cold Spring Harb Perspect Med* 2012, **2**:a006288.

84. Theuns J, Marjaux E, Vandenbulcke M, Van Laere K, Kumar-Singh S, Bormans G, Brouwers N, Van den Broeck M, Vennekens K, Corsmit E, Cruts M, De Strooper B, Van Broeckhoven C, Vandenberghe R: **Alzheimer dementia caused by a novel mutation located in the APP C-terminal intracytosolic fragment**. *Hum Mutat* 2006, **27**:888–896.

85. Rogaev EI, Sherrington R, Rogaeva EA, Levesque G, Ikeda M, Liang Y, Chi H, Lin C, Holman K, Tsuda T, Mar L, Sorbi S, Nacmias B, Piacentini S, Amaducci L, Chumakov I, Cohen D, Lannfelt L, Fraser PE, Rommens JM, George-Hyslop PHS: **Familial Alzheimer's disease in kindreds with missense mutations in a gene on chromosome 1 related to the Alzheimer's disease type 3 gene**. *Nature* 1995, **376**:775–778.

86. Gardell SJ, Li Y-M, Xu M, Lai M-T, Huang Q, Castro JL, DiMuzio-Mower J, Harrison T, Lellis C, Nadin A, Neduvelil JG, Register RB, Sardana MK, Shearman MS, Smith AL, Shi X-P, Yin K-C, Shafer JA: **Photoactivated gamma-secretase inhibitors directed to the active site covalently label presenilin 1.** *Nature* 2000, **405**:689–694.

87. Saito T, Suemoto T, Brouwers N, Sleegers K, Funamoto S, Mihira N, Matsuba Y, Yamada K, Nilsson P, Takano J, Nishimura M, Iwata N, Van Broeckhoven C, Ihara Y, Saido TC: **Potent amyloidogenicity and pathogenicity of Aβ43**. *Nat Neurosci* 2011, **14**:1023–1032.

88. Corder EH, Saunders AM, Strittmatter WJ, Schmechel DE, Gaskell PC, Small GW, Roses AD, Haines JL, Pericak-Vance MA: **Gene dose of apolipoprotein E type 4 allele and the risk of Alzheimer's disease in late onset families.** *Science* 1993, **261**:921–3.

89. Corder EH, Saunders AM, Risch NJ, Strittmatter WJ, Schmechel DE, Gaskell PC, Rimmler JB, Locke PA, Conneally PM, Schmader KE, Small GW, Roses AD, Haines JL, Pericak-Vance MA: **Protective effect of apolipoprotein E type 2 allele for late onset Alzheimer disease**. *Nat Genet* 1994, **7**:180–184.

90. Dosunmu R, Wu J, Basha MR, Zawia NH: **Environmental and dietary risk factors in Alzheimer's disease**. *Expert Rev Neurother* 2007, **7**:887–900.

91. Esch FS, Keim PS, Beattie EC, Blacher RW, Culwell AR, Oltersdorf T, McClure D, Ward PJ: **Cleavage of amyloid beta peptide during constitutive processing of its precursor.** *Science* 1990, **248**:1122–4.

92. Sisodia SS, Koo EH, Beyreuther K, Unterbeck A, Price DL: **Evidence that beta-amyloid protein in Alzheimer's disease is not derived by normal processing.** *Science* 1990, **248**:492–5.

93. Sastre M, Steiner H, Fuchs K, Capell A, Multhaup G, Condron MM, Teplow DB, Haass C: **Presenilin-dependent γ-secretase processing of β-amyloid precursor protein at a site corresponding to the S3 cleavage of Notch**. *EMBO Rep* 2001, **2**:835–841.

94. Haass C, Selkoe DJ: **Cellular processing of beta-amyloid precursor protein and the genesis of amyloid beta-peptide.** *Cell* 1993, **75**:1039–42.

95. Gu Y, Misonou H, Sato T, Dohmae N, Takio K, Ihara Y: **Distinct Intramembrane Cleavage of the -Amyloid Precursor Protein Family Resembling -Secretase-like Cleavage of Notch**. *J Biol Chem* 2001, **276**:35235–35238.

96. Gowing E, Roher AE, Woods AS, Cotter RJ, Chaney M, Little SP, Ball MJ: **Chemical characterization of Abeta 17-42 peptide, a component of diffuse amyloid deposits of Alzheimer disease.** *J Biol Chem* 1994, **269**:10987–90.

97. Higgins LS, Murphy GM, Forno LS, Catalano R, Cordell B, Cordell B: **P3 beta-amyloid peptide has a unique and potentially pathogenic immunohistochemical profile in Alzheimer's disease brain.** *Am J Pathol* 1996, **149**:585–96.

98. Dulin F, Léveillé F, Ortega JB, Mornon J-P, Buisson A, Callebaut I, Colloc'h N: **p3 peptide, a truncated form of Aβ devoid of synaptotoxic effect, does not assemble into soluble oligomers**. *FEBS Lett* 2008, **582**:1865–1870.

99. Sisodia SS: **Beta-amyloid precursor protein cleavage by a membrane-bound protease.** *Proc Natl Acad Sci U S A* 1992, **89**:6075–9.

100. Roberts SB, Ripellino JA, Ingalls KM, Robakis NK, Felsenstein KM: **Non-amyloidogenic cleavage of the beta-amyloid precursor protein by an integral membrane metalloendopeptidase.** *J Biol Chem* 1994, **269**:3111–6.

101. Koike H, Tomioka S, Sorimachi H, Saido TC, Maruyama K, Okuyama A, Fujisawa-Sehara A, Ohno S, Suzuki K, Ishiura S: **Membrane-anchored metalloprotease MDC9 has an alpha-secretase activity responsible for processing the amyloid precursor protein.** *Biochem J* 1999, **343 Pt 2**:371–5.

102. Asai M, Hattori C, Szabó B, Sasagawa N, Maruyama K, Tanuma S, Ishiura S: **Putative function of ADAM9, ADAM10, and ADAM17 as APP alpha-secretase.** *Biochem Biophys Res Commun* 2003, **301**:231–5.

103. Lammich S, Kojro E, Postina R, Gilbert S, Pfeiffer R, Jasionowski M, Haass C, Fahrenholz F: **Constitutive and regulated alpha-secretase cleavage of Alzheimer's amyloid precursor protein by a disintegrin metalloprotease.** *Proc Natl Acad Sci U S A* 1999, **96**:3922–7.

104. Buxbaum JD, Liu KN, Luo Y, Slack JL, Stocking KL, Peschon JJ, Johnson RS, Castner BJ, Cerretti DP, Black RA: **Evidence that tumor necrosis factor alpha converting enzyme is involved in regulated alpha-secretase cleavage of the Alzheimer amyloid protein precursor.** *J Biol Chem* 1998, **273**:27765–7.

105. Tanabe C, Hotoda N, Sasagawa N, Sehara-Fujisawa A, Maruyama K, Ishiura S: **ADAM19 is tightly associated with constitutive Alzheimer's disease APP α-secretase in A172 cells**. *Biochem Biophys Res Commun* 2007, **352**:111–117.

106. Blacker M, Noe MC, Carty TJ, Goodyer CG, LeBlanc AC: **Effect of tumor necrosis factor-alpha converting enzyme (TACE) and metalloprotease inhibitor on amyloid precursor protein metabolism in human neurons.** *J Neurochem* 2002, **83**:1349–57.

107. Kuhn P-H, Wang H, Dislich B, Colombo A, Zeitschel U, Ellwart JW, Kremmer E, Roßner S, Lichtenthaler SF: **ADAM10 is the physiologically relevant, constitutive α-secretase of the amyloid precursor protein in primary neurons**. *EMBO J* 2010, **29**:3020–3032.

108. Hotoda N, Koike H, Sasagawa N, Ishiura S: **A secreted form of human ADAM9 has an α-secretase activity for APP**. *Biochem Biophys Res Commun* 2002, **293**:800–805.

109. Marballi K, Cruz D, Thompson P, Walss-Bass C: **Differential neuregulin 1 cleavage in the prefrontal cortex and hippocampus in schizophrenia and bipolar disorder: preliminary findings.** *PLoS One* 2012, **7**:e36431.

110. Hussain I, Powell D, Howlett DR, Tew DG, Meek TD, Chapman C, Gloger IS, Murphy KE, Southan CD, Ryan DM, Smith TS, Simmons DL, Walsh FS, Dingwall C, Christie G: **Identification of a Novel Aspartic Protease (Asp 2) as β-Secretase**. *Mol Cell Neurosci* 1999, **14**:419–427.

111. Vassar R, Bennett BD, Babu-Khan S, Kahn S, Mendiaz EA, Denis P, Teplow DB, Ross S, Amarante P, Loeloff R, Luo Y, Fisher S, Fuller J, Edenson S, Lile J, Jarosinski MA, Biere AL, Curran E, Burgess T, Louis JC, Collins F, Treanor J, Rogers G, Citron M: **Beta-secretase cleavage of Alzheimer's amyloid precursor protein by the transmembrane aspartic protease BACE.** *Science* 1999, **286**:735–41.

112. Yan R, Gurney ME, Bienkowski MJ, Shuck ME, Miao H, Tory MC, Pauley AM, Brashler JR, Stratman NC, Mathews WR, Buhl AE, Carter DB, Tomasselli AG, Parodi LA, Heinrikson RL: **Membrane-anchored aspartyl protease with Alzheimer's disease beta-secretase activity.** *Nature* 1999, **402**:533–537.

113. Sinha S, Anderson JP, Barbour R, Basi GS, Caccavello R, Davis D, Doan M, Dovey HF, Frigon N, Hong J, Jacobson-Croak K, Jewett N, Keim P, Knops J, Lieberburg I, Power M, Tan H, Tatsuno G, Tung J, Schenk D, Seubert P, Suomensaari SM, Wang S, Walker D, Zhao J, McConlogue L, John V: **Purification and cloning of amyloid precursor protein beta-secretase from human brain.** *Nature* 1999, **402**:537–540.

114. Lin X, Koelsch G, Wu S, Downs D, Dashti A, Tang J: **Human aspartic protease memapsin 2 cleaves the beta-secretase site of beta-amyloid precursor protein.** *Proc Natl Acad Sci U S A* 2000, **97**:1456–60.

115. Marcinkiewicz M, Seidah NG: **Coordinated expression of beta-amyloid precursor protein and the putative beta-secretase BACE and alpha-secretase ADAM10 in mouse and human brain.** *J Neurochem* 2000, **75**:2133–43.

116. Huse JT, Pijak DS, Leslie GJ, Lee VM-Y, Doms RW: **Maturation and endosomal targeting of beta-site amyloid precursor protein-cleaving enzyme. The Alzheimer's disease beta-secretase.** *J Biol Chem* 2000, **275**:33729–33737.

117. Walter J, Fluhrer R, Hartung B, Willem M, Kaether C, Capell A, Lammich S, Multhaup G, Haass C: **Phosphorylation Regulates Intracellular Trafficking of Beta Secretase**. *J Biol Chem* 2001, **276**:14634–14641.

118. Huse JT, Liu K, Pijak DS, Carlin D, Lee VM-Y, Doms RW: **Beta-secretase Processing in the**

Trans-Golgi Network Preferentially Generates Truncated Amyloid Species That Accumulate in Alzheimer's Disease Brain. *J Biol Chem* 2002, **277**:16278–16284.

119. Hook V, Toneff T, Bogyo M, Greenbaum D, Medzihradszky KF, Neveu J, Lane W, Hook G, Reisine T: **Inhibition of cathepsin B reduces β-amyloid production in regulated secretory vesicles of neuronal chromaffin cells: evidence for cathepsin B as a candidate β-secretase of Alzheimer's disease**. *Biol Chem* 2005, **386**:931–40.

120. Hook VYH, Kindy M, Reinheckel T, Peters C, Hook G: **Genetic cathepsin B deficiency reduces β-amyloid in transgenic mice expressing human wild-type amyloid precursor protein**. *Biochem Biophys Res Commun* 2009, **386**:284–288.

121. Thinakaran G, Borchelt DR, Lee MK, Slunt HH, Spitzer L, Kim G, Ratovitsky T, Davenport F, Nordstedt C, Seeger M, Hardy J, Levey AI, Gandy SE, Jenkins NA, Copeland NG, Price DL, Sisodia SS: **Endoproteolysis of presenilin 1 and accumulation of processed derivatives in vivo.** *Neuron* 1996, **17**:181–90.

122. Wolfe MS, Selkoe DJ, Xia W, Ostaszewski BL, Diehl TS, Kimberly WT: **Two transmembrane aspartates in presenilin-1 required for presenilin endoproteolysis and gamma-secretase activity.** *Nature* 1999, **398**:513–517.

123. St George-Hyslop P, Yu G, Nishimura M, Arawaka S, Levitan D, Zhang L, Tandon A, Song Y-Q, Rogaeva E, Chen F, Kawarai T, Supala A, Levesque L, Yu H, Yang D-S, Holmes E, Milman P, Liang Y, Zhang DM, Xu DH, Sato C, Rogaev E, Smith M, Janus C, Zhang Y, Aebersold R, Farrer L, Sorbi S, Bruni A, Fraser P: **Nicastrin modulates presenilin-mediated notch/glp-1 signal transduction and betaAPP processing.** *Nature* 2000, **407**:48–54.

124. Francis R, McGrath G, Zhang J, Ruddy DA, Sym M, Apfeld J, Nicoll M, Maxwell M, Hai B, Ellis MC, Parks AL, Xu W, Li J, Gurney M, Myers RL, Himes CS, Hiebsch R, Ruble C, Nye JS, Curtis D: **Aph-1 and pen-2 are required for Notch pathway signaling, gamma-secretase cleavage of betaAPP, and presenilin protein accumulation.** *Dev Cell* 2002, **3**:85–97.

125. Goutte C, Tsunozaki M, Hale VA, Priess JR: **APH-1 is a multipass membrane protein essential for the Notch signaling pathway in Caenorhabditis elegans embryos**. *Proc Natl Acad Sci* 2002, **99**:775–779.

126. Greenfield JP, Xu H, Greengard P, Gandy S, Seeger M: **Generation of the amyloid-beta peptide N terminus in Saccharomyces cerevisiae expressing human Alzheimer's amyloid-beta precursor protein.** *J Biol Chem* 1999, **274**:33843–6.

127. Edbauer D, Winkler E, Regula JT, Pesold B, Steiner H, Haass C: **Reconstitution of γ-secretase activity**. *Nat Cell Biol* 2003, **5**:486–488.

128. Chávez-Gutiérrez L, Tolia A, Maes E, Li T, Wong PC, de Strooper B: **Glu(332) in the Nicastrin ectodomain is essential for gamma-secretase complex maturation but not for its activity.** *J Biol Chem* 2008, **283**:20096–105.

129. Kimberly WT, LaVoie MJ, Ostaszewski BL, Ye W, Wolfe MS, Selkoe DJ: **Gamma-Secretase is a membrane protein complex comprised of presenilin, nicastrin, aph-1, and pen-2**. *Proc Natl Acad Sci* 2003, **100**:6382–6387.

130. Luo W -j., Wang H, Li H, Kim BS, Shah S, Lee H-J, Thinakaran G, Kim T-W, Yu G, Xu H: **PEN-2 and APH-1 Coordinately Regulate Proteolytic Processing of Presenilin 1**. *J Biol Chem* 2003, **278**:7850–7854.

131. Zhou S, Zhou H, Walian PJ, Jap BK: **CD147 is a regulatory subunit of the gamma-secretase complex in Alzheimer's disease amyloid beta-peptide production.** *Proc Natl Acad Sci* 2005,

102:7499–7504.

132. Vetrivel KS, Gong P, Bowen JW, Cheng H, Chen Y, Carter M, Nguyen PD, Placanica L, Wieland FT, Li Y-M, Kounnas MZ, Thinakaran G: **Dual roles of the transmembrane protein p23/TMP21 in the modulation of amyloid precursor protein metabolism.** *Mol Neurodegener* 2007, **2**:4.

133. He G, Luo W, Li P, Remmers C, Netzer WJ, Hendrick J, Bettayeb K, Flajolet M, Gorelick F, Wennogle LP, Greengard P: **Gamma-secretase activating protein is a therapeutic target for Alzheimer's disease**. *Nature* 2010, **467**:95–98.

134. Walter J, Haass C: **Posttranslational Modifications of Amyloid Precursor Protein: Ectodomain Phosphorylation and Sulfation**. In *Alzheimer's Disease*. *Volume 32*. New Jersey: Humana Press; 2000:149–168.

135. Ehehalt R, Keller P, Haass C, Thiele C, Simons K: **Amyloidogenic processing of the Alzheimer beta-amyloid precursor protein depends on lipid rafts.** *J Cell Biol* 2003, **160**:113–23.

136. Riddell DR, Christie G, Hussain I, Dingwall C: **Compartmentalization of beta-secretase (Asp2) into low-buoyant density, noncaveolar lipid rafts.** *Curr Biol* 2001, **11**:1288–93.

137. Vetrivel KS, Cheng H, Lin W, Sakurai T, Li T, Nukina N, Wong PC, Xu H, Thinakaran G: **Association of γ-Secretase with Lipid Rafts in Post-Golgi and Endosome Membranes**. *J Biol Chem* 2004, **279**:44945–44954.

138. Vetrivel KS, Cheng H, Kim S-H, Chen Y, Barnes NY, Parent AT, Sisodia SS, Thinakaran G: **Spatial Segregation of γ-Secretase and Substrates in Distinct Membrane Domains**. *J Biol Chem* 2005, **280**:25892–25900.

139. Rajendran L, Honsho M, Zahn TR, Keller P, Geiger KD, Verkade P, Simons K: **Alzheimer's disease beta-amyloid peptides are released in association with exosomes.** *Proc Natl Acad Sci U S A* 2006, **103**:11172–7.

140. Hutton M, Heutink P, Lendon CL, Rizzu P, Baker M, Froelich S, Houlden H, Pickering-Brown S, Chakraverty S, Isaacs A, Grover A, Hackett J, Adamson J, Lincoln S, Dickson D, Davies P, Petersen RC, Stevens M, de Graaff E, Wauters E, van Baren J, Hillebrand M, Joosse M, Kwon JM, Nowotny P, Che LK, Norton J, Morris JC, Reed LA, Trojanowski J, et al.: **Association of missense and 5'-splice-site mutations in tau with the inherited dementia FTDP-17.** *Nature* 1998, **393**:702–705.

141. Poorkaj P, Bird TD, Wijsman E, Nemens E, Garruto RM, Anderson L, Andreadis A, Wiederholt WC, Raskind M, Schellenberg GD: **Tau is a candidate gene for chromosome 17 frontotemporal dementia**. *Ann Neurol* 1998, **43**:815–825.

142. Spillantini MG, Bird TD, Ghetti B: **Frontotemporal dementia and Parkinsonism linked to chromosome 17: a new group of tauopathies.** *Brain Pathol* 1998, **8**:387–402.

143. Lewis J, Dickson DW, Lin WL, Chisholm L, Corral A, Jones G, Yen SH, Sahara N, Skipper L, Yager D, Eckman C, Hardy J, Hutton M, McGowan E: **Enhanced Neurofibrillary Degeneration in Transgenic Mice Expressing Mutant Tau and APP**. *Science (80-)* 2001, **293**:1487–1491.

144. Lambert MP, Barlow AK, Chromy BA, Edwards C, Freed R, Liosatos M, Morgan TE, Rozovsky I, Trommer B, Viola KL, Wals P, Zhang C, Finch CE, Krafft GA, Klein WL: **Diffusible, nonfibrillar ligands derived from Abeta1-42 are potent central nervous system neurotoxins.** *Proc Natl Acad Sci U S A* 1998, **95**:6448–53.

145. Shankar GM, Li S, Mehta TH, Garcia-Munoz A, Shepardson NE, Smith I, Brett FM, Farrell MA, Rowan MJ, Lemere CA, Regan CM, Walsh DM, Sabatini BL, Selkoe DJ: **Amyloid-beta protein dimers isolated directly from Alzheimer's brains impair synaptic plasticity and memory.** *Nat*

Med 2008, **14**:837–42.

146. Walsh DM, Klyubin I, Fadeeva J V., Cullen WK, Anwyl R, Wolfe MS, Rowan MJ, Selkoe DJ: **Naturally secreted oligomers of amyloid β protein potently inhibit hippocampal long-term potentiation in vivo**. *Nature* 2002, **416**:535–539.

147. Lesné S, Koh MT, Kotilinek L, Kayed R, Glabe CG, Yang A, Gallagher M, Ashe KH: **A specific amyloid-β protein assembly in the brain impairs memory**. *Nature* 2006, **440**:352–357.

148. Esparza TJ, Zhao H, Cirrito JR, Cairns NJ, Bateman RJ, Holtzman DM, Brody DL: **Amyloid-β oligomerization in Alzheimer dementia versus high-pathology controls.** *Ann Neurol* 2013, **73**:104–19.

149. Selkoe DJ, Hardy J: **The amyloid hypothesis of Alzheimer's disease at 25 years**. *EMBO Mol Med* 2016, **8**:595–608.

150. Braak H, Braak E: **Frequency of stages of Alzheimer-related lesions in different age categories.** *Neurobiol Aging* 1997, **18**:351–7.

151. de Leon MJ, Convit A, Wolf OT, Tarshish CY, DeSanti S, Rusinek H, Tsui W, Kandil E, Scherer AJ, Roche A, Imossi A, Thorn E, Bobinski M, Caraos C, Lesbre P, Schlyer D, Poirier J, Reisberg B, Fowler J: **Prediction of cognitive decline in normal elderly subjects with 2-[18F]fluoro-2-deoxy-D-glucose/positron-emission tomography (FDG/PET)**. *Proc Natl Acad Sci* 2001, **98**:10966–10971.

152. de Leon MJ, Golomb J, George AE, Convit A, Tarshish CY, McRae T, De Santi S, Smith G, Ferris SH, Noz M: **The radiologic prediction of Alzheimer disease: the atrophic hippocampal formation.** *AJNR Am J Neuroradiol* 1993, **14**:897–906.

153. Visser PJ, Verhey FRJ, Hofman PAM, Scheltens P, Jolles J: **Medial temporal lobe atrophy predicts Alzheimer's disease in patients with minor cognitive impairment.** *J Neurol Neurosurg Psychiatry* 2002, **72**:491–7.

154. Dubois B, Feldman HH, Jacova C, DeKosky ST, Barberger-Gateau P, Cummings J, Delacourte A, Galasko D, Gauthier S, Jicha G, Meguro K, O'Brien J, Pasquier F, Robert P, Rossor M, Salloway S, Stern Y, Visser PJ, Scheltens P: **Research criteria for the diagnosis of Alzheimer's disease: revising the NINCDS–ADRDA criteria**. *Lancet Neurol* 2007, **6**:734–746.

155. Mayeux R: **Evaluation and use of diagnostic tests in Alzheimer's disease.** *Neurobiol Aging* 1998, **19**:139–43.

156. Beach TG, Monsell SE, Phillips LE, Kukull W: **Accuracy of the clinical diagnosis of Alzheimer disease at National Institute on Aging Alzheimer Disease Centers, 2005-2010.** *J Neuropathol Exp Neurol* 2012, **71**:266–73.

157. Bibl M, Esselmann H, Wiltfang J: **Neurochemical biomarkers in Alzheimer's disease and related disorders.** *Ther Adv Neurol Disord* 2012, **5**:335–48.

158. Motter R, Vigo-Pelfrey C, Kholodenko D, Barbour R, Johnson-Wood K, Galasko D, Chang L, Miller B, Clark C, Green R, Olson D, Southwick P, Wolfert R, Munroe B, Lieberburg I, Seubert P, Schenk D: **Reduction of beta-amyloid peptide42 in the cerebrospinal fluid of patients with Alzheimer's disease**. *Ann Neurol* 1995, **38**:643–648.

159. Lewczuk P, Esselmann H, Otto M, Maler JM, Henkel AW, Henkel MK, Eikenberg O, Antz C, Krause W-R, Reulbach U, Kornhuber J, Wiltfang J: **Neurochemical diagnosis of Alzheimer's dementia by CSF Aβ42, Aβ42/Aβ40 ratio and total tau**. *Neurobiol Aging* 2004, **25**:273–281.

160. Wiltfang J, Esselmann H, Smirnov A, Bibl M, Cepek L, Steinacker P, Mollenhauer B, Buerger K, Hampel H, Paul S, Neumann M, Maler M, Zerr I, Kornhuber J, Kretzschmar HA, Poser S, Otto M:

Beta-amyloid peptides in cerebrospinal fluid of patients with Creutzfeldt-Jakob disease. *Ann Neurol* 2003, **54**:263–267.

161. Sjögren M, Gisslén M, Vanmechelen E, Blennow K: **Low cerebrospinal fluid beta-amyloid 42 in patients with acute bacterial meningitis and normalization after treatment.** *Neurosci Lett* 2001, **314**:33–6.

162. Hulstaert F, Blennow K, Ivanoiu A, Schoonderwaldt HC, Riemenschneider M, De Deyn PP, Bancher C, Cras P, Wiltfang J, Mehta PD, Iqbal K, Pottel H, Vanmechelen E, Vanderstichele H: **Improved discrimination of AD patients using beta-amyloid(1-42) and tau levels in CSF.** *Neurology* 1999, **52**:1555–62.

163. Blennow K: **Cerebrospinal fluid protein biomarkers for Alzheimer's disease**. *NeuroRX* 2004, **1**:213–225.

164. Bibl M, Mollenhauer B, Esselmann H, Lewczuk P, Klafki H-W, Sparbier K, Smirnov A, Cepek L, Trenkwalder C, Rüther E, Kornhuber J, Otto M, Wiltfang J: **CSF amyloid-beta-peptides in Alzheimer's disease, dementia with Lewy bodies and Parkinson's disease dementia**. *Brain* 2006, **129**:1177–1187.

165. Wiltfang J, Esselmann H, Bibl M, Smirnov A, Otto M, Paul S, Schmidt B, Klafki H-W, Maler M, Dyrks T, Bienert M, Beyermann M, Rüther E, Kornhuber J: **Highly conserved and disease-specific patterns of carboxyterminally truncated Abeta peptides 1-37/38/39 in addition to 1-40/42 in Alzheimer's disease and in patients with chronic neuroinflammation.** *J Neurochem* 2002, **81**:481–96.

166. Lewczuk P, Kamrowski-Kruck H, Peters O, Heuser I, Jessen F, Popp J, Bürger K, Hampel H, Frölich L, Wolf S, Prinz B, Jahn H, Luckhaus C, Perneczky R, Hüll M, Schröder J, Kessler H, Pantel J, Gertz H-J, Klafki H-W, Kölsch H, Reulbach U, Esselmann H, Maler JM, Bibl M, Kornhuber J, Wiltfang J: **Soluble amyloid precursor proteins in the cerebrospinal fluid as novel potential biomarkers of Alzheimer's disease: a multicenter study.** *Mol Psychiatry* 2010, **15**:138–45.

167. Jensen M, Basun H, Lannfelt L: **Increased cerebrospinal fluid tau in patients with Alzheimer's disease.** *Neurosci Lett* 1995, **186**:189–91.

168. Vigo-Pelfrey C, Seubert P, Barbour R, Blomquist C, Lee M, Lee D, Coria F, Chang L, Miller B, Lieberburg I: **Elevation of microtubule-associated protein tau in the cerebrospinal fluid of patients with Alzheimer's disease.** *Neurology* 1995, **45**:788–93.

169. Blennow K, Wallin A, Ågren H, Spenger C, Siegfried J, Vanmechelen E: **Tau protein in cerebrospinal fluid.** *Mol Chem Neuropathol* 1995, **26**:231–245.

170. Andreasen N, Minthon L, Clarberg A, Davidsson P, Gottfries J, Vanmechelen E, Vanderstichele H, Winblad B, Blennow K: **Sensitivity, specificity, and stability of CSF-tau in AD in a community-based patient sample.** *Neurology* 1999, **53**:1488–94.

171. Lewczuk P, Esselmann H, Bibl M, Beck G, Maler JM, Otto M, Kornhuber J, Wiltfang J: **Tau Protein Phosphorylated at Threonine 181 in CSF as a Neurochemical Biomarker in Alzheimer's Disease: Original Data and Review of the Literature**. *J Mol Neurosci* 2004, **23**:115–122.

172. Itoh N, Arai H, Urakami K, Ishiguro K, Ohno H, Hampel H, Buerger K, Wiltfang J, Otto M, Kretzschmar H, Moeller HJ, Imagawa M, Kohno H, Nakashima K, Kuzuhara S, Sasaki H, Imahori K: **Large-scale, multicenter study of cerebrospinal fluid tau protein phosphorylated at serine 199 for the antemortem diagnosis of Alzheimer's disease.** *Ann Neurol* 2001, **50**:150–6.

173. Hampel H, Buerger K, Kohnken R, Teipel SJ, Zinkowski R, Moeller HJ, Rapoport SI, Davies P: **Tracking of Alzheimer's disease progression with cerebrospinal fluid tau protein phosphorylated**

at threonine 231. *Ann Neurol* 2001, **49**:545–6.

174. Shaw LM, Vanderstichele H, Knapik-Czajka M, Figurski M, Coart E, Blennow K, Soares H, Simon AJ, Lewczuk P, Dean RA, Siemers E, Potter W, Lee VM-Y, Trojanowski JQ, Alzheimer's Disease Neuroimaging Initiative: **Qualification of the analytical and clinical performance of CSF biomarker analyses in ADNI**. *Acta Neuropathol* 2011, **121**:597–609.

175. Shoji M, Kanai M, Matsubara E, Ikeda M, Harigaya Y, Okamoto K, Hirai S: **Taps to Alzheimer's patients: A continuous Japanese study of cerebrospinal fluid biomarkers**. *Ann Neurol* 2000, **48**:402–402.

176. Welge V, Fiege O, Lewczuk P, Mollenhauer B, Esselmann H, Klafki H-W, Wolf S, Trenkwalder C, Otto M, Kornhuber J, Wiltfang J, Bibl M: **Combined CSF tau, p-tau181 and amyloid-beta 38/40/42 for diagnosing Alzheimer's disease.** *J Neural Transm* 2009, **116**:203–12.

177. Zetterberg H, Wahlund L-O, Blennow K: **Cerebrospinal fluid markers for prediction of Alzheimer's disease.** *Neurosci Lett* 2003, **352**:67–9.

178. Struyfs H, Molinuevo JL, Martin J-J, De Deyn PP, Engelborghs S: **Validation of the AD-CSF-index in autopsy-confirmed Alzheimer's disease patients and healthy controls.** *J Alzheimers Dis* 2014, **41**:903–9.

179. Reiber H: **Dynamics of brain-derived proteins in cerebrospinal fluid.** *Clin Chim Acta* 2001, **310**:173–86.

180. Preston SD, Steart P V, Wilkinson A, Nicoll JAR, Weller RO: **Capillary and arterial cerebral amyloid angiopathy in Alzheimer's disease: defining the perivascular route for the elimination of amyloid beta from the human brain.** *Neuropathol Appl Neurobiol* 2003, **29**:106–17.

181. Lewczuk P, Esselmann H, Bibl M, Paul S, Svitek J, Miertschischk J, Meyrer R, Smirnov A, Maler JM, Klein C, Otto M, Bleich S, Sperling W, Kornhuber J, Rüther E, Wiltfang J: **Electrophoretic separation of amyloid β peptides in plasma**. *Electrophoresis* 2004, **25**:3336–3343.

182. van Oijen M, Hofman A, Soares HD, Koudstaal PJ, Breteler MM: **Plasma Aβ1–40 and Aβ1–42 and the risk of dementia: a prospective case-cohort study**. *Lancet Neurol* 2006, **5**:655–660.

183. Mayeux R, Honig LS, Tang M-X, Manly J, Stern Y, Schupf N, Mehta PD: **Plasma A[beta]40 and A[beta]42 and Alzheimer's disease: relation to age, mortality, and risk.** *Neurology* 2003, **61**:1185–90.

184. Abdullah L, Paris D, Luis C, Quadros A, Parrish J, Valdes L, Keegan AP, Mathura V, Crawford F, Mullan M: **The influence of diagnosis, intra- and inter-person variability on serum and plasma Aβ levels**. *Neurosci Lett* 2007, **428**:53–58.

185. Graff-Radford NR, Crook JE, Lucas J, Boeve BF, Knopman DS, Ivnik RJ, Smith GE, Younkin LH, Petersen RC, Younkin SG: **Association of Low Plasma Aβ42/Aβ40 Ratios With Increased Imminent Risk for Mild Cognitive Impairment and Alzheimer Disease**. *Arch Neurol* 2007, **64**:354.

186. Lui JK, Laws SM, Li Q-X, Villemagne VL, Ames D, Brown B, Bush AI, De Ruyck K, Dromey J, Ellis KA, Faux NG, Foster J, Fowler C, Gupta V, Hudson P, Laughton K, Masters CL, Pertile K, Rembach A, Rimajova M, Rodrigues M, Rowe CC, Rumble R, Szoeke C, Taddei K, Taddei T, Trounson B, Ward V, Martins RN: **Plasma Amyloid-β as a Biomarker in Alzheimer's Disease: The AIBL Study of Aging**. *J Alzheimer's Dis* 2010, **20**:1233–1242.

187. Lewczuk P, Kornhuber J, Vanmechelen E, Peters O, Heuser I, Maier W, Jessen F, Bürger K, Hampel H, Frölich L, Henn F, Falkai P, Rüther E, Jahn H, Luckhaus C, Perneczky R, Schmidtke K, Schröder J, Kessler H, Pantel J, Gertz H-J, Vanderstichele H, de Meyer G, Shapiro F, Wolf S, Bibl M,

Wiltfang J: **Amyloid β peptides in plasma in early diagnosis of Alzheimer's disease: A multicenter study with multiplexing**. *Exp Neurol* 2010, **223**:366–370.

188. Perneczky R, Guo LH, Kagerbauer SM, Werle L, Kurz A, Martin J, Alexopoulos P: **Soluble amyloid precursor protein β as blood-based biomarker of Alzheimer's disease.** *Transl Psychiatry* 2013, **3**:e227.

189. Takahashi RH, Milner TA, Li F, Nam EE, Edgar MA, Yamaguchi H, Beal MF, Xu H, Greengard P, Gouras GK: **Intraneuronal Alzheimer abeta42 accumulates in multivesicular bodies and is associated with synaptic pathology.** *Am J Pathol* 2002, **161**:1869–79.

190. Joshi P, Turola E, Ruiz A, Bergami A, Libera DD, Benussi L, Giussani P, Magnani G, Comi G, Legname G, Ghidoni R, Furlan R, Matteoli M, Verderio C: **Microglia convert aggregated amyloid-β into neurotoxic forms through the shedding of microvesicles.** *Cell Death Differ* 2014, **21**:582–93.

191. Vingtdeux V, Hamdane M, Loyens A, Gelé P, Drobeck H, Bégard S, Galas M-C, Delacourte A, Beauvillain J-C, Buée L, Sergeant N: **Alkalizing drugs induce accumulation of amyloid precursor protein by-products in luminal vesicles of multivesicular bodies.** *J Biol Chem* 2007, **282**:18197–205.

192. Perez-Gonzalez R, Gauthier SA, Kumar A, Levy E: **The exosome secretory pathway transports amyloid precursor protein carboxyl-terminal fragments from the cell into the brain extracellular space.** *J Biol Chem* 2012, **287**:43108–15.

193. Sharples RA, Vella LJ, Nisbet RM, Naylor R, Perez K, Barnham KJ, Masters CL, Hill AF: **Inhibition of gamma-secretase causes increased secretion of amyloid precursor protein C-terminal fragments in association with exosomes.** *FASEB J* 2008, **22**:1469–78.

194. Sugiura Y, Ikeda K, Nakano M: **High Membrane Curvature Enhances Binding, Conformational Changes, and Fibrillation of Amyloid-β on Lipid Bilayer Surfaces.** *Langmuir* 2015, **31**:11549–57.

195. Goetzl EJ, Mustapic M, Kapogiannis D, Eitan E, Lobach I V, Goetzl L, Schwartz JB, Miller BL: **Cargo proteins of plasma astrocyte-derived exosomes in Alzheimer's disease.** *FASEB J* 2016.

196. Wang G, Dinkins M, He Q, Zhu G, Poirier C, Campbell A, Mayer-Proschel M, Bieberich E: **Astrocytes secrete exosomes enriched with proapoptotic ceramide and prostate apoptosis response 4 (PAR-4): potential mechanism of apoptosis induction in Alzheimer disease (AD).** *J Biol Chem* 2012, **287**:21384–95.

197. Yuyama K, Sun H, Mitsutake S, Igarashi Y: **Sphingolipid-modulated exosome secretion promotes clearance of amyloid-β by microglia.** *J Biol Chem* 2012, **287**:10977–89.

198. An K, Klyubin I, Kim Y, Jung JH, Mably AJ, O'Dowd ST, Lynch T, Kanmert D, Lemere CA, Finan GM, Park JW, Kim T-W, Walsh DM, Rowan MJ, Kim J-H: **Exosomes neutralize synaptic-plasticity-disrupting activity of Aβ assemblies in vivo.** *Mol Brain* 2013, **6**:47.

199. Bulloj A, Leal MC, Xu H, Castaño EM, Morelli L: **Insulin-degrading enzyme sorting in exosomes: a secretory pathway for a key brain amyloid-beta degrading protease.** *J Alzheimers Dis* 2010, **19**:79–95.

200. Tamboli IY, Barth E, Christian L, Siepmann M, Kumar S, Singh S, Tolksdorf K, Heneka MT, Lütjohann D, Wunderlich P, Walter J: **Statins promote the degradation of extracellular amyloid beta-peptide by microglia via stimulation of exosome-associated insulin-degrading enzyme (IDE) secretion.** *J Biol Chem* 2010, **285**:37405–14.

201. Katsuda T, Tsuchiya R, Kosaka N, Yoshioka Y, Takagaki K, Oki K, Takeshita F, Sakai Y, Kuroda M, Ochiya T: **Human adipose tissue-derived mesenchymal stem cells secrete functional**

neprilysin-bound exosomes. *Sci Rep* 2013, **3**:1197.

202. Alvarez-Erviti L, Seow Y, Yin H, Betts C, Lakhal S, Wood MJA: **Delivery of siRNA to the mouse brain by systemic injection of targeted exosomes.** *Nat Biotechnol* 2011, **29**:341–5.

203. Haney MJ, Klyachko NL, Zhao Y, Gupta R, Plotnikova EG, He Z, Patel T, Piroyan A, Sokolsky M, Kabanov A V, Batrakova E V: **Exosomes as drug delivery vehicles for Parkinson's disease therapy.** *J Control Release* 2015, **207**:18–30.

204. Yang T, Martin P, Fogarty B, Brown A, Schurman K, Phipps R, Yin VP, Lockman P, Bai S: **Exosome delivered anticancer drugs across the blood-brain barrier for brain cancer therapy in Danio rerio.** *Pharm Res* 2015, **32**:2003–14.

205. Dinkins MB, Dasgupta S, Wang G, Zhu G, Bieberich E: **Exosome reduction in vivo is associated with lower amyloid plaque load in the 5XFAD mouse model of Alzheimer's disease.** *Neurobiol Aging* 2014, **35**:1792–800.

206. Dinkins MB, Dasgupta S, Wang G, Zhu G, He Q, Kong JN, Bieberich E: **The 5XFAD Mouse Model of Alzheimer's Disease Exhibits an Age-Dependent Increase in Anti-Ceramide IgG and Exogenous Administration of Ceramide Further Increases Anti-Ceramide Titers and Amyloid Plaque Burden.** *J Alzheimers Dis* 2015, **46**:55–61.

207. Saman S, Kim W, Raya M, Visnick Y, Miro S, Saman S, Jackson B, McKee AC, Alvarez VE, Lee NCY, Hall GF: **Exosome-associated tau is secreted in tauopathy models and is selectively phosphorylated in cerebrospinal fluid in early Alzheimer disease.** *J Biol Chem* 2012, **287**:3842–9.

208. Kanmert D, Cantlon A, Muratore CR, Jin M, O'Malley TT, Lee G, Young-Pearse TL, Selkoe DJ, Walsh DM: **C-Terminally Truncated Forms of Tau, But Not Full-Length Tau or Its C-Terminal Fragments, Are Released from Neurons Independently of Cell Death.** *J Neurosci* 2015, **35**:10851–65.

209. Asai H, Ikezu S, Tsunoda S, Medalla M, Luebke J, Haydar T, Wolozin B, Butovsky O, Kügler S, Ikezu T: **Depletion of microglia and inhibition of exosome synthesis halt tau propagation.** *Nat Neurosci* 2015, **18**:1584–93.

210. Polanco JC, Scicluna BJ, Hill AF, Götz J: **Extracellular Vesicles Isolated from the Brains of rTg4510 Mice Seed Tau Protein Aggregation in a Threshold-dependent Manner.** *J Biol Chem* 2016, **291**:12445–66.

211. Santa-Maria I, Varghese M, Ksiezak-Reding H, Dzhun A, Wang J, Pasinetti GM: **Paired helical filaments from Alzheimer disease brain induce intracellular accumulation of Tau protein in aggresomes.** *J Biol Chem* 2012, **287**:20522–33.

212. Fauré J, Lachenal G, Court M, Hirrlinger J, Chatellard-Causse C, Blot B, Grange J, Schoehn G, Goldberg Y, Boyer V, Kirchhoff F, Raposo G, Garin J, Sadoul R: **Exosomes are released by cultured cortical neurones.** *Mol Cell Neurosci* 2006, **31**:642–8.

213. Simpson RJ, Jensen SS, Lim JWE: **Proteomic profiling of exosomes: current perspectives.** *Proteomics* 2008, **8**:4083–99.

214. Fiandaca MS, Kapogiannis D, Mapstone M, Boxer A, Eitan E, Schwartz JB, Abner EL, Petersen RC, Federoff HJ, Miller BL, Goetzl EJ: **Identification of preclinical Alzheimer's disease by a profile of pathogenic proteins in neurally derived blood exosomes: A case-control study.** *Alzheimers Dement* 2015, **11**:600–7.e1.

215. Kapogiannis D, Boxer A, Schwartz JB, Abner EL, Biragyn A, Masharani U, Frassetto L, Petersen RC, Miller BL, Goetzl EJ: **Dysfunctionally phosphorylated type 1 insulin receptor substrate in**

neural-derived blood exosomes of preclinical Alzheimer's disease. *FASEB J* 2015, **29**:589–96.

216. Goetzl EJ, Boxer A, Schwartz JB, Abner EL, Petersen RC, Miller BL, Kapogiannis D: **Altered lysosomal proteins in neural-derived plasma exosomes in preclinical Alzheimer disease.** *Neurology* 2015, **85**:40–7.

217. Winston CN, Goetzl EJ, Akers JC, Carter BS, Rockenstein EM, Galasko D, Masliah E, Rissman RA: **Prediction of conversion from mild cognitive impairment to dementia with neuronally derived blood exosome protein profile.** *Alzheimer's Dement (Amsterdam, Netherlands)* 2016, **3**:63–72.

218. Lugli G, Cohen AM, Bennett DA, Shah RC, Fields CJ, Hernandez AG, Smalheiser NR: **Plasma Exosomal miRNAs in Persons with and without Alzheimer Disease: Altered Expression and Prospects for Biomarkers.** *PLoS One* 2015, **10**:e0139233.

219. Liu C-G, Song J, Zhang Y-Q, Wang P-C: **MicroRNA-193b is a regulator of amyloid precursor protein in the blood and cerebrospinal fluid derived exosomal microRNA-193b is a biomarker of Alzheimer's disease.** *Mol Med Rep* 2014, **10**:2395–400.

220. Cheng L, Doecke JD, Sharples RA, Villemagne VL, Fowler CJ, Rembach A, Martins RN, Rowe CC, Macaulay SL, Masters CL, Hill AF, Australian Imaging, Biomarkers and Lifestyle (AIBL) Research Group: **Prognostic serum miRNA biomarkers associated with Alzheimer's disease shows concordance with neuropsychological and neuroimaging assessment.** *Mol Psychiatry* 2015, **20**:1188–96.

221. Sarkar S, Jun S, Rellick S, Quintana DD, Cavendish JZ, Simpkins JW: **Expression of microRNA-34a in Alzheimer's disease brain targets genes linked to synaptic plasticity, energy metabolism, and resting state network activity.** *Brain Res* 2016, **1646**:139–51.

222. Crawford N: **The presence of contractile proteins in platelet microparticles isolated from human and animal platelet-free plasma.** *Br J Haematol* 1971, **21**:53–69.

223. Dalton AJ: **Microvesicles and vesicles of multivesicular bodies versus "virus-like" particles.** *J Natl Cancer Inst* 1975, **54**:1137–48.

224. Caby M-P, Lankar D, Vincendeau-Scherrer C, Raposo G, Bonnerot C: **Exosomal-like vesicles are present in human blood plasma**. *Int Immunol* 2005, **17**:879–887.

225. Hunter MP, Ismail N, Zhang X, Aguda BD, Lee EJ, Yu L, Xiao T, Schafer J, Lee M-LT, Schmittgen TD, Nana-Sinkam SP, Jarjoura D, Marsh CB: **Detection of microRNA expression in human peripheral blood microvesicles.** *PLoS One* 2008, **3**:e3694.

226. Skog J, Würdinger T, van Rijn S, Meijer DH, Gainche L, Sena-Esteves M, Curry WT, Carter BS, Krichevsky AM, Breakefield XO, Breakefield XO: **Glioblastoma microvesicles transport RNA and proteins that promote tumour growth and provide diagnostic biomarkers.** *Nat Cell Biol* 2008, **10**:1470–6.

227. Lässer C, Seyed Alikhani V, Ekström K, Eldh M, Torregrosa Paredes P, Bossios A, Sjöstrand M, Gabrielsson S, Lötvall J, Valadi H: **Human saliva, plasma and breast milk exosomes contain RNA: uptake by macrophages**. *J Transl Med* 2011, **9**:9.

228. Gui Y, Liu H, Zhang L, Lv W, Hu X: **Altered microRNA profiles in cerebrospinal fluid exosome in Parkinson disease and Alzheimer disease.** *Oncotarget* 2015, **6**:37043–53.

229. Conde-Vancells J, Falcon-Perez JM: **Isolation of Urinary Exosomes from Animal Models to Unravel Noninvasive Disease Biomarkers**. In *Liver Proteomics*. *Volume 909*. Totowa, NJ: Humana Press; 2012:321–340.

230. Wolfers J, Lozier A, Raposo G, Regnault A, Théry C, Masurier C, Flament C, Pouzieux S, Faure F, Tursz T, Angevin E, Amigorena S, Zitvogel L: **Tumor-derived exosomes are a source of shared tumor rejection antigens for CTL cross-priming.** *Nat Med* 2001, **7**:297–303.

231. Taylor DD, Gerçel-Taylor C: **Tumour-derived exosomes and their role in cancer-associated T-cell signalling defects**. *Br J Cancer* 2005, **92**:305–11.

232. Grad LI, Pokrishevsky E, Silverman JM, Cashman NR: **Exosome-dependent and independent mechanisms are involved in prion-like transmission of propagated Cu/Zn superoxide dismutase misfolding**. *Prion* 2014, **8**:331–335.

233. Witwer KW, Buzás EI, Bemis LT, Bora A, Lässer C, Lötvall J, Nolte-'t Hoen EN, Piper MG, Sivaraman S, Skog J, Théry C, Wauben MH, Hochberg F: **Standardization of sample collection, isolation and analysis methods in extracellular vesicle research.** *J Extracell vesicles* 2013, **2**.

234. Welton JL, Webber JP, Botos L-A, Jones M, Clayton A: **Ready-made chromatography columns for extracellular vesicle isolation from plasma.** *J Extracell vesicles* 2015, **4**:27269.

235. **Dynamic light scattering common terms defined Z-Average size** [www.malvern.com/contact]

236. **Dynamic Light Scattering Training Achieving reliable nano particle sizing** [http://149.171.168.221/partcat/wp-content/uploads/Malvern-Zetasizer-LS.pdf]

237. **Dynamic Light Scattering for Nanoparticle Size Analysis - HORIBA** [http://www.horiba.com/scientific/products/particle-characterization/technology/dynamic-light-scattering/]

238. Egerton RF: *Physical Principles of Electron Microscopy : An Introduction to TEM, SEM, and AEM*. Springer Science+Business Media; 2005.

239. **The Transmission Electron Microscope** [http://www.nobelprize.org/educational/physics/microscopes/tem/]

240. **Transmission Electron Microscopy | Central Microscopy Research Facility** [https://cmrf.research.uiowa.edu/transmission-electron-microscopy]

241. Savina A, Vidal M, Colombo MI: **The exosome pathway in K562 cells is regulated by Rab11.** *J Cell Sci* 2002, **115**(Pt 12):2505–15.

242. Rosa IM, Henriques AG, Carvalho L, Oliveira J, da Cruz e Silva OAB: **Screening Younger Individuals in a Primary Care Setting Flags Putative Dementia Cases and Correlates Gastrointestinal Diseases with Poor Cognitive Performance**. *Dement Geriatr Cogn Disord* 2017, **43**:15–28.

243. Morris JC: **The Clinical Dementia Rating (CDR): current version and scoring rules.** *Neurology* 1993, **43**:2412–4.

244. Caradec J, Kharmate G, Hosseini-Beheshti E, Adomat H, Gleave M, Guns E: **Reproducibility and efficiency of serum-derived exosome extraction methods.** *Clin Biochem* 2014, **47**:1286–92.

245. Helwa I, Cai J, Drewry MD, Zimmerman A, Dinkins MB, Khaled ML, Seremwe M, Dismuke WM, Bieberich E, Stamer WD, Hamrick MW, Liu Y: **A Comparative Study of Serum Exosome Isolation Using Differential Ultracentrifugation and Three Commercial Reagents.** *PLoS One* 2017, **12**:e0170628.

246. Andreu Z, Rivas E, Sanguino-Pascual A, Lamana A, Marazuela M, González-Alvaro I, Sánchez-Madrid F, de la Fuente H, Yáñez-Mó M: **Comparative analysis of EV isolation procedures for**

miRNAs detection in serum samples. *J Extracell vesicles* 2016, **5**:31655.

247. Lobb RJ, Becker M, Wen SW, Wong CSF, Wiegmans AP, Leimgruber A, Möller A: **Optimized exosome isolation protocol for cell culture supernatant and human plasma.** *J Extracell vesicles* 2015, **4**:27031.

248. Ge Q, Zhou Y, Lu J, Bai Y, Xie X, Lu Z: **miRNA in Plasma Exosome is Stable under Different Storage Conditions**. *Molecules* 2014, **19**:1568–1575.

249. Kuchinskiene Z, Carlson LA: **Composition, concentration, and size of low density lipoproteins and of subfractions of very low density lipoproteins from serum of normal men and women.** *J Lipid Res* 1982, **23**:762–9.

250. Scheffer PG, Bakker SJ, Heine RJ, Teerlink T: **Measurement of low-density lipoprotein particle size by high-performance gel-filtration chromatography.** *Clin Chem* 1997, **43**:1904–12.

251. Krauss RM: **Lipids and lipoproteins in patients with type 2 diabetes.** *Diabetes Care* 2004, **27**:1496–504.

252. Grigor'eva AE, Dyrkheeva NS, Bryzgunova OE, Tamkovich SN, Chelobanov BP, Ryabchikova EI: **Contamination of exosome preparations, isolated from biological fluids.** *Biomed Khim* 2017, **63**:91–96.

253. Gyorgy B, Modos K, Pallinger E, Paloczi K, Pasztoi M, Misjak P, Deli MA, Sipos A, Szalai A, Voszka I, Polgar A, Toth K, Csete M, Nagy G, Gay S, Falus A, Kittel A, Buzas EI: **Detection and isolation of cell-derived microparticles are compromised by protein complexes resulting from shared biophysical parameters**. *Blood* 2011, **117**:e39–e48.

254. Kalra H, Adda CG, Liem M, Ang C-S, Mechler A, Simpson RJ, Hulett MD, Mathivanan S: **Comparative proteomics evaluation of plasma exosome isolation techniques and assessment of the stability of exosomes in normal human blood plasma.** *Proteomics* 2013, **13**:3354–64.

255. Sokolova V, Ludwig A-K, Hornung S, Rotan O, Horn PA, Epple M, Giebel B: **Characterisation of exosomes derived from human cells by nanoparticle tracking analysis and scanning electron microscopy.** *Colloids Surf B Biointerfaces* 2011, **87**:146–50.

256. Kato K, Kobayashi M, Hanamura N, Akagi T, Kosaka N, Ochiya T, Ichiki T: **Electrokinetic Evaluation of Individual Exosomes by On-Chip Microcapillary Electrophoresis with Laser Dark-Field Microscopy**. *Jpn J Appl Phys* 2013, **52**:06GK10.

257. Lőrincz ÁM, Timár CI, Marosvári KA, Veres DS, Otrokocsi L, Kittel Á, Ligeti E: **Effect of storage on physical and functional properties of extracellular vesicles derived from neutrophilic granulocytes.** *J Extracell vesicles* 2014, **3**:25465.

258. Lee M, Ban J-J, Im W, Kim M: **Influence of storage condition on exosome recovery**. *Biotechnol Bioprocess Eng* 2016, **21**:299–304.

259. Akagi T, Ichiki T, Ohshima H: **Evaluation of Zeta-Potential of Individual Exosomes Secreted from Biological Cells Using a Microcapillary Electrophoresis Chip**. In *Encyclopedia of Biocolloid and Biointerface Science 2V Set*. Hoboken, NJ, USA: John Wiley & Sons, Inc.; 2016:469–473.

260. Deregibus MC, Figliolini F, D'Antico S, Manzini PM, Pasquino C, De Lena M, Tetta C, Brizzi MF, Camussi G: **Charge-based precipitation of extracellular vesicles.** *Int J Mol Med* 2016, **38**:1359–1366.

261. Gupta S, Knowlton AA: **HSP60 trafficking in adult cardiac myocytes: role of the exosomal pathway**. *AJP Hear Circ Physiol* 2007, **292**:H3052–H3056.

262. Caradec J, Kharmate G, Hosseini-Beheshti E, Adomat H, Gleave M, Guns E: **Reproducibility and efficiency of serum-derived exosome extraction methods.** *Clin Biochem* 2014, **47**:1286–92.

263. Sáenz-Cuesta M, Arbelaiz A, Oregi A, Irizar H, Osorio-Querejeta I, Muñoz-Culla M, Banales JM, Falcón-Pérez JM, Olascoaga J, Otaegui D: **Methods for extracellular vesicles isolation in a hospital setting.** *Front Immunol* 2015, **6**:50.

Annexes

Exosome isolation

- PBS (1x)

  Dissolve 1 pack of BupH Modified Dulbecco's PBS in 500 ml of deionised water. Filter solution through a 0.2 µm filter and store at 4 ºC. The final concentration should be 8 mM sodium phosphate, 2 mM potassium phosphate, 140 mM NaCl, 10 mM KCl, pH 7.4.

- RIPA buffer (Sigma-aldrich)

  Add 50 µl protease cocktail inhibitors to 950 µl of RIPA buffer. Store at 4ºC.

Transmission electron microscopy (TEM)

- PBS (1x)

  Dissolve 1 pack of BupH Modified Dulbecco's Phosphate Buffered Saline (Pierce) in 500 ml of deionised water. Filter solution through a 0.2 µm filter and store at 4 ºC. The final concentration should be 8 mM sodium phosphate, 2 mM potassium phosphate, 140 mM NaCl, 10 mM KCl, pH 7.4.

- Paraformaldehyde fixating solution (100 ml):

  Add 4g of paraformaldehyde to 80 ml of filtered H_2O. Dissolve by heating the mixture, with agitation, at 58ºC. Add one or two drops of 1M NaOH to clarify the solution. Filter solution through a 0.2 µm filter, adjust the volume with deionised water and store at 4ºC.

- Phosphotungstic acid hydrate solution (5 ml):

  Add 0.15g of phosphotungstic acid hydrate to 3 ml of sterilized deionised water. Adjust pH to 7 by adding 3 or 4 drops of 1M NaOH. Ajust the volume to 5 ml and store at 4ºC.

Protein quantification

- Working reagent:

  Prepare working reagent considering the proportion 50 reagent A: 1 reagent B. The reagent A contains sodium carbonate, sodium bicarbonate, bicinchoninic acid and sodium tartrate in 0.1 sodium hydroxide. Reagent B contains 4% cupric azide.

SDS-PAGE

- Lower gel buffer (LGB) (4x) (1L):

  Add 181.65 g of Tris to 900 ml of deionised H_2O and mix until complete dissolution. Adjust to pH 8.9, adjust the volume to 1L with deionized water and store at 4ºC.

- Upper gel buffer (UGB) (1L):

  Add 75.69 g of Tris to 900 ml of deionised H_2O and mix until complete dissolution. Adjust to pH 6.8, adjust the volume to 1L with deionized water and store at 4ºC.

- Ammonium Persulfate (APS) 10x (10 ml):

  Dissolve 1g of APS in 10 ml of deionized H_2O. Prepare it always fresh before use.

- 10% Sodium docecilsulfate (SDS) (100 ml):

  Dissolve 10g of SDS in 100 ml of deionized H_2O.

- Stacking and resolving gel (60 ml):

Reagents	Stacking gel 3.5%	Resolving gel 5%	Resolving gel 20%
H_2O	13.2 ml	17.4 ml	2.2 ml
Acrylamide	2.4 ml	5 ml	20 ml
LGB (4x)	-	7.5 ml	7.5 ml
UGB (5x)	4.0 ml	-	-
10% APS	200 µl	150 µl	150 µl
10% SDS	200 µl	-	-
TEMED	20 µl	15 µl	15 µl

- Loading gel buffer (4x) (10 ml):

  To a final volume 10 ml add:

Reagents	V= 10 ml
Tris 1M	2.5 ml
SDS	0.8 g
Glicerol	4 ml
β-Mercaptoetanol	2 ml
Azul bromofenol	1 mg

- Tris 1M (250 ml):

  Dissolve 30.3g of Tris in 250 ml of deionized H_2O. Adjust pH to 6.8.

- Running buffer (10x) (1L):

  Dissolve 30.3g of Tris (250 mM), 144.2g of glycine (2.5 M) and 10g of SDS (1%) in deionized H_2O. Adjust pH to 8.3 and adjust the volume to 1L.

Western blotting

- Transfer buffer (1x) (1L):

  To 700 ml of deionized H_2O add 3.03g of Tris (25mM) and 14.41g of Glycine (192mM). Mix it until dissolution and the adjust the pH to 8.3. Adjust the volume to 800 ml of deionized H_2O. Just before use add 200 ml of methanol (20%).

- Tris buffered saline (TBS) (10x) (1L):

  To 700 ml of deionized H_2O add 12.11g of Tris (10 mM) and 87.66g of NaCl (150 mM). Adjust the pH to 8.0 and the volume to 1L with deionized H_2O.

- Tris buffered saline + Tween (TBS-T) (10x) (1L):

  Add 12.11g of Tris (10 mM), 87.66g of NaCl (150 Mm) and 5 ml of Tween 20 (0.05%) of deionized H_2O. Adjust the pH to 8.0 with HCl and adjust the volume to 1L with deionized H_2O.

- Blocking solution (5%) (100 ml):

  Dissolve 5g of non-fat dry milk in 100 ml of 1x TBS-T.

- Antibody solution (3%) (25 ml):

  Dissolve 0.75g of non-fat dry milk in 25 ml of 1x TBS-T. Add antibody according to pretended dilution, mix gently (no vortex) and store at -20ºC.

- Ponceau S Staining solution (0.1%) (50 ml):

  Dissolve 1g of Ponceau S in 50 ml acetic acid and adjust the volume to 1L with deionized H_2O. Store at 4ºC, protected from light.

- Membranes stripping solution (500 ml):

  Dissolve 3.76g of Tris-HCl (pH 6.7) and 10g of SDS (2%) in deionized H_2O. Add 3.5 ml of β-mercaptoethanol (100 mM) and adjust the volum